

CENTRAL LIBRARY

TEZPUR UNIVERSITY

Accession No. T319

Date

**SYNTHESIS, CHARACTERIZATION AND APPLICATION
OF NOVEL SOLID BASE GREEN CATALYSTS FOR
NUCLEOPHILIC ADDITION REACTIONS**

A thesis submitted in partial fulfillment of the requirements

for the degree of

Doctor of Philosophy

By

Rasna Devi

Registration No: 058 of 2010



Department of Chemical Sciences

Tezpur University, Napaam

Assam, India

784028

August 2014

*Dedicated to my parents and
teachers*



TEZPUR UNIVERSITY
(A CENTRAL UNIVERSITY)
Napaam, Tezpur -784028

Declaration

I do hereby declare that the matter embodied in this thesis is the result of investigations carried out by me in the Department of Chemical Sciences, Tezpur University, India under the guidance of Professor Ramesh Ch. Deka, Head, Department of Chemical Sciences, Tezpur University.

In keeping with the general practice of reporting scientific observations, due acknowledgements have been made wherever the work described is based on the findings of other investigators.

Date: 29th August 2014
Tezpur University

Rasna Devi
Rasna Devi



Prof. Ramesh C. Deka
Professor, Department of Chemical Sciences
Tezpur University, Napaam
Tezpur - 784 028, Assam, INDIA
E-mail: ramesh@tezu.ernet.in
Web: www.tezu.ernet.in
Mobile: +91 94353 80221

Certificate from Supervisor


This is to certify that the thesis entitled "*Synthesis, Characterization and Application of Novel Solid Base Green Catalysts for Nucleophilic addition reactions*" submitted to the School of Sciences, Tezpur University in partial fulfillment of the requirements for the degree of Doctor of Philosophy in Chemical Sciences is a record of research work carried out by Ms. Rasna Devi under my supervision. She has fulfilled all the requirements specified in the regulations of Tezpur University including course work for the award of Doctor of Philosophy in Chemical Sciences (School of Sciences).

All help received by her from various sources have been sincerely acknowledged.

No part of this thesis has been submitted elsewhere for award of any other degree or diploma by this or any other university/institution.

Place: Tezpur University

Date: 29th August 2014


(Prof. Ramesh C. Deka)

Professor and Head
Department of Chemical Sciences
Tezpur University,
Napaam, 784 028, India

ACKNOWLEDGEMENT

I extend my esteemed gratitude and indebtedness to my supervisor, Professor Ramesh Chandra Deka, head of the department, Chemical Sciences, Tezpur University for giving me the opportunity to carry out my research work under his able guidance. I am very much indebted for his precious suggestions and help during my entire Ph.D. research work and shouldering the responsibility in completing the thesis.

It is my heartfelt thanks to Professor Mihir K. Chaudhuri, Vice-Chancellor, Tezpur University for allowing me to take the advantages of the resources from this institute.

I am glad to offer my gratefulness to Madam Dr. Ruli Borah, Associate Professor, Department of Chemical Sciences, Tezpur University for her invaluable suggestions and help during my research period.

I offer my sincere gratitude to Dr. Pankaj Bharali, Assistant Professor, Department of Chemical Sciences, Tezpur University for helping me throughout my Ph.D. work by constantly discussing the subject matter and dedicating his appreciable efforts in completing my research work.

I thank all the faculty members of department of Chemical Sciences, Tezpur University and all teachers in my life who gave me precious knowledge and blessings throughout my life.

I thank Council of Scientific and Industrial Research and Department of Science and Technology (DST), New Delhi for the financial support offered to me.

I offer my sincere thanks to my labmates and friends specially Pangkita, Dipshikha, Himadri, Dhruba and Parijat for their constant help and support during my Ph. D. work.

I honestly thank my parents, grandparents and brother Biman for their love and respect towards me and being my greatest strength in every step of my life.

Date: 29th August 2014

Rasna Devi
Rasna Devi

CONTENTS

Chapter names	Title	Page Number
Initials	List of tables	i-iii
	List of figures	iv-vi
	List of schemes	vii
	List of abbreviations	viii-ix
	Abstract	x-xvii
1	Introduction	1-49
2	Materials and details of experimental methods	50-58
3	Design of zeolite catalysts for Henry reaction	59-96
	<i>Section 3A: Modification NaY and KL zeolites by potassium fluoride and their application for Henry reaction under mild conditions</i>	59-75
	<i>Section 3B: Study of structural change and basicity of KF loaded NaY zeolite and its application for Henry reaction under microwave irradiation condition</i>	76-96
4	Synthesis and modification MgAl-Hydrotalcite for Knoevenagel condensation reaction	97-133
	<i>Section 4A: Comparative study of structure and basicity of potassium salt modified MgAl-hydrotalcite and their application for Knoevenagel condensation reaction</i>	97-117
	<i>Section 4B: KNO₃ supported MgAl-mixed oxide as solid base catalyst for liquid phase Knoevenagel condensation reaction under microwave irradiation condition</i>	118-133
5	Synthesis of MgO by hydrothermal and solvothermal methods and their application for Claisen-Schmidt condensation reaction	134-145
6	Conclusions and future scope	146-149
	Appendices	150-151

List of Tables

Table Number	Table Caption	Page Number
Table 1.1	List of Nobel Prize winners in the field of catalysis	4
Table 1.2	Comparison of homogeneous versus heterogeneous catalysts	5
Table 1.3	Types of solid base catalysts	8
Table 1.4	Important industrial processes catalysed by solid bases	10
Table 1.5	List of indicators and their base strength ranges	11
Table 1.6	Classification of zeolites based on pores or channel system	17
Table 3A.1	Basic properties of zeolite NaY and KL before and after loading with KF	64
Table 3A.2	Effect of solvents on Henry reaction of 4-nitrobenzaldehyde and Nitromethane catalyzed by KF/NaY	66
Table 3A.3	Effect of temperature on Henry reaction of 4- nitro benzaldehyde and nitromethane catalyzed by KF/NaY	67
Table 3A.4	Effect of amount of nitromethane on conversion (%) and selectivity (%) on Henry reactions	68
Table 3A.5	Effect of the amount of catalyst on Henry reaction	69
Table 3A.6	Effect of catalysts on Henry reaction	69
Table 3A.7	Henry reaction of nitromethane with different aldehydes	71
Table 3A.8	Reusability study of KF/NaY for Henry reaction	73
Table 3B.1	Surface properties and particle size of zeolites	79
Table 3B.2	Base strength of zeolites modified with KF	81
Table 3B.3	Henry reaction of 4-nitrobenzaldehyde and nitromethane catalyzed by 10% KF/NaY in different solvents under M	84

Table 3B.4	Henry reactions with various aldehydes under MW ^a	88
Table 3B.5	Reusabiliy study of KF/NaY for Henry reaction under MW	89
Table 4A.1	Calculation of lattice parameter and basal spacings for potassium salt loaded hydrotalcites	100
Table 4A.2	Thermogravimetric and Differential thermal analysis results of the potassium salt loaded hydrotalcites	102
Table 4A.3	Textural properties of potassium salt loaded hydrotalcites	107
Table 4A.4	The values of Fukui functions with respect to Mulliken and Hirshfeld charges of the basic oxygen atoms of the metal oxide	109
Table 4A.5	Knoevenagel condensation reaction with different potassium salt loaded hydrotalcites at room temperature	111
Table 4A.6	Effect of various solvents on Knoevenagel condensation reaction at room temperature	112
Table 4A.7	Knoevenagel condensation reaction of different aldehydes and active methylene compounds with 10% KOH/HT	114
Table 4B.1	Textural properties of potassium salt loaded hydrotalcites calcined at 450 °C	125
Table 4B.2	Basic properties of potassium salt loaded hydrotalcites calcined at 450 °C	126
Table 4B.3	Catalyst study for knoevenagel condensation reaction	127
Table 4B.4	Knoevenagel condensation reaction catalyzed by KNO ₃ /MgAl(O)	128
Table 4B.5	Reusabiliy study of 10 % KNO ₃ /MgAl(O)	129
Table 5.1	Surface are and pore volumes of MgO calcined at 500 °C	141

Table 5.2	Effect of various MgO catalyst calcined at 500 °C	143
Table 5.3	Claisen-Schmidt reaction with MgO at 130° C.	144

List of Figures

Figure Number	Figure Caption	Page Number
Figure 1.1	Design of green synthesis in laboratory	2
Figure 1.2	Typical classification of catalysts	5
Figure 1.3	Comparison of solid acid and solid base catalysis	7
Figure 1.4	Effect of electric field on dipolar molecules (a) without any field (b) under influence of continuous electric field (c) under influence of alternating electric field at high frequency.	13
Figure 1.5	Structures of four large pore zeolites, faujasite, zeolite-L, mordenite and ZSM-12	16
Figure 1.6	Schematic diagram of Hydrotalcite and reconstructed hydrotalcite	28
Figure 3A.1	XRD pattern of (a) NH ₄ Y (b) NaY zeolite (c) KF/NaY (d) KL zeolite (e) KF/KL after calcinations at 450 °C	61
Figure 3A.2	The intensity ratio of the modified zeolites with parent zeolites at some 2θ points for (a) NaY zeolites (b) KL zeolites.	61
Figure 3A.3	The relative crystallinity (%) of modified zeolites with parent zeolites (a) NaY, KF/NaY zeolites (b) KL, KF/KL zeolites	62
Figure 3A.4	FTIR spectra of (a) NH ₄ Y (b) NaY (c) KF/NaY (d) KL and (e) KF/KL zeolites after activation at 450 °C	63
Figure 3A.5	SEM images of (a) NaY (b) KF/NaY (c) KL (d) KF/KL	64
Figure 3A.6	Plot of yield (%) against Hammett substituent constant (σ).	72
Figure 3B.1	XRD patterns of NaY and KF/NaY zeolites calcined at 450 °C	78
Figure 3B.2	Intensity differences of crystallinity of NaY and different KF/NaY zeolites calcined at 450 °C	78

Figure 3B.3	Differences of (%) crystallinity of NaY and different KF/NaY zeolites calcined at 450 °C	79
Figure 3B.4	FTIR spectra of parent as well as KF modified samples calcined at various temperatures. (a1) NaY, (a2) 0.5% KF/NaY, (a3) 1% KF/NaY, (a4) 2% KF/NaY, (a5) 3% KF/NaY, (a6) 5% KF/NaY, (a7) 10% KF/NaY, (a8) 15% KF/NaY and (a9) 20% KF/NaY [calcined at 450 °C]; (b1) 5% KF/NaY [calcined at 600 °C]; (b2) 5% KF/NaY [calcined at 800 °C]; (b3) 10% KF/NaY [calcined at 800 °C]	80
Figure 3B.5	Effect of microwave irradiation time on different polar solvents	85
Figure 3B.6	Effect of microwave irradiation power on amount of solvent	86
Figure 4A.1	Powder x-ray diffraction pattern of potassium loaded hydrotalcites	98
Figure 4A.2	Crystallinity (%) of different potassium loaded hydrotalcites	99
Figure 4A.3	Thermogravimetric analysis (a) and differential thermal analysis (b) patterns of different hydrotalcites	103
Figure 4A.4	FTIR patterns of hydrotalcites loaded with potassium salts	103
Figure 4A.5	Nitrogen adsorption/desorption isotherms and corresponding pore size distribution curves of (a) HT and (b) KOH/HT dried at 80 °C for 15 h	106
Figure 4A.6	Scanning electron micrographs of (a) HT and (b) KOH/HT at two different resolutions	107
Figure 4A.7	Optimized structure for most stable geometry of $Mg_3Al(OH)_8KOH$. The green balls represent Magnesium, pink represent Aluminium, purple represent Potassium, red represent oxygen and the grey balls represent Hydrogen atoms in the optimized geometry. The Oxygen atoms having larger values of $f(-)$ (higher basicity) are numbered and the bond lengths are in Å	109
Figure 4B.1	Powder x-ray diffraction pattern of potassium loaded MgAl-mixed oxides, (a) at 450 °C and (b) 550 °C	120

Figure 4B.2	Relative crystallinity (%) of loaded hydrotalcites calcined at 450 °C	121
Figure 4B.3	FTIR patterns of MgAl-mixed oxides loaded with potassium salts (a) calcined at 450 °C (b) calcined at 550 °C	122
Figure 4B.4	Scanning electron micrographs of (a) HT and (b) KNO ₃ /HT (c) KF/HT at two different resolutions	124
Figure 5.1	XRD pattern of MgO precursors synthesized under hydrothermal treatment for 6 h with different ratio of base versus salt; urea [a1-a3, a1(1 : 0.1), a2 (0.1 : 1), a3 (1 : 1) a4 (1 : 0.1, 24h)], NaOH [a5 (1 : 0.1), a6 (1 : 1)] and Na ₂ CO ₃ [a7 (1 : 0.1), a8 (1 : 1)]	136
Figure 5.2	Relative crystallinity (%) of MgO precursors obtained from urea	137
Figure 5.3	XRD pattern of MgO precursors obtained via solvothermal route with ethanol (SEt), ethylene glycol (SEg) and glycerol (SGly)	137
Figure 5.4	Relative crystallinity (%) of MgO precursors obtained via solvothermal route	138
Figure 5.5	XRD pattern of MgO calcined at 500 °C	138
Figure 5.6	SEM images of MgO precursors (a1, a3, a5 and a7) by hydrothermal route	139
Figure 5.7	SEM images of MgO precursors obtained by solvothermal route	140
Figure 5.8	BET isotherm of Calcined MgO at 500 °C.	142

List of Schemes

Scheme Number	Caption	Page Number
Scheme 1.1	Henry reaction between nitroalkane and carbonyl compound	22
Scheme 1.2	General mechanism of Henry reaction	23
Scheme 1.3	Application of Henry product β -nitroaldol	24
Scheme 1.4	Knoevenagel condensation reaction of carbonyl compound and active methylene compound in presence of base catalyst	29
Scheme 1.5	Mechanism of Knoevenagel condensation reaction	30
Scheme 1.6	General Scheme of Aldol Condensation and cross-aldol reaction	36
Scheme 1.7	Mechanism of Claisen-Schmidt condensation reaction	36
Scheme 3A.1	Henry reaction catalyzed by KF/NaY and KF/KL zeolites	60
Scheme 3B.1	Henry reaction catalyzed by KF/NaY under microwave	77
Scheme 4A.1	Knoevenagel condensation reaction catalyzed by KOH/HT at room temperature	110
Scheme 4B.1	Knoevenagel condensation reaction catalyzed by $\text{KNO}_3/\text{MgAl}(\text{O})$	128
Scheme 5.1	Claisen-Schmidt condensation reaction catalyzed by MgO calcined at 500 °C	143

List of Abbreviations

The following are the abbreviations used in the thesis

°C	Degree Celsius
¹³ C	Carbon-13-isotope
Å	Angstrom
BET	Brunauer-Emmett-Teller
BJH	Barrett–Joyner– Halenda
brs	Broad singlet
CDCl ₃	Deuterated chloroform
d	Doublet (spectral)
DCM	Dichloromethane
DMF	Dimethyl formamide
DTA	Differential Thermal Analysis
EDAX	Energy dispersive X-ray elemental analysis
EtOH	Ethanol
FTIR	Fourier Transformed Infra-Red
FWHM	Full Width at Half Maximum
g	Grams
h	Hour
HPA	Hirshfeld population analysis
HT	Hydrotalcite
IR	Infra-Red
LDH	Layered Double Hydroxide
m	Multiplet (spectral)
m.p.	Melting Point
MeOH	Methanol
MHz	Mega hertz
ml	Milliliter
mmol	Mili mole
MPA	Mulliken population analysis
MWI	Microwave Irradiation
NMR	Nuclear magnetic resonance

rt	Room temperature
s	Singlet (spectral)
ScCO ₂	Super Critical Carbondioxide
SEM	Scannig Electron Microscopy
STP	Standard Temperature and Pressure
t	Triplet (spectral)
TEM	Transmission Electron Microscopy
TGA	Thermo Gravimetric Analysis
THF	Tetrahydrofuran
UV	Ultra violet
XRD	X-ray Diffraction

Abstract

The growing interests of green chemical synthesis have led to the development of newer catalytic processes day by day. The term “Green chemistry” is often said with a term called “sustainable technology” which is defined as “Meeting the needs of present generation without compromising the ability of future generation to meet their own needs”. It is said that sustainability is the goal where green chemistry is the way to achieve it. Therefore, green chemical synthesis is an exciting field to introduce in this thesis.

The main contents of this thesis have been divided into six chapters. **Chapter 1** includes the introduction part and **Chapter 2** describes the details of materials, experimental methods and characterization techniques used in this thesis. The results of the present investigation are covered in **Chapter 3**, **Chapter 4** and **Chapter 5**. Conclusion of this thesis is given in **Chapter 6**.

Chapter 1: Introduction

This chapter describes the general introduction of catalysis, acid and base catalyzed organic reactions, key aspects of green chemistry principles and utilization of solid acid and solid base catalysts in the field of catalysis. It also focuses on literature methods of developing solid base catalysts and reaction strategies mainly in three areas of importance on which research have been carried out. The history and properties of three interesting solid base materials namely, zeolite, layered double hydroxide and magnesium oxide have been elaborated in this chapter. Included herein is also the general introduction of three important organic reactions namely Henry reaction, Knoevenagel condensation reaction and Claisen-Schmidt condensation reaction along with their previous literature reviews.

Zeolites possessing varieties of pore architecture and acid-base sites in their structures are considered as benign catalysts due to their aluminosilicate compositions. The entire surface area of zeolites is found nearly inside the micropores which are accessible to molecules of varying dimensions. Reactant molecules can access through the pores and give selective products. Due to tunable characteristics of these materials and their porous structures, zeolite materials have been selected for my Ph. D work to find benign solid base catalyst and to follow green chemical route of synthesis. Another important class of solid base materials which have been

Abstract

described in this thesis is the layered double hydroxides (LDHs) or commonly known as hydrotalcites. As the name imply, these are layered materials having positively charged brucite like sheets of dipositive and tripositive cations (e.g $M^{+2} = Mg^{+2}$, $M^{+3}=Al^{+3}$) and negatively charged anions (e.g. CO_3^{2-}) in the interlayer spaces. The strong basic nature and possibility of changing their properties through alteration of the cations and interlayer anions led us to select these materials for our research work. What makes these materials most fascinating in the field of catalysis are due to the typical acid-base properties and possibility to synthesize a large number of this family in the laboratory by varying the aforementioned compositions. Besides, physicochemical properties of these materials can be easily tuned by varying the synthesis procedure as well as their thermal treatment, which make them excellent support and catalysts for a good number of organic reactions. We have also introduced in this part of thesis the synthesis procedure and properties of magnesium oxide, which act as admirable solid base material for various reactions. Magnesium oxide or magnesia (MgO) is a hygroscopic white solid mineral having important acid-base properties. The superior catalytic performances of these materials are mainly governed by their physicochemical properties like morphologies, particles size and shapes, crystallinities as well as their surface area and basic properties. The synthesis of structurally diverse MgO can be obtained through thermal decomposition of the precursor such as magnesium carbonate or magnesium hydroxides obtained from different methods. Therefore, synthesis of these precursors to get varied morphologies, searching proper calcination temperature to obtain MgO and tuning their properties would be interesting in the field of catalysis.

This chapter also describes the basic properties of the three solid base materials and their procedure of measurements. Investigation of basic properties of solid bases and supported solid bases is a necessary tool for understanding their catalytic activities, nature of solid surfaces as well as the guest-host interactions. The catalytic activity of the aforementioned solid bases has been checked through their practical application in three important base catalyzed organic reactions i.e. Henry reaction, Knoevenagel condensation reaction and Claisen-Schmidt condensation reaction. Henry (or nitroaldol) reaction is a classic example of atom economic C-C bond forming reaction between a nitroalkane and an aldehyde or a ketone in presence

Abstract

of a base to give β -nitroaldols as the major product. It has got considerable interests from very early days due to synthetic utility of the product β -nitroaldol which can be easily converted into various important compounds such as β -amino alcohols, ketones, carboxylic acids, nitroalkenes etc. The literature review and importance of the reaction are included in the thesis. Knoevenagel condensation reaction is a versatile C–C bond forming reaction between, a carbonyl compound and an active hydrogen compound in presence of a basic catalyst to give α , β -unsaturated carbonyl compounds. The beauty of this reaction is due to its application in getting various chemically and biologically important intermediates such as alpha-cyanocinnamates, α,β -unsaturated esters and α,β -unsaturated nitriles which are useful for synthesis of drugs like nifendipine and nitrendipine, anionic polymerizations etc. The general mechanism, reaction strategies and literature reviews of this reaction also have been elaborated in this part of the thesis. Herein are also included the catalytic reviews, mechanism and reaction strategies of another important base catalyzed organic reaction named Claisen-Schmidt condensation reaction. It is the reaction of an aromatic aldehyde with another carbonyl compound containing an α -H atom in presence of a base to give α , β -unsaturated carbonyl compound. The importance, history and catalytic reviews are described herein this thesis.

Objectives of the present investigation

Going through the literature reviews, we have set our objectives as follows:

1. Modification of NaY and KL zeolites by potassium metal salts to check their structural and basic properties for Henry reaction.
2. Synthesis and modification of MgAl-hydrotalcites by potassium salts and their application for Knoevenagel condensation reaction.
3. Synthesis and modification of magnesium oxide via hydrothermal and solvothermal methods and their application for Claisen-Schmidt condensation reaction.

Chapter 2: Materials and details of experimental methods

This chapter gives the detail of reaction strategies, synthesis and modification of solid bases, chemicals and solvents used, procedures for quantitative and qualitative

Abstract

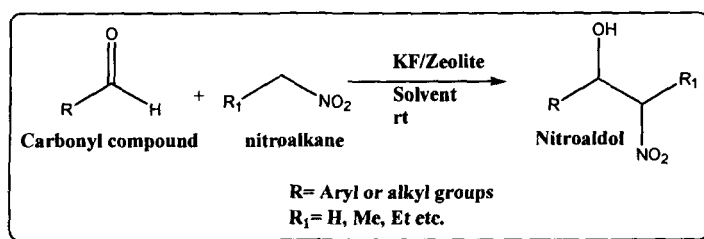
determination of the physicochemical properties as well as details of all the equipments used for these studies. This chapter also contains different characterization procedures for the solid catalysts.

Chapter 3: Design of zeolite catalysts for Henry reaction

This chapter describes the modification of NaY and KL zeolites and their application for Henry reaction. It has been divided into Section 3A and Section 3B.

Section 3A: Modification NaY and KL zeolites by potassium fluoride and their application for Henry reaction under mild conditions

This section concentrates on modification of NaY and KL zeolites with KF by a wet impregnation method, investigation of change of their basic properties and catalytic activities towards Henry reaction under classical conditions. Classical nitroaldol reaction is routinely performed by homogeneous bases like amines, alkoxides, and alkali metal hydroxides which are not acknowledged from the point of green chemistry. In this work, 5 wt % KF are loaded with NaY and KL zeolites and calcined them at 450 °C to check their base strength and catalytic activities for Henry reaction. Interestingly, the base strengths of both zeolites increase after introduction of potassium fluoride and catalyze Henry reaction efficiently with high conversions and selectivities. Effects of reaction parameters such as temperature, solvents, amount of catalysts and ratio of substrates versus reagents on Henry reaction have been explained. It is found that KF/NaY is the optimum catalyst for this reaction and active for variety of substrates to give respectable yields in H₂O-MeOH medium at room temperature. Addition of water in pure solvents speed up the reaction. Results of complete characterization of the catalysts are correlated to the catalytic activities of the catalysts and thus described herein.

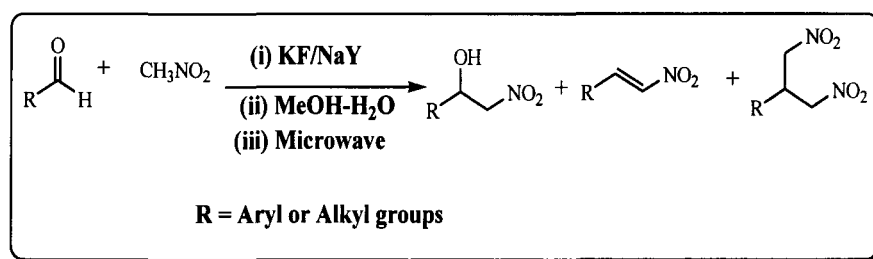


Scheme 1: Henry reaction catalyzed by zeolites

Abstract

Section 3B: Study of structural change and basicities of KF loaded NaY zeolite and its application for Henry reaction under microwave irradiation condition

This section continues with the investigation of effective catalysts and suitable reaction conditions for Henry reaction by combining the knowledge from previous section to carry out the reaction under microwave irradiation. Synthetic protocol using microwave irradiation are gaining value now a days due to its core heating mechanism and shorter reaction time than classical conditions. The green approach lies in getting higher yields within short reaction time, energy efficiency, higher selectivities and possibility to carry out reactions under solventless conditions.



Scheme 2: Henry reaction catalyzed by KF/NaY under microwave irradiation

In this section, the effect of guest potassium salt over the structural features and basic properties of NaY zeolite was explored by impregnating KF amounts of 0.5-20 % (w/w) over NaY zeolite. The research was focused on getting selective products and minimizing reaction time using microwave energy without compromising the yield. Accordingly, effect of amount of solvents, nature of solvents, microwave power and microwave irradiation time were studied and described herein. To our expectation, the catalysts efficiently catalyze the reaction under microwave irradiation to give β -nitroalcohols with high yield and selectivities within short time.

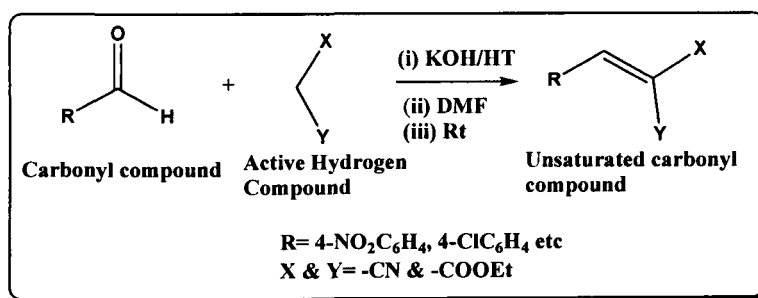
Chapter 4: Synthesis and modification MgAl-Hydrotalcite for Knoevenagel condensation reaction

This chapter describes the synthesis and modification MgAl-Hydrotalcite for Knoevenagel condensation reaction. It has been further divided into Section 4A and Section 4B

Abstract

Section 4A: Comparative study of structure and basicity of potassium salt modified MgAl hydrotalcite and their application for Knoevenagel condensation reaction

This section deals with the synthesis of MgAl layered double hydroxide, loading of KNO_3 , KOH , K_2CO_3 , KHCO_3 and KF salts over calcined Mg-Al hydrotalcite (Mg : Al = 3:1), investigation of their structure, basicities and catalytic activities towards Knoevenagel condensation reaction under mild conditions. Hydrotalcite, due to its layered structure and tunable properties is considered as interesting material for wide applications such as catalyst, catalyst support, flame retardant, ion-exchanger etc. In this work, hydrotalcites were modified by wet impregnation method and used for Knoevenagel condensation reaction at room temperature. Knoevenagel condensation reaction is the base catalyzed aldol type condensation reaction between a carbonyl compound and an active hydrogen compound giving an aldol type intermediate followed by dehydration to get substituted olefins. The olefin bearing electron withdrawing groups have numerous applications. Herein, we have described the effect various solvents and potassium loaded hydrotalcites over yield and selectivities of Knoevenagel condensation reaction. Furthermore, stability of host hydrotalcite structure and change in their physicochemical properties after modification have been explored by different characterization techniques. This study shows that KOH loaded MgAl hydrotalcite is the optimum catalyst for Knoevenagel condensation reaction and shows excellent conversions and selectivities within short time.

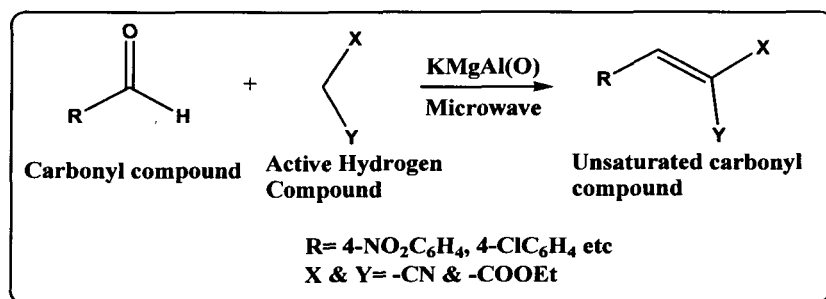


Scheme 3: Knoevenagel condensation catalyzed by hydrotalcites

Abstract

Section 4B: KNO₃ supported MgAl-mixed oxide as solid base catalyst for liquid phase Knoevenagel condensation reaction under microwave irradiation condition

This section of the thesis is the continuation of the work as described in section 4A. Hydrotalcites after activation gains interesting properties like high surface area, strong basicities and memory effect. This section concentrates on loading of activated MgAl hydrotalcite with KNO₃, KOH, K₂CO₃, KHCO₃ and KF salts, further activation of the loaded materials, investigation of change of structure, basicities and surface properties after loading and their catalytic activities for Knoevenagel condensation reaction under microwave irradiation condition. Herein, we have developed an optimized reaction strategy for this reaction. Effect of catalysts, microwave power and solvents have been explored and described herein. It is found that KNO₃ loaded mixed oxide is the optimum catalyst in this study and active for a variety of aldehydes containing functional groups such as -NO₂, -Cl, -OH, and -Me to afford good yield of the Knoevenagel product within short time.



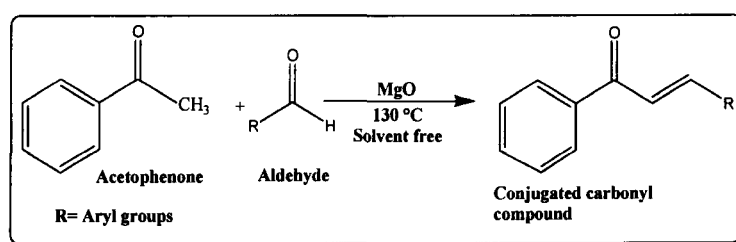
Scheme 4: Knoevenagel condensation catalyzed by potassium promoted MgAl-mixed oxides

Chapter 5: Synthesis of MgO by hydrothermal and solvothermal methods and their application for Claisen-Schmidt condensation reaction

This section comprises of synthesis of MgO precursors from nitrate salts of magnesium in presence of a base by hydrothermal and solvothermal methods, complete characterization of these materials through XRD, FTIR, SEM, TGA, DSC, N₂ adsorption desorption measurements and their application for Claisen-Schmidt condensation reaction under classical heating conditions. Motivation behind this

Abstract

work lies in the tunable characteristics of MgO with their superior activities for a good number of organic reactions. MgO is one of the most fascinating solid base catalyst in organic chemistry due to their excellent basic properties and tunable characteristic which can be obtained via alteration of particle arrangements through various synthesis strategies. Synthesis of MgO through different routes have been a promising field of catalysis since the catalytic properties of these materials are governed by particle size, surface area, crystallinity as well as morphologies. This section exclusively describes the formation of different MgO precursors under hydrothermal and solvothermal routes. Furthermore, the effect of three bases namely NaOH, Urea and Na₂CO₃, effect of ratio of magnesium salt versus bases upon growth of particles, phase obtained, crystallinity and particle sizes were explored and described herein. Interestingly, the amount of magnesium salt and the base in the mixture has crucial role over the crystal growth. It is observed that 1: 0.1 molar ratio of base versus Mg(NO₃)₂.6H₂O salt gives optimum conditions for crystal growth with high crystallinity in hydrothermal route. This section also describes the basic properties of the as synthesized MgO precursors, calcined MgO as well as their catalytic activities towards Claisen-Schmidt condensation reaction. In this respect detailed study of effect of catalysts, reaction time and temperatures on yield was investigated and explained herein. The scope of the reaction was further enhanced by performing the reaction under microwave condition where the reaction time reduced from hours to minutes to afford good yield.



Scheme 5: Claisen-Schmidt condensation catalyzed by MgO

Chapter 6: Conclusions and future scope

This chapter of this thesis describes the overall conclusions and future scope of the studied area in this thesis.

Chapter 1

Introduction

1. Introduction

Since the ancient age chemistry plays a key role in the progress of new civilizations. It is reflected in the history of various civilizations which were classified according to the development of new materials in that particular civilization *viz.* Copper age, Iron age etc. In short, progress of a civilization is widely influenced by the discovery of new materials. In this modern civilization, high demand for new materials, chemicals and medicines have resulted an increase in complexity of targeted molecules day by day. To synthesize such complex molecules development of new chemical processes has become an important aspect of organic chemistry. Development of new processes is receiving special interest in the context of green chemistry and sustainable development. It was Prof. Paul T. Anastas in 1991 who first introduced the term “Green Chemistry” to signify sustainable development of academic and industrial chemical processes [1,2]. According to him, *green chemistry is defined as “utilization of a set of principles that reduces or eliminates the use or generation of hazardous substances in the design, manufacture and application of chemical products”*.

Prof. Anastas put forwarded a set of twelve principles for making a chemical process green [3,4] which are as follows:

1. Prevention of waste/by-products
2. Maximum incorporation of the reactants (starting materials and reagents)
3. Prevention or minimization of hazardous products
4. Designing of safer chemicals
5. Minimization of energy requirement for any synthesis
6. Selecting the most appropriate solvent
7. Selecting the appropriate starting materials
8. Avoiding the use of protecting groups whenever possible
9. Use of catalysts should be preferred wherever possible
10. Products obtained should be biodegradable
11. The manufacturing plants should be designed so as to eliminate the possibility of accidents during operations
12. Strengthening of analytical techniques to control hazardous compounds

According to IUPAC system, green chemistry is defined as “The invention, design and application of chemical products and processes to reduce or to eliminate the use and generation of hazardous substances” [5]. The term “sustainable technology” is often said with “Green chemistry” particularly applicable for industrial processes, is defined as “Meeting the needs of present generation without compromising the ability of future generation to meet their own needs”. It is said that sustainability is the goal where green chemistry is the way to achieve it. Therefore, green chemistry is a global term for a sustainable modern world [1,6].

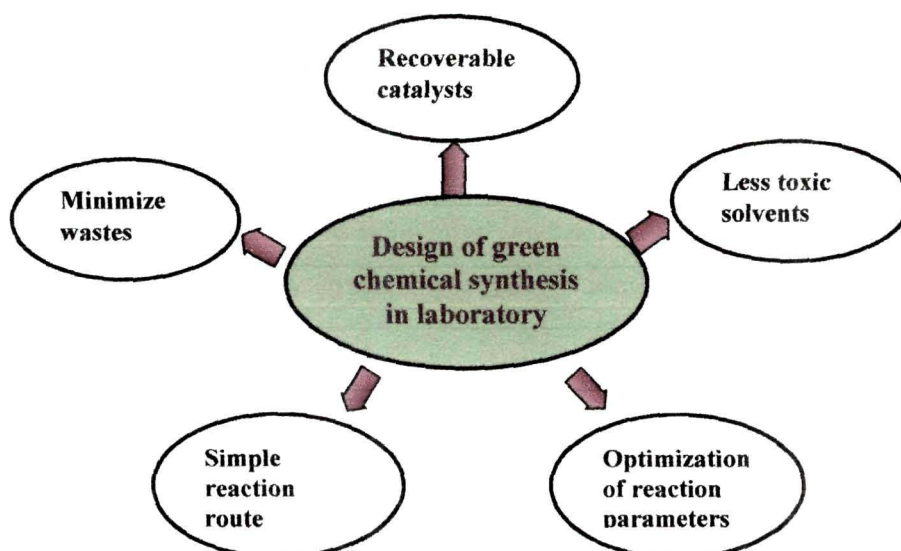


Figure 1.1: Design of green synthesis in laboratory

Design of green methodologies is generally framed by use of less toxic solvents, recoverable catalyst systems, appropriate starting materials, optimized reaction parameters and simple reaction routes (Figure 1.1). Among these, solvent plays crucial role in various reactions. However, most of the traditionally used solvents are hazardous to human health and the environments. It is found that benzene can cause cancer in animals and humans while toluene can damage brain, liver as well as kidney in humans. Chlorofluoro- carbons (CFCs) used widely until 20th century are dangerous for depletion of ozone layers. Therefore, it is always desirable to replace the traditional hazardous

organic solvents by the non/less hazardous solvents. In this respect, use of supercritical CO₂, ionic liquids and water as solvents have solved the problems to a great extent. Supercritical CO₂ has become a new hope for textile and metal industries and for dry cleaning of clothes. It is non-flammable, cheap and easily available. Ionic liquids are easy to perform, they are liquids at or below room temperatures and non-volatile. Similarly, water has been applied in numerous reactions due to its benign nature [7]. Solventless synthesis is another strategy in this respect due to faster reaction rate, minimization of costs for purification and separation process. However, not all reactions can be performed without solvents. Thus, no any single strategy can be termed as universal for building benign synthetic methodologies. One of the most important factor of green chemical synthesis is the use of catalysts whenever possible.

1.1 Catalysis and its importance

The beauty of catalysis has revolutionary aspects in every domain of sciences since early days. The word “catalysis” coined by Jöns Jacob Berzelius in 1835, comes from Greek words *kata* (cata) means down and *lyein* (lysis) means loosen. It was a great German chemist named Friedrich Wilhelm Ostwald got Nobel prize in chemistry in 1909 for his outstanding work on catalysis and developed the concept of catalysis which stated that a catalyst did not initiate a reaction but rather accelerated the rate of reaction without formation of intermediate compounds [8]. The phenomenon of performing a reaction in presence of catalysts is called *catalysis*. According to the definition, a catalyst can provide a different reaction energy pathway and decreases the activation energy barrier between reactants and products. Most of the complex chemical reactions in human and animal body, plant physiology are catalyzed by some efficient catalysts found in nature. Similarly, most of the chemical reactions in laboratories and industries would not have been possible without the use of catalysts. For example hydrolysis of esters become rapid in presence of a small amount of an acid or a base and these are called acid or base catalyzed. In the entire process, -OH ions act as the catalyst and does not consumed in the process. Therefore, catalysis has been an exciting area in the context of green chemistry. The importance of catalysis reflects from the outstanding work of various scientists who got Nobel prizes in the field of catalysis as listed in Table 1.1.

Table 1.1: List of Nobel Prize winners in the field of catalysis

Serial No	Name of Scientists	Area of discovery	Year
1	Friedrich Wilhelm Ostwald	<i>Catalysis, Chemical equilibrium and reaction rates.</i>	1909
2	Fritz Haber	<i>Synthesis of Ammonia from atmospheric N₂ and H₂ molecules.</i>	1918
3	Karl Waldemar Ziegler and Giulio Natta	<i>Controlled polymerization of hydrocarbons by Ziegler-Natta catalyst</i>	1963
4	William S. Knowles Ryoji Noyori	<i>Chirally catalysed hydrogenation reactions</i>	2001
5	K. Barry Sharpless	<i>Chirally catalysed oxidation reactions</i>	2001
6	Yves Chauvin, Robert H. Grubbs and Richard H. Schrock	<i>Development of the metathesis method in organic synthesis catalyzed by transition methods</i>	2005
7	Gerhard Ertl	<i>Chemical processes on solid surfaces</i>	2007
8	Richard F. Heck Ei-ichi Negishi Akira Suzuki	<i>Palladium-catalyzed cross couplings in organic synthesis.</i>	2010

1.1.1 Types of catalysts

Catalysts are broadly classified into homogeneous and heterogeneous ones. The following diagram shows the sub-divisions of various types of catalysts (Figure 1.2). In homogeneous catalysis, the catalysts present in the same phase as that of the reactants and products and generally are liquids while in heterogeneous one, catalysts present in different phase from the reactants or products and these are generally solids. Most of the traditionally used catalysts are homogeneous in nature which is dominating some major catalytic processes in the industries till now [9]. In spite of some excellent benefits, serious difficulties arise in separation of the homogeneous catalysts from reaction mixtures. Particularly, removal of heavy metal catalysts from reaction mixtures in various

metal catalyzed reactions create severe problem to the environment due to their toxic nature [10].

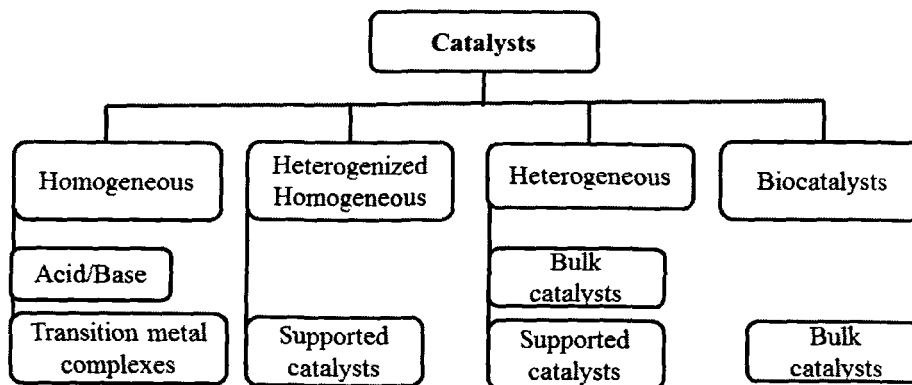


Figure 1.2: Typical classification of catalysts

The use of heterogenized catalysts are found advantageous in many processes in which homogeneous catalysts are anchored onto heterogeneous surfaces to get benefits of both homogeneous (high activity) and heterogeneous system (recovery) [11]. However, major drawbacks with these catalysts lies in leaching of catalysts from the heterogeneous surfaces during the course of reaction or in recycling process [11]. Hence, design of efficient and environmentally benign catalysts have been a common issue in the field of catalysis. In this regard, heterogeneous catalysts play a major role in establishing the economic strength of industries as well as laboratories due to cleaner synthesis. The advantages of heterogeneous catalysts over homogeneous ones can be understood from Table 1.2 as shown below [12].

Table 1.2: Comparison of homogeneous versus heterogeneous catalysts

Catalyst property	Homogeneous	Heterogeneous
Catalyst recovery	Difficult and Expensive	Easy and cheap
Thermal stability	Poor	Good
Selectivity	Excellent/good	Good/poor
Active sites	Single active site	Multiple active site

1.1.2 Acid and Base catalysis

Acid and base catalysis occupy a cardinal position in the domain of organic synthesis [13,14]. The use of traditional acids such as BF_3 , AlCl_3 , TiCl_4 and HF create severe difficulties in the chemical and industrial processes due to their corrosive nature, toxicity and problems associated with effluent disposal and product separation. Similarly, traditional liquid bases such as NaOH, LiOH etc. are disadvantageous for human health and to the environment. It is found that aqueous hydroxide solution having $\text{pH} > 11$ cause saponification of fats and solubilization of proteins when comes in contact with skin [15]. Concentrated caustic solutions are corrosive in nature and leads to prevent to cracking of tanks and vessels. Disposal of caustic solutions both in concentrated and dilute form are dangerous to the environment due to their strong basic nature. Neutralization of these basic solutions by other acidic solutions is generally employed for this problem prior to their disposal to the environment. However, this is quite problematic and costly. Again, commonly used molecular liquid bases such as ammonia and amines have sufficient volatility and gives toxic vapors. Due to these serious difficulties with the commonly used liquid solid acids and bases, the use for solid acid and solid base catalysts have emerged in vast number of chemical processes. Solid acid catalysts have got large attentions due to their high demand in petrochemical industries for catalytic cracking. Over the past 40 years, large varieties of solid acid catalysts such as Al_2O_3 , ZSM-5, zeolite-Y, SiO_2 and P_2O_5 have been extensively studied for wide spectrum of reactions such as alkylations, biodiesel production, catalytic cracking, isomerization, hydration, dehydration and polymerization reactions. On the other hand, the number of use of solid bases is very less in comparison to solid acids. According to the survey made by Kozo Tanabe and Wolfgang F. Hoelderich in the industrial processes till 1999, it was found that out of 127 acid and base catalyzed commercial processes, 103 were catalyzed by solid acid catalysts, 14 were catalyzed by solid acid-base bifunctional catalysts while only 10 were catalyzed by solid bases [16] (Figure 1.3). Thus, solid base catalysts are not well explored in comparison to solid-acids. Ground-breaking paper on the use of solid base catalysts was reported by Pines and his co-workers in 1955 [17], where they found that the sodium metal dispersed on alumina effectively catalyzed double bond migration of alkenes. Since then, a good number of solid bases including single component metal

oxides such as MgO and CaO to porous zeolites, mesoporous aluminosilicates and clays have been developed [18] over the period.

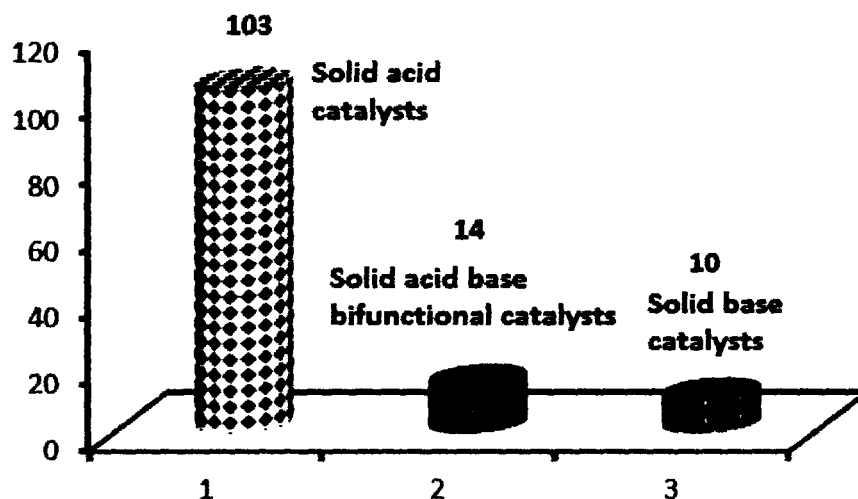


Figure 1.3: Comparison of solid acid and solid base catalysis

Heterogenization of the classical base catalysts and supporting basic guests over these single component oxides hosts and porous hosts have been applied over the years to prepare a variety of base catalysts [13, 19]. Table 1.3 shows some of the important solid bases developed in last 50 years.

The most important reasons for recognizing the listed materials as solid bases can be evidenced from the following points [20].

- (i) Evidence of the existence of basic sites on the surfaces are found from different surface characterizations such as colour change of the acid-base indicators, adsorption of acidic molecules on the surface, and spectroscopic studies (UV, IR, XPS, ESR, etc.).
- (ii) The catalytic activities correlate well with the amount of basic sites, strength of the basic sites and these are usually poisoned by acidic molecules such as HCl, H₂O and CO₂.

- (iii) The materials exhibit similar activities to “base-catalyzed reactions” similar to homogeneous basic catalysts and the mechanisms are similar to the homogeneous system.
- (iv) Mechanistic studies of the reactions, product distributions, and spectroscopic observations of the surface species indicate that anionic intermediates are involved in the reactions

Table 1.3: Types of solid base catalysts

Types	Typical types	Examples
1. <i>Single component metal oxides</i>	<i>Alkali metal oxides</i>	<i>LiO,</i>
	<i>Alkaline earth metal oxides</i>	<i>CaO, MgO</i>
	<i>Rare earth oxides</i>	<i>La₂O₃, YbO₂</i>
	<i>Transition metal oxides</i>	<i>ZrO₂, TiO₂</i>
2. <i>Zeolites</i>	<i>Alkali ion-exchanged zeolites</i>	<i>NaY</i>
	<i>Alkali metal or metal oxide occluded zeolites</i>	<i>KF/NaY, KNO₃/NaX, Cs-occluded zeolite</i>
3. <i>Supported catalyst</i>	<i>Alkali metal or metal ions such as Na, K, KNO₃, K₂CO₃ etc. supported on alkaline earth oxides, SiO₂, Al₂O₃ etc.</i>	<i>KF/MgO, KF/Al₂O₃</i>
4. <i>Clay minerals or modified clays</i>	<i>Hydrotalcite,</i>	<i>Mg-Al-Hydrotalcite</i>
	<i>Sapiolite,</i>	
	<i>Chrysolite etc</i>	
5. <i>Mesoporous material</i>	<i>Modified mesoporous material</i>	<i>MgO/SBA-15</i>
	<i>Functionalized mesoporous</i>	<i>MCM-41 functionalized with amino groups</i>
6. <i>Others</i>	<i>Oxynitride, Natural phosphate,</i>	<i>Silicon oxynitride (SiON) Aluminophosphate oxynitride (AIPON)</i>

However, most of the solid surfaces are not as strong as the liquid bases under ordinary conditions and thus requires proper pretreatment method before utilizing them in reactions. Hence, creating basic sites through their proper pretreatment is an essential step for solid catalysts. Generation of strong base sites is usually carried out by two methods: activation of the materials at high temperatures and supporting various guest species over porous materials. High temperature activation is necessary to activate the solid surfaces, since adsorption of CO₂ and water vapors poisons the surface basicity when exposed to air. Supporting guest species on porous hosts is attractive for the fact that the amount of basic sites as well the base strengths can be adjusted by varying the ratio of guest host amount and their activation temperature according to the need of a particular reaction. Besides, porous hosts have the ability to accommodate varieties of guest species inside their structures. Among various supports, porous oxides such as ZrO₂ and Al₂O₃ are widely used as host materials to generate strong basic sites [21,22]. Handa et al. have shown that metal and alkali metal compounds supported on γ -Al₂O₃ are much more active than a variety of single component solid bases such as BaO, Al₂O₃, KY zeolite and mixed oxide like 4MgO.Al₂O₃ for isomerization of 2,3-dimethyl-but-1-ene at 313K [23]. They have found that among varieties of catalysts tested, RbNH₂/Al₂O₃ and KNH₂/Al₂O₃ are the most active for this reaction while potassium exchanged zeolite Y is inactive under same reaction conditions. They have also found that KY zeolite is weaker than alkali amides on alumina, alkali compounds loaded alumina, MgO and CaO. Potassium amide supported on alumina (KNH₂/Al₂O₃) is a promising solid base for various other base catalyzed reactions [24-26]. Moreover, ZrO₂ and Al₂O₃ in presence KNO₃ can create superbasic sites after activation [27,28]. However, relatively low surface area of these oxide hosts limits their use in many cases. Similarly, ordered mesoporous silicas, in spite of their use as support for creating strong basicities [29], face limitations due to poor stability of the amorphous walls due to guest-host interactions [30]. Zeolites, due to their high surface area, high thermal stability, ordered pore architecture and surface acid-base properties can be good alternative for generating strong basicities. Therefore, searching of suitable guest hosts for preparation of strong, reusable solid bases is an ongoing research in the field of catalysis. Some of the important industrial processes catalyzed by supported and unsupported solid bases are listed in Table 1.4 [20].

Table 1.4: Important industrial processes catalyzed by solid bases

Process	Reaction	Catalyst	Company/Year
Alkylation	1. Alkylation of phenol with methanol	MgO	Gen.l Elect./1970, BASF/1985
	2. Alkylation of cumene with ethylene	Na/KOH/Al ₂ O ₃	Sumitomo/1988
Isomerization	3. Isomerization of 2,3-dimethyl-1-butene	Na/NaOH/Al ₂ O ₃	Sumitomo/1988
	4. Isomeri. of 3,5-vinylbicyclo[2.2.1]heptene	Na/NaOH/Al ₂ O ₃	Sumitomo/1988
	5. Isomerization of 1,2-propadiene to propyne	K ₂ O/Al ₂ O ₃	Shell/1996
Dehydration/ Condensation	6. Dehydration of 1-cyclohexylethanol	ZrO ₂	Sumitomo/1986
	7. Dehydration of propylamine-2-ol	ZrO ₂ -KOH ZrO ₂	Koei Chem/1992 Chisso/1974
	8. Isobutyraldehyde to isobutylisobutyrate		
Esterification	9. Esterification of ethylene oxide with alcohol	Hydrotalcite	Henkel/1994
Others	10. Thiols from alcohols with	Alkali/Al ₂ O ₃	Orgsintez

1.1.3 Determination of basic properties of catalysts

Investigation of basic properties of solid bases such as strength of basic sites and concentration of basic sites is a necessary tool for understanding their catalytic activities, nature of solid surfaces as well as the guest-host interactions. The existence of surface basic character was first understood through the indicator technique followed by a number of methods such as temperature-programmed-desorption (TPD) of CO₂ [31], NMR studies [32], poisoning by CO₂ and NH₃ [33], XPS binding energy of probe molecules adsorbed on solid surfaces [34] and adsorption of organic acids [35]. Among

these, TPD technique and indicator techniques are commonly employed for measurement of basic sites and base strengths, respectively.

Studies on basicities of solid surfaces have been reviewed well in different literatures [36,37]. The theory behind the indicator technique is similar to simple acid-base indicator in the solution phase chemistry where the colour of an acidic indicator change when it get adsorbed onto a basic surface. Base strength of a solid surface is defined as its ability to convert an adsorbed electrically neutral acid to its conjugate base [38]. If a neutral acidic indicator (InH) transfers the proton to the basic sites (B) of the catalyst, base strength is represented by Hammett basicity function (H_-) as shown below:

$$H_- = pK_{IH} + \log [In^-]/[IH] \dots\dots\dots (i)$$

where [IH] and [I⁻] are the concentrations of acidic indicator and its conjugate base respectively. Table 1.5 lists some commonly used indicators for measurement of basicity along with their respective colours in acidic and basic surface.

Table 1.5: List of indicators and their base strength ranges

Indicators	Colour		H_- range
	Acid form	Basic form	
<i>Bromothymol blue</i>	<i>Yellow</i>	<i>Green</i>	7.2
<i>Phenolphthalein</i>	<i>Colorless</i>	<i>Red</i>	9.3
<i>Tropaeolin-O</i>	<i>Red</i>	<i>Yellow</i>	11.1
<i>2,4,6-Trinitroaniline</i>	<i>Yellow</i>	<i>Reddish orange</i>	12.2
<i>2,4-Dinitroaniline</i>	<i>Yellow</i>	<i>Violet</i>	15.0
<i>4Chloro-2-nitroaniline</i>	<i>Yellow</i>	<i>Orange</i>	17.2
<i>4-Nitroaniline</i>	<i>Yellow</i>	<i>Orange</i>	18.4
<i>4.Chloroaniline</i>	<i>Colorless</i>	<i>Pink</i>	26.5

Hammett basicity function (H_-) was proposed for the first time by Paul and Long in 1957 [39]. Practically, base strength of a basic surface is determined by addition of a known concentration of indicator solution in non-polar solvent to the tested solid and checking well to ease adsorption. When the indicator gets adsorbed onto the solid, the

colour of the indicator will change provided the solid surface has enough strength to convert the indicator into its conjugate base form and thus shows the colour of its basic form. Similarly, quantitative determination of amount of basic sites is determined by using the theory of acid base indicators. We have found that titration method is commonly employed for this purpose. In this method, titration of a suspension of the solid base in a non-polar solvent such as benzene, containing the indicator in its conjugate base form is titrated with benzene solution of benzoic acid. Here, the acid neutralizes the conjugate base and shows end points from which amount of basic sites are measured in mmol g^{-1} of the titrated acid.

1.2 Microwave heating for chemical reactions

Microwave heating technology is gaining special interest in the last few years for improving the organic transformations [40]. Using microwave technology traditional organic transformation can be carried out within short period of time. It is well known that enhancement of reaction rate and conversions are achieved through heating of reaction mixtures under thermal heating conditions in oil bath. Microwave irradiation as non-conventional energy source provides an alternative way to activate reaction systems. The direct use of microwave energy in chemical reactions was started in 1986 from the pioneering papers by Gedye and co-workers [41] and Giguere and co-workers [42]. Since then it has become an essential tool for faster synthesis for wide areas of sciences like organic synthesis, polymer synthesis, material sciences, medicinal chemistry and nanotechnology [43-47]. The main advantage of the protocol lies in its “core heating” mechanism or dipolar mechanism [48]. The acceleration of reactions is due to interaction of dipolar molecules with microwave energy leading to both thermal and nonthermal effects. To be active for microwave adsorption, a substance or a molecule must possess some dipole moment. A dipole is sensitive to an external electric field and tries to orient itself with the direction of field. When microwave is irradiated, due to rapidly oscillating electric field of strength of about 2450 MHz, the dipoles try to orient themselves along with the oscillating field and thus induce some rotation and intermolecular friction between them (Figure 1.4). Internal core heating is the result of dissipation of microwave energy as heat due to these induced rotations. The ability of a substance to convert

electromagnetic energy into heat at a given temperature and frequency can be calculated by using the formula,

$$\varepsilon''/\varepsilon' = \tan \delta,$$

where δ is the dissipation factor of the molecule, and ε'' is the dielectric loss and measures the efficiency with which heat is generated from electromagnetic radiation and ε' is the dielectric loss which gives the ability of a molecule to be polarized by an electromagnetic field [49].

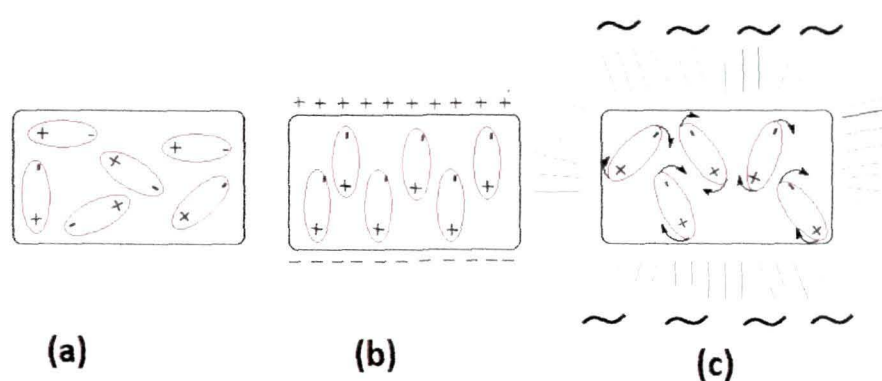


Figure 1.4: Effect of electric field on dipolar molecules (a) without any field (b) under influence of continuous electric field (c) under influence of alternating electric field at high frequency.

The high value of δ indicates high susceptibility to microwave energy [50]. This has special advantage for polar solvent molecules where “superheating effect” occurs under microwave and boiling point increases than their conventional values [51]. Both solvent free and solvent mediated microwave synthesis have been reviewed in the recent years describing the advantages of microwave heating over classical heating [52,53].

1.3. Aqueous phase reactions

Being non-toxic, cheapest and safest solvent in the world, water plays an important role in green chemical synthesis [54,55]. The replacement of volatile organic solvents with environmentally friendly solvents is essential due to unlimited use of solvents in various purposes like reactions, extractions and separations in both

laboratories and chemical industries. Although aqueous media reactions were tried in the beginning of 19th century, water was not utilized for organic synthesis due to low solubility of organic reactants and reagents in it. It was Breslow in 1980 who showed for the first time the enhancement of reaction rate with H₂O as solvent and made a remarkable beginning for utilization of water in organic synthesis [56,57]. He observed that the rate of Diels-Alder reaction of cyclopentadiene and butenone with water medium was more than 700 times faster than that with isooctane. The unique properties of water have been understood well during these times and have been utilized for green synthetic methodologies. Water has low volatility due to association of the molecules through hydrogen bonding and thus becomes an interesting replacement to the commonly used volatile organic solvents. Water being a small molecule, large cohesive energy density due to three dimensional hydrogen-bonded structures, high dielectric constant and high heat capacity, gives rise to an important property called hydrophobic effect. This hydrophobic effect is the driving force for interaction of organic reactants in aqueous medium, formation of micelles and bilayers, determination of the structures of proteins and nucleic acid, binding of substrates to enzymes, binding of antigens to antibodies etc. [58,59]. High cohesive energy of water drives the non polar organic molecules in organic reactions to aggregate in water and thus help in the progress of the reaction and increases selectivity [60,61]. In spite of the large cohesive energy of water, some solute molecules cannot aggregate and interact in water due to *hydrophobic hydration* [62,63]. This effect is responsible for decrease of reactions in aqueous medium. The properties of water are also controlled by pressure and temperature. On increasing temperature, hydrophobic hydration effect decreases and the association of hydrophobic molecules becomes easier i.e. hydrophobic interaction effect comes into play. Water behaves differently under high temperature and pressure. At high pressure, electrical conductance of aqueous solutions increases on increasing pressure due to their peculiar associative properties while for all solvents, electrical conductance decreases on increasing pressure. On increasing temperature, density of water goes on decreasing due to thermal expansion of the molecules. This value of dielectric constant is comparable to the commonly used organic solvents such as acetone at ambient temperatures [64]. Thus water can behave like pseudo-organic solvents at high temperature and high pressure. This increases solubility

of hydrophobic molecules and speed up reactions. At critical temperature, water called supercritical water, the density of water becomes 0.3 g/cm^3 . At the supercritical region, the heat capacity at constant pressure becomes very high and electrical conductance rises sharply. Therefore, supercritical water is used as green solvent in many processes. Despite of these advantages, water mediated synthesis are limited due to insolubility of most of the organic substrates. Again, evaporation of water from the reaction medium requires further difficulty in the process. Hence, efforts have been going on to add advantages of water with other strategies to get benefited from the combined effect. In this respect, microwave heating of reaction mixtures in presence of water medium is quite impressive.

When water is heated under microwave, due to its polar nature it can absorb microwave radiation easily and thus convert microwave energy into heat energy as a result of dissipation of absorbed energy in the form of heat. This can lead to rapid heating of the reaction mixtures and accelerates reactions faster than conventional heating. The use of water is further advantageous for reactions with nonpolar solvents under microwave. Addition of small amount of water with non-polar solvent like toluene can heat the reaction mixture as a whole. Besides, polar molecules can easily dissipate energy to the non-polar molecules and heats the whole reaction mixture rapidly [65]. Hence, addition of small amount of polar solvents to non polar solvents is an effective way to use non polar solvents for accelerating reactions under microwave. With these beneficial properties, water has been used in a good number of organic reactions.

1.4 Introduction of Zeolite

Zeolites form an important class of solid catalysts in the fine chemical industries as well as in the laboratories. It was Weisz and Frilette who reported the pioneering work on catalysis by zeolite in 1960 when they found some “unexpected intrinsic catalytic activities” of a faujasite like synthetic zeolite [66]. After the discovery, rapid increase of publications have been noticed year after year with practice of zeolite catalysts in all field of sciences. It was Swedish mineralogist Axel Fredrik Cronstedt who discovered zeolite mineral “stilbite” for the first time in 1756. Cronstedt in 1756 coined the term “zeolite” (comes from Greek words “zeo” meaning “to boil” and “lithos” meaning

“stone”) when he observed that heating stilbite mineral produced large amount of steam from water which was contained in their structure [67].

Structurally, zeolites are crystalline aluminosilicates having general formula $M^{n+}_{x/n}[(AlO_2)_x(SiO_2)_y].zH_2O$, where M^{n+} is the cation, x,y,z are numbers and the ratio of y/x is the governing factor of acidity or basicity of zeolites. The primary building block of zeolites is the SiO_4 tetrahedron with each apical oxygen atom shared with an adjacent tetrahedron. In zeolites, some of the SiO_4 tetrahedra are replaced by AlO_4 tetrahedra which creates extra negative charge in the structure and thus the resulting imbalance of charge is compensated by some positive ions. Some of these compensating cations are called the extra framework cations of zeolites and are exchangeable by other positive ions. Structurally, zeolites are complex inorganic polymers with infinite three dimensional network of TO_4 tetrahedra ($T =$ tetrahedral atom, e.g., Si, Al) and each apical oxygen atom is shared with an adjacent tetrahedron.

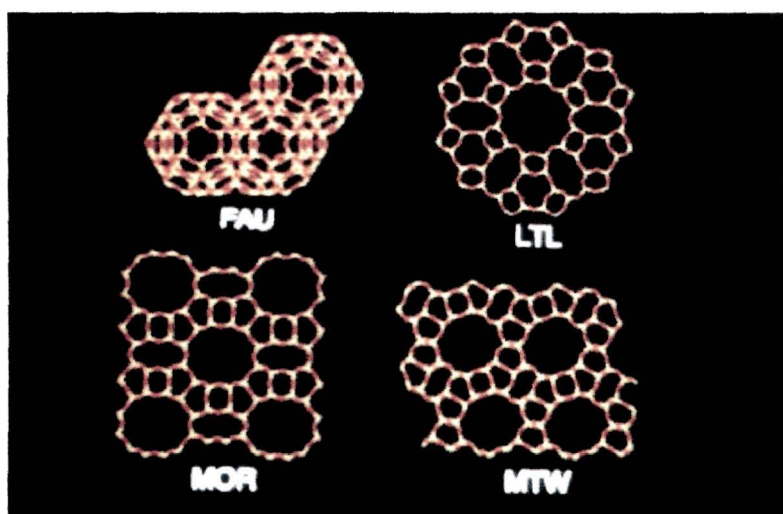


Figure 1.5: Structures of four large pore zeolites, faujasite, zeolite-L, mordenite and ZSM-12

The three dimensional network of zeolites possess intracrystalline porous channels containing water molecules and the replaceable cations. Removal of these water molecules through heat treatment leaves the void space free and makes them porous. The porous nature of zeolites is the principal reason why these are charming in the field of catalysis. In zeolites, the primary building units join in different ways to form secondary

building unit such as cubes, hexagonal prism and simple polyhedra which again join to form a varied types of zeolite frameworks (Figure 1.5). The structural nomenclature of zeolites was given by Structure Commission of International Zeolite Association (IZA) [68]. The international zeolite association (IZA) was formed in 1973 at the third international molecular sieve conference to develop the field of zeolite science and technology. This was followed by the formation of “Structure Commission” in the 4th international conference on molecular sieves in 1977 [69]. The Structure Commission was given authority by IUPAC to assign framework type codes (consisting of three capital letters) to all unique and confirmed framework topologies. Accordingly, each distinct framework type was assigned a three letter code called Framework Type Code (FTC) by the IZA Structure Commission irrespective of their compositions and published the details in *Atlas of Zeolite Framework Types* [70,71].

Table 1.6: Classification of zeolites based on pores or channel system [72].

Zeolite Type	Channel system Å (Number of oxygen atoms in the ring, channel dimension)	Porous Cavity, Å
Small Pore		
<i>Linde A</i>	4.1 (8, 3D)	6.6, 11.4
<i>Erionite</i>	3.6 × 5.2 (8, 3D)	6.3 × 13
Medium Pore		
<i>ZSM-5</i>	5.3 × 5.6 (10, 1D) 5.1 × 5.5 (10, 1D)	<i>Interconnencted channels</i>
<i>Ferrierite</i>	3.4 × 4.8 (8, 1D) 4.3 × 5.5 (10, 1D)	<i>Interconnencted channels</i>
Large Pore		
<i>Fauzasite</i>	7.4 (12, 3D)	6.6, 13
<i>Mordenite</i>	2.9 × 5.7 (8, 1D) 6.7 × 7.0 (12, 1D)	<i>Interconnencted channels</i>
<i>Zeolite L</i>	7.1 (12, 1D)	10.7

Till date more than 200 types of framework structures of zeolite are identified. According to the nomenclature, “FAU” was given to the fauhasite type framework (e.g. NaY, zeolite Y, NaX etc), “LTA” for Linde Type A framework and MOR was given to mordenite topology. The most important features of zeolite framework are the presence of pores upto 8-12 member oxygen rings and variations in Si/Al ratio from member to member.

The entire surface areas of zeolites are nearly inside the micropores and are accessible to molecules of varying dimensions. Reactant molecules can access through the pores and gives selective products. Depending upon the pore sizes, zeolites are classified as small pore, medium pore and large pore zeolites as shown in Table 1.6.

1.4.1 Catalysis by zeolites

Historically, zeolites have been widely used as solid acid catalysts in the industries for petroleum refining applications such as catalytic cracking and oil refining [73]. Besides, zeolites are used extensively in the chemical processes such as conversion of benzene to ethylbenzene, production of xylene, side chain alkylation of toluene; gas conversions such as methanol to gasolines (MTG), methanol to olefins (MTO), conversion of light petroleum gas (LPG) to aromatics and in oil conversion processes like hydrowaxing and hydrocracking [74]. ZSM-5 zeolite has been commercialized as additive for increasing octane numbers in fluidized catalytic cracking (FCC) [74]. Similarly, zeolite Y in its rare earth exchanged form was found admirable for FCC processes where the low octane number was further improved by utilizing ultrastable zeolite Y (USY i.e. high silicon zeolite Y) or a mixture of both USY and zeolite Y in the processes. However, zeolite as base catalysts was not practiced until the end of 19th century. It has been found that zeolites were used as solid base catalysts in their ion-exchanged form and impregnated form in the beginning of 1990s [75]. In spite of their great potential as shape selectivity and green catalysts, use of zeolites as solid bases are limited due to their weak base strengths and difficulty in generating strong basic sites in their structures. Therefore, tuning of basic properties through modification has been an exciting field of research till now.

1.4.2 Basic properties of zeolites

There are two main kinds of base zeolites i.e. alkali ion-exchanged zeolites and metals or metal oxides loaded zeolites. In general, the base sites in alkali ion-exchanged zeolites are the framework oxygens adjacent to the alkali cations and therefore related to the negative charge density on the oxygen atoms, which depend on the zeolite structure and chemical composition [76]. The base strength and the density of basic sites in alkali ion-exchanged zeolites decrease with an increase in framework Si/Al ratio, while basic strength increases with an increase in electropositivity of the counter cation in zeolites [77]. High aluminum content of zeolite X (Si/Al = 1–1.5) increase the framework negative charges, which makes zeolite X an excellent base catalyst in its alkali exchanged form [78,79]. It is found that the basic strength of alkali ion-exchanged zeolites decreases in the following order: $\text{Cs}^+ > \text{Rb}^+ > \text{K}^+ > \text{Na}^+ > \text{Li}^+$ and these are regarded as weak bases. Therefore they can be handled in ambient atmosphere, since adsorption of carbon dioxide or water is not too strong and they can be removed by high-temperature treatment. Occlusion of alkali metal oxide clusters in zeolite cages via decomposition of impregnated alkali salts results in a further increase in the basicity of base zeolites. Preparation of fine particles of alkali oxides inside the cavities of zeolites was developed by Hathaway and Davis [80-82]. They impregnated CsNaX and CsNaY zeolite with cesium acetate aqueous solution and calcined at 723 K to decompose cesium acetate into cesium oxide inside the cavities. Highly active basic sites were formed by this method. The work of Hathaway and Davis was extended by Tsuji et al. and found that potassium and rubidium oxide could be formed in addition to cesium oxide [83,84]. The resulting zeolite created basic sites stronger than those of simple ion-exchanged zeolites and able could isomerize 1-butene to 2-butene at 273 K with high *cis/trans* ratios. Recently, alkali earth oxides such as MgO and BaO are introduced into zeolites to produce strong basic sites [85,86].

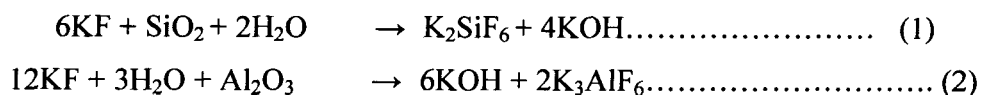
The basicity (amount and strength) of base zeolites have been extensively studied by theoretical approaches and experimental characterizations, including infrared (IR) spectroscopy of adsorbed probe molecules such as carbon dioxide [87], pyrrole [88,89], chloroform [90] and characterization techniques like TPD [91], XPS [92,94], UV-Vis spectroscopy [95,96], microcalorimetry [97,98] and NMR [99,101] etc. By generating

framework and/or extra-framework basic sites mentioned above, it is possible to prepare base zeolites having medium to strong basicities. Depending on the reaction to be catalyzed, it is possible to tune and select the most suitable base zeolite. Therefore, zeolites have been used as base catalysts in a number of base-catalyzed reactions, such as toluene alkylations with methanol or ethylene [102,103], dehydrogenation of alcohols [104], double bond isomerizations [105], Knoevenagel condensations [106,107], aldol condensations [108,109], cycloaddition of CO₂ to epoxides [2] and nitroaldol condensation [110,111].

In the flow of current research, a group of basic materials have been prepared by exchanging extra framework cations of zeolites with alkali and alkaline earth metal cations [112] and loading alkali metal salts over a variety of solid supports where potassium salt is the most common among other alkali salts [113-116]. Supported catalysts have caught considerable attention in these days due to their superior properties. Various supports such as porous oxides Al₂O₃, ZnO, ZrO₂ and SiO₂, zeolite NaX, NaY, ZSM-5, KL zeolite etc. are used to prepare solid bases by using potassium salts as guest material [117-119]. Although Al₂O₃ and ZrO₂ have been found as excellent basic materials in presence of potassium salts, their use is limited due to low surface area and disordered pore arrangements. Zeolites having aluminosilicate compositions, high surface area, well organized pore channels; stability towards heating and its benign nature are preferred as host material over the low surface area oxide hosts. Potassium fluoride has been supported onto a variety of solid host materials due to its different advantages such as it is easy to handle, inexpensive, thermally stable and can be easily dried.

According to the report by Weinstock et al. in 1986, the high basicity of KF/ Al₂O₃ is responsible for KOH formed as a result of interaction of KF with Al₂O₃ where F⁻ ions form H-bonding to the -OH group of hydroxylated surface of alumina and exert high basicity [120]. Zhu et al. loaded KF over Al₂O₃ and found higher basicity and higher catalytic activity than KOH/Al₂O₃ for isomerization of 1-butene at 273K [-124]. Yamaguchi et al. in 1997 showed that potassium compounds such as KNO₃ loaded on Al₂O₃ and activated at 773-873K is highly basic and active for isomerisation of but-1-ene [125]. Similarly, KF loaded over SiO₂ was reported by Jhu et al. and showed that F⁻

reacted with the surface of SiO₂ to give a crystalline phase of K₂SiF₆ and liberated KOH similar to KF/Al₂O₃ according to the equations-1 and 2 [126].



In their study, acidic SiO₂ became basic after loading of KF and basicity was responsible on concentration of F⁻ ion. Since zeolites have both AlO₄ and SiO₄ units in their structure, similar type of basic nature and reaction with F⁻ ions can be expected from loading fluoride support. ZeoliteY having high surface area attracted the chemists from long time to support various guest species over it. Due to unique selectivities [127,128] and benign nature, it would be a potential solid base catalysts if strong basic sites can be generated onto it. In this issue, potassium salts such as KOH, KF and KNO₃ are practiced by a number of groups in the past years. Supported fluorides have been found as potential base catalysts for a long time [129].

In 1979, Yamawaki et al. supported KF over fauzasite zeolite and utilized it for O-alkylation of phenol. In the experiment the basic properties was not well understood and the activity was found very low [130]. In 1998, Zhu and his co-workers reported only mild basicity of NaY zeolite (H_L =9.3) after loading 16 wt % KF and activated at 400 °C. They observed that 16 wt % KF over alumina coated NaY zeolite and activated at 400 °C generated strong basic sites (H_L =17.2) without significant change in zeolite pore architecture. Again, Sun et al. in 2009 have reported quite low basicity of KF /NaY (H_L = 7.2,) after activation at 600 °C. They have showed that the zeolite structure collapsed upon activation at 600 °C [131].

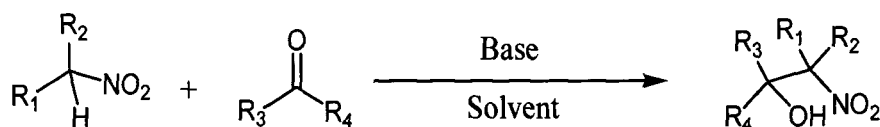
Similarly, zeolite KL has been loaded with potassium salts like KOH and KNO₃ to increase the basic properties [132-134]. Jo et al. showed that KL zeolite loaded with KOH and calcined at 500 °C increased base strength from H_L = 7.2-9.6 of parent KL to H_L = 9.6-15 of the loaded one and showed high catalytic activities for transesterification of soyabean oil [135].

Recently, we have modified NaY zeolite with 2-20 wt % KF and found that low loading of KF zeolite over NaY and their activation can generate strong basic sites

without damaging the framework structure. We have observed that zeolite structure remain intact upto 10 wt % loading of KF and activated at 450 °C without forming any other crystalline phase. Consequently, loading of NaY zeolite with different amount of KF and activation at 450-800 °C were done to observe their effect upon the structure, base strengths and catalytic activities.

1.5 Henry reaction

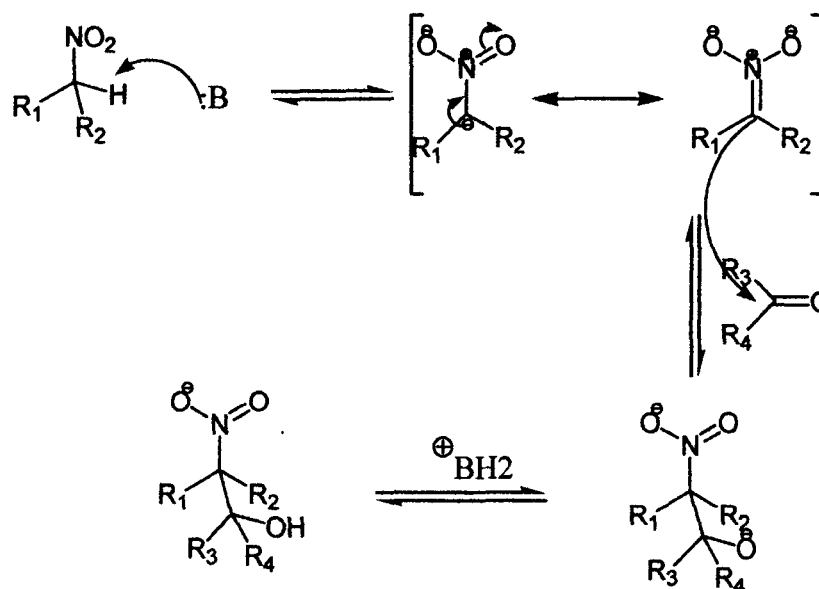
Henry (or nitroaldol) reaction is a classic example of atom economic C-C bond forming reaction between a nitroalkane and an aldehyde or a ketone in presence of a base to give β -nitroalcohols as the major product [136] (Scheme 1). It was L. Henry who discovered this reaction for the first time in 1895 which become a useful reaction for various chemical and biological syntheses since then [137,138].



Scheme 1.1: Henry reaction between nitroalkane and carbonyl compound

The mechanism of the reaction involves abstraction of a proton by the base from the active methylene center of the nitroalkane to form a reactive nitronate species in the first step followed by attack of the nitronate species on electrophilic centre of the carbonyl compound to form corresponding β -nitroalcohol [139] (Scheme 2). The reaction has got considerable interests from very early days due to synthetic utility of the product β -nitroaldol which can be easily converted into various important compounds such as β -amino alcohols, ketones, carboxylic acids, nitroalkenes etc [140-143]. Moreover, it can act as suitable intermediate for synthesis of various biologically important compounds such as aminosugars, anti-HIV drug amprenavir and α -hydroxy- β -amino acids which is a valuable backbone for peptide formation [144-148] (Scheme 3).

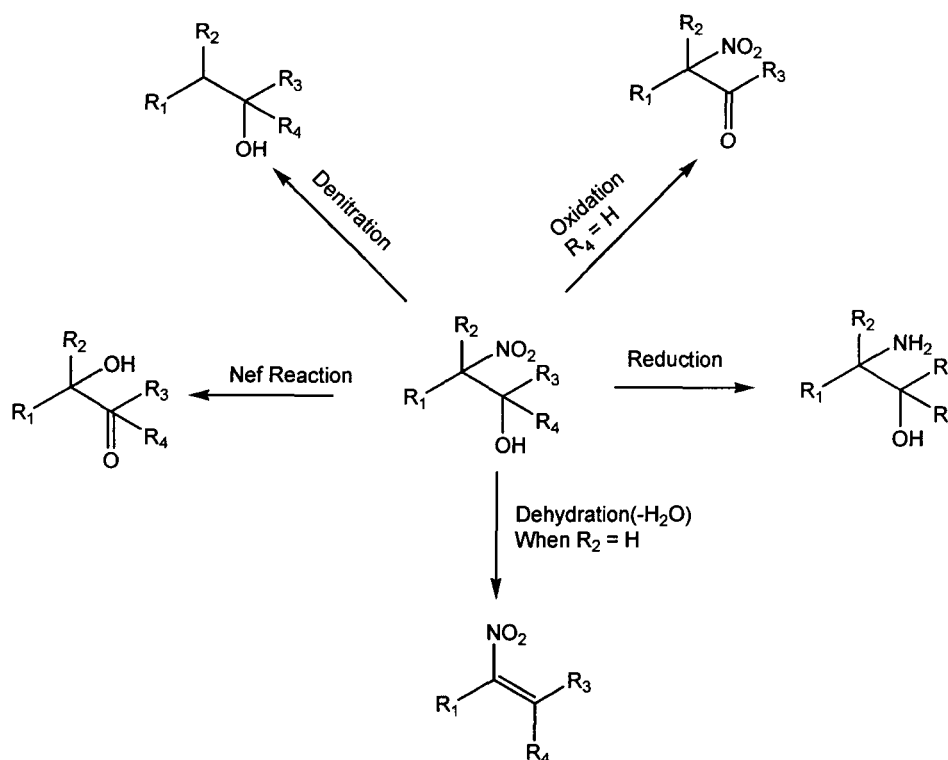
Typically, nitroaldol reactions were performed in presence of homogeneous bases such as NaOH, KOH, NaOMe etc. in either alcoholic or aqueous medium [149,150]. However, these traditional catalysts have got limitations in formation of nitroalkenes and polymerized products as side products due to strong basic nature of the catalysts. On the other hand, removal of the homogeneous catalysts from the reaction mixture is a difficult task.



Scheme 1.2: General mechanism of Henry reaction

A good number of homogeneous catalysts have been found successful for this reaction over the years. In 1989, Watt et al. studied the reaction with 1,1,3,3-tetramethylguanidine (TMG) in presence of diethyl ether and tetrahydrofuran [151,152]. Besides, amines such as triethylamine and diisopropylethylamine were used in presence of alcoholic solvents [153]. Verkade et al. in 1999 reported efficient promotion of nitroaldol reaction of ketones and aldehydes by a series of proazaphosphatranes [154]. They showed that the competitive self-condensation reaction of ketones was suppressed to a greater extent due to the protonated structure of phosphatranes and gave good yield of nitroaldol product with ketonic substrates. Youn et al. in 2000 reported that LiAlH₄ (10 mol %) in THF can

effectively catalyze the nitroaldol reaction between a variety of aliphatic and aromatic aldehydes with simple nitroalkanes such as nitromethane and nitroethane [155]. The reaction gave 71 % yield within 2-8 hours. The promotion of the reaction by moisture and impurity LiOH was ruled out by carrying out the reaction with 10 mol % LiOH with dried THF.



Scheme 1.3: Application of Henry product β -nitroaldol

A variety of catalysts like tetramethyl guanidine, NaOH in presence of cetyltrimethylammonium chloride (CTACl) [156], tetramethylethylene diamine (TMEDA) are found successful for this reaction [157]. The impressive works on Henry reaction has been carried out by different groups like Chisholm et al. with trialkyl phosphine catalysts [158], Desai et al. with potassium phosphate [159], Morao and Cossio with dendritically encapsulated amine complexes [160].

Demand of green chemical synthesis led various group of chemists to improve the reaction conditions as well as to minimize side products with the help of new catalyst systems and suitable reaction media [161-164]. Use of solid base catalysts, solventless reaction, water mediated reaction and use of microwave as alternating heating source have solved this problem to a great extent. Ballini et al. in 1994 used Amberlyst A-21 to synthesize nitroaldols with good to moderate yield of the product (65-86%) from a series of aldehydes and 4-nitro-2-butanol under solvent free conditions [165]. In 2008, Ballini et al. used Al_2O_3 in supercritical CO_2 to get controlled product with good yield [166]. They showed that nitroaldol product predominates at low temperature and low pressure (40 °C) while nitroalkene predominates on increasing temperature and pressure (60 °C, 100 bar). In the recent years, a group of catalysts like hydrotalcites, MgO catalysts, silica etc. have been practiced for this reaction under suitable reaction conditions. Bulbule et al. have reported that activated MgAl-hydrotalcite in THF solvent can effectively catalyze nitroaldol reaction to afford *threo* isomer in a highly diastereoselective manner. At the same time Choudhary et al. found high yield of nitroaldol product with activated MgAl-O-tBu catalyst under mild condition [167]. Despite of a variety of solid bases used for this reaction, searching of better catalyst is an ongoing research to obtain high yield and simultaneous control of the side reactions. Particularly, solid base catalysts like alkali and alkaline earth metal exchanged zeolite X and zeolite Y, supported zeolites and metal oxides, hydrotalcites etc. have been used for this reaction to take advantage of their tunable basicity, easy product isolation and catalyst recycling [168-171]. We have observed that zeolite catalyzed nitroaldol reactions is not very common. In 2014, Keller et al. have found that cation free high silica containing ultrastable zeolite Y (USY) shows high catalytic activities for liquid phase nitroaldol reaction [172]. On the other hand, functionalized mesoporous silica materials were found to catalyze this reaction selectively. The high selectivity of mesoporous silica is controlled by the typical coordination of the heterogenized group on the surface of silica where the silica acts as inert host for the reactions [173,174]. Anan et al. showed that grafting of aminopropyl group on mesoporous silica in polar solvent like ethanol formed selective nanoporous catalysts which gave nitroaldol product upto 100 % conversion selectively within 15-30 minutes

[175]. In another report, Huh et al. found high selectivity of the product with bifunctionalized mesoporous silica nanospheres [176].

Therefore, it is believed that KF loaded NaY zeolite can selectively catalyze nitroaldol condensation reaction. Further improvement of yield has been achieved through microwave irradiation of the reaction mixture. Henry reaction under microwave has been practiced in the years under solventless conditions with both homogeneous and heterogeneous catalytic systems. Verma et al. in 1997 obtained high yield of the dehydrated nitroalkene from NH_4OAc as catalysts under solventless conditions without isolation of intermediate β -nitroalcohols [177]. Gan et al. found high yield of nitroaldol product with 1,4-diazabicyclo[2,2,2]octane (DABCO) as base under microwave [178]. Powdered KOH can also furnish good yield of the product within few minutes for both aliphatic and aromatic aldehydes [179]. In another report, Kumar et al. have shown that reaction of aromatic aldehyde and nitroalkanes on activated SiO_2 affords 2-nitroalcohols in moderate to high yields [180]. However, the use of solvents along with heterogeneous base under microwave is not very common for this reaction. Herein, we have coupled the benefits of aqueous medium with alcoholic solvents under microwave for this reaction.

1.6 Layered Double Hydroxides (LDHs) Introduction

Another important class of solid base materials are the layered double hydroxides (LDHs) or commonly known as hydrotalcites [181]. The word “*hydrotalcite*” was derived from the word “*talc*” and its high water content because it can be easily crushed into powder like “*talc*” and it possesses high water content in the interlayers [182]. These are two dimensional anionic clays whose structures can be derived from brucite like $\text{Mg}(\text{OH})_2$ structures as shown in Figure 1. The divalent (Mg^{+2}) cations are surrounded octahedrally by hydroxyl groups in the brucite structures [183]. When some of the divalent Mg^{+2} cations in the brucite like layers are replaced isomorphously by trivalent cations like Al^{+3} , generation of extra positive charge occurs in the structures and thus accommodates some charge balancing anions in the hydrated interlayer region to form hydrated layered structures or hydrotalcite structure [183]. The structure of LDHs can be represented by the general formula $[\text{M}^{\text{II}}_{1-x} \text{M}^{\text{III}}_x(\text{OH})_2]^{x+} (\text{A}^{n-})_{x/n} \cdot y\text{H}_2\text{O}$, where M(II) are divalent cations

(M=Mg, Fe, Co, Ni, Cu, Ni etc.), M(III) are the trivalent cations (M=Al, Cr, Mn, Fe, Cr etc.), A^{n-} are the charge balancing anions such as CO_3^{2-} , NO_3^- , Cl^- , SO_4^- and OH^- in the interlayer regions and x is the ratio of $\text{M(II)}/[\text{M(II)} + \text{M(III)}]$ which generally lies in the range of 0.2-0.33 [184]. Among the varied possibility of anions in hydrotalcite structure, CO_3^{2-} is the most common among naturally occurring hydrotalcites. What makes these materials most fascinating in the field of catalysis are due to the typical acid-base properties and possibility of synthesizing a large number of this family in the laboratory by varying the aforementioned compositions. Besides, physicochemical properties of these materials can be easily tuned by varying the synthesis procedures as well as their thermal treatment. Hydrotalcites possess different properties in three different forms namely *as synthesized form*, *activated form* and *rehydrated form* due to which they are found as important materials for various purposes such as catalysts, catalysts supports, pharmaceuticals, ion-exchange materials, absorbers etc. The *as synthesized* hydrotalcite generally possesses low surface area and low base strengths due to the presence of water and charge compensating anions in the interlayer galleries. Therefore, they are generally activated to create strong basic sites and larger surface area. However, due to the presence of interlayer anions, they can act as catalysts for anion exchange reactions. In the halide ion exchange reactions between alkyl chloride and Br^- or I^- ions, use of hydrotalcites possessing Cl^- , Br^- or I^- ions in the interlayers act as catalysts for this reaction [185]. As synthesized hydrotalcites are also used as flame retardant and adsorbent for waste water in the industries [186]. The *activated form* of hydrotalcites are obtained upon thermal treatment of the *as synthesized* form in temperature ranges 450-500 °C, when the hydrotalcite phase converts to the most widely used mixed oxide phase. The mixed oxide form possesses the most important properties as catalytic materials i.e. high surface area, strong basic properties as well as memory effect [187]. Mixed oxides are used in catalytic applications such as aldol condensation, polymerization, epoxidation, hydrocarbon stream reforming, transesterification etc. [188,189]. When calcined hydrotalcites are rehydrated directly in water or in presence of water vapor, *rehydrated forms* of hydrotalcite occurs and the OH^- ions occupy in the interlayer galleries [190]. This property of hydrotalcites is called the *memory effect* [191]. It has been reported that reconstructed hydrotalcites having OH^- ions are stronger bases than

the as synthesized hydrotalcite possessing CO_3^{2-} ions [192]. These $-\text{OH}^-$ ions on the surface are claimed to be responsible for excellent catalytic activities of a number of base catalyzed reactions such as Knoevenagel condensation, Micheal addition, nitroaldol reaction etc [193,194].

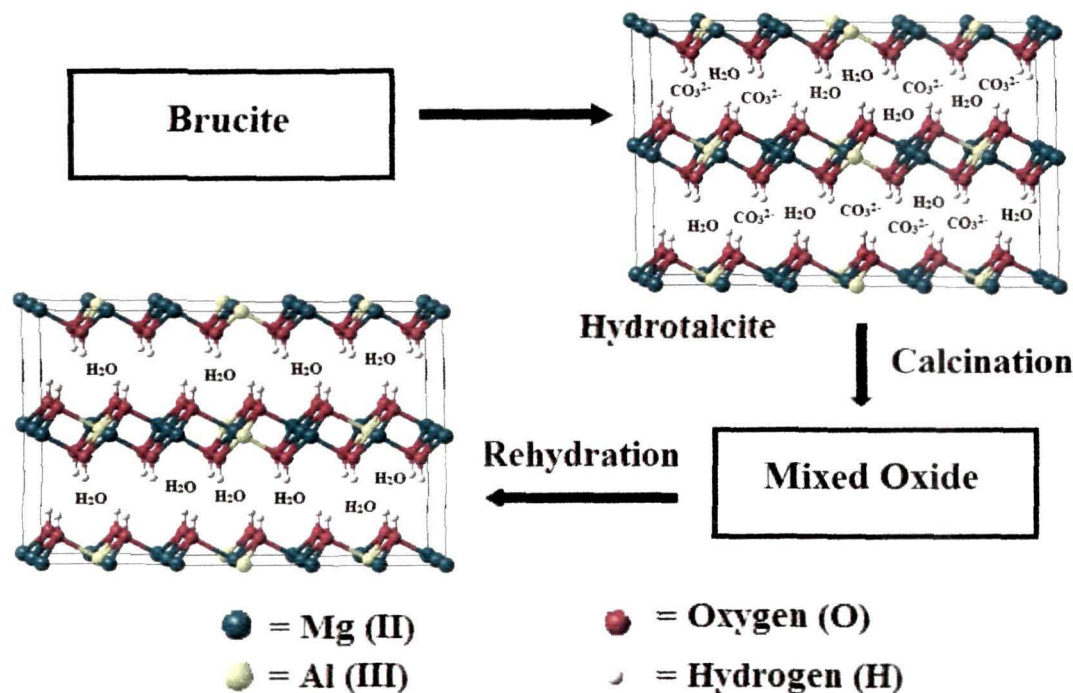
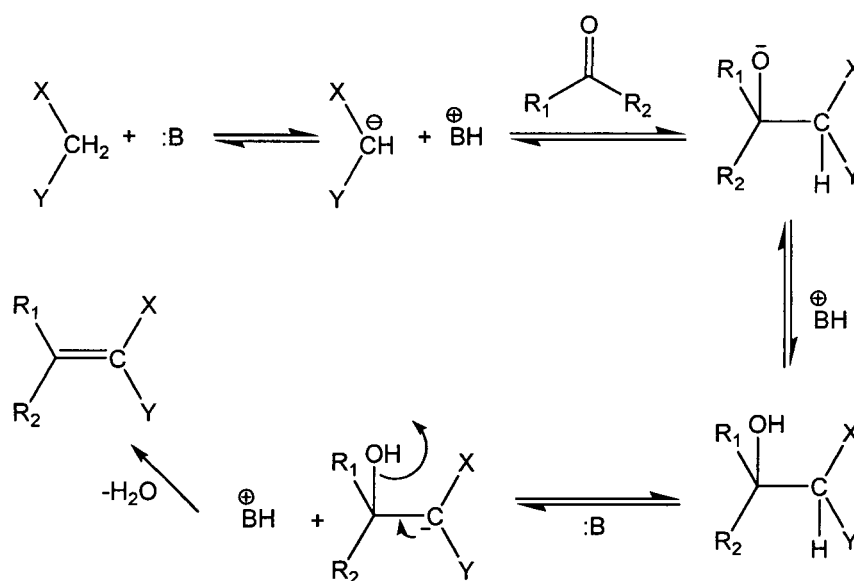


Figure 1.6: Schematic diagram of Hydrotalcite and reconstructed hydrotalcite

Thus, LDHs in *activated form*, *rehydrated form* and *as synthesized form* are excellent materials for large number of applications in the areas such as catalysis, photochemistry, pharmaceuticals, adsorption, electrochemistry etc. (Figure 1.6) [195]. Over the past years, considerable attentions are given to occlusion of guest species inside layered structure to enhance basic properties. Interestingly, use of MgAl mixed oxides as host materials to generate strong basicities by loading of solid guest species such as alkali or alkaline earth metals are proving to be beneficial for base catalyzed reactions. Among various guest species, potassium salts are the most common [196]. However, selection of the metal salt to suit the host material, effect of guest over the structure and generation of basicity are not well studied for hydrotalcite like compounds. Besides, conditions for a suitable catalyst in terms of its base strength, catalytic activity, stability of the host material,

niphendipine and nitrendipine, α,β -unsaturated nitriles useful for anionic polymerizations, cinnamic acid etc [203].

The mechanism of the reaction involves deprotonation of the active hydrogen compound by the base to form a nucleophile in the initial step followed by nucleophilic attack at the carbonyl carbon atom of the carbonyl compound to form an aldol type intermediate in the second step (Scheme 1.5). The aldol type intermediate eliminates water to form the corresponding α,β -unsaturated carbonyl compound.



Scheme 1.5: Mechanism of Knoevenagel condensation reaction

Traditional catalysts for this reaction are mainly alkali metal hydroxides (NaOH, KOH), piperidine and pyridine. Demand of green chemistry has led to the development of varieties of solid base catalysts and different strategies for this reaction [204]. McCluskey et al. in 2002 reported that solvent free synthesis is superior to traditional water reflux and ethanol reflux methods in presence of piperidine catalyst [205]. Use of solid bases with solventless synthesis is interesting in the field of green chemistry. Gawande et al. prepared MgO/ZrO₂ composite and performed solvent free Knoevenagel condensation and reported high yield of product [206]. It has been reported that basic zeolites such as GeX, Cs-exchanged NaX and Cs and Ln impregnated mesoporous MCM-41 can effectively catalyze this reaction under mild condition [207-210]. However, more basic

sites in comparison to ion exchanged method were generated in zeolites upon nitridation of zeolites with ammonia and after activation, where $-OH$ groups of zeolites were replaced by amino groups [211]. Zhang et al. grafted amino group onto NaX and CsNaX zeolite and found them as excellent catalysts for Knoevenagel condensation reaction under solventless condition [212]. Bigi and co-workers showed water mediated synthesis [213] of this reaction without any catalyst. In another report, Wang et al. found that use of water as solvent can catalyze the reaction of ketones and malononitrile [214]. Banothu et al. shows that use of solid base SeO_2/ZrO_2 catalysts under water medium and solventless condition gives better result for Knoevenagel condensation than commonly used polar solvents DMF, EtOH and acetonitrile where the high catalytic activity of selenium promoted ZrO_2 is believed to be due to the lattice defect created by promoter selenium and considerable redox properties [215]. Other solid bases like ZnO, MgO, alumina, potassium carbonates, zeolites and modified zeolites, natural phosphates etc. are reported as potential catalysts for this reaction [216]. These are considered as more benign in comparison to traditionally used alkaline hydroxides [217]. Kantam et al. reported a modified method for the activation of MgAl-hydrotalcite and quantitative formation of Knoevenagel condensation product in liquid phase at a faster rate with these catalysts [218]. In another report [219], Ebitani et al. have also showed that reconstructed hydrotalcite is more active than untreated hydrotalcite and provide a unique acid-base bifunctional surface capable of promoting the Knoevenagel and Michael reactions. They have also found that reconstructed hydrotalcite gives almost three times more yield than untreated hydrotalcites for aldol and Knoevenagel condensation reaction. Besides, other catalysts such as modified Mg-Al hydrotalcite with tert-butoxide anion, layered double hydroxide fluoride, hydrotalcite in ionic liquid medium etc. are also reported to be efficient catalyst for this reaction [220].

1.8 MgO catalysts for Claisen-Schmidt condensation reaction

Among various solid base catalysts practiced in the recent years, nano crystalline metal oxides such as MgO, CoO, CuO, ZnO, TiO_2 etc. have got considerable interests due to their structural variances that allow them to exhibit outstanding properties of chemical,

physical or material research interests like acid-base, redox, metallic, semiconductors and insulator properties. In particular, nanostructured MgO have extensively been studied as promising catalysts, catalysts supports and promoters in the field of heterogeneous catalysis due to its unique chemical and physical properties. Magnesium oxide or magnesia (MgO) is a hygroscopic white solid mineral occur naturally as *periclase*. The formula of MgO consists of lattice of Mg^{+2} and O^{2-} ions held together by ionic bonds. It reacts with water according to the reaction $MgO + H_2O = Mg(OH)_2$, which can be reversed to get MgO through thermal treatment. Some of the fascinating properties of MgO include its high thermal stability, high melting point (2850 °C) and high boiling point (3600 °C). MgO is generally obtained by calcination of magnesium hydroxide [$Mg(OH)_2$], magnesium carbonate [$MgCO_3$] or reaction of magnesium chloride with lime followed by heating. The basic properties of MgO are due to the presence of O^{2-} ions on the surface. Et al showed a surface model of decarbonated and dehydrated MgO where $Mg^{+2}-O^{2-}$ ion pairs present in different co-ordination environment. They have shown that $Mg^{+2}-O^{2-}$ ion pairs with co-ordination number three is the most active, less stable and requires high pretreatment temperature for their appearance [221]. Thus, activation temperature is crucial for tuning basic properties of MgO [222]. The superior catalytic performances of these materials are mainly governed by their physicochemical properties like morphologies, particles size, shapes, crystallinities as well as their surface area and basic properties. MgO having the aforementioned properties can be achieved through alteration of synthetic strategies.

1.8.1 Synthesis procedures of MgO

In the recent years, MgO having large variations of morphologies have been successfully synthesized via different synthetic routes such as solution phase hydrothermal and solvothermal methods, chemical precipitation, chemical vapour deposition, combustion, thermal evaporation and solid stabilized emulsion method [223-226]. However, most of the above methods require sophisticated equipments and are not cost effective. Moreover, MgO materials prepared through these methods exhibits relatively large crystallite sizes, low surface area, inhomogeneous morphologies, and low surface to volume ratio which make them disadvantageous in the field of catalysis. It has

been reported that sol-gel method of synthesis can give MgO having improved surface area, high surface to volume ratio, narrow particle size distributions and smaller crystallite sizes. However, requirement of environmentally hazardous and costly metal-organic precursors make this process inconvenient in view of green chemistry.

(a) Hydrothermal Synthesis

Solution based synthesis, particularly hydrothermal and solvothermal routes are the most conventionally used route for this purpose and thus provide an important technique to synthesize MgO with controlled size and shape [227,228]. The hydrothermal synthesis can be understood from the name itself as “hydro” means water and “thermal” means heat. Hydrothermal synthesis involves various techniques of crystallization in which crystals are allowed to grow from high temperature aqueous solutions of the metal salts at high vapour pressure. The term *hydrothermal* was first used by British geologist Roderick Murchinson to describe the formation of rocks and minerals due to the action of water with earth’s crust at elevated temperature and pressure [229]. According to Morey and Niggli, hydrothermal synthesis is defined as the process in which “components are subjected to the action of water at temperatures generally near though often considerably above the critical temperature of water, and therefore, under the corresponding high pressure developed by such solutions” [230]. Different scientists have presented the definition in different ways where the basic definition of all of them describes the action of water at high temperature or at ambient temperatures [231-234]. A variety of precursors like $\text{Mg}(\text{NO}_3)_2$, MgCO_3 , MgCl_2 , $\text{Mg}(\text{OH})_2$ etc. have been synthesized via hydrothermal method to synthesize MgO powder. General method of hydrothermal preparation of MgO involves homogeneous mixing of Mg salt solution of water with a basic solution of water under normal temperature and stirring condition, transferring the homogeneous mixture to a special stainless steel apparatus called autoclave and allowing crystal growth at the required temperature. In the method, a temperature gradient is maintained at the opposite ends of the growth chamber where the high temperature end favours dissolving the salts and the low temperature end favours crystal growth [235]. The growth of crystals and their physicochemical properties are dependent on the temperature, amount of salts in the

mixture, concentration of base, time of hydrothermal treatment, precursor types as well as treatment of the precursors after synthesis.

(b) Solvothermal Synthesis

Solvothermal route is again an important method of synthesizing MgO nanoparticles [236, 237]. In this method, similar to the hydrothermal route, nutrients are supplied along with different solvents into the growth chamber and crystals are allowed to grow at particular temperature. Numerous structures such as cubes, ellipsoids, spheroids, pyramids and bipyramids are synthesized via this route. Control over growth and agglomeration has been achieved through addition of suitable capping agents like long chain amine or thiols in the mixture [238]. Various MgO morphologies have been successfully synthesized through this route by solvent mediated, surfactant mediated or pH dependent growth of crystals [239,240].

(c) Synthesis of MgO from precursors

Magnesium oxide is generally synthesized by thermal decomposition of magnesium carbonate or magnesium hydroxides [241,242]. Among various basic precursors, magnesium carbonate hydrates (MCH) is interesting for its fascinating morphologies. It has been found that nesquehonite phase i.e. $\text{Mg}(\text{HCO}_3)\text{OH}\cdot 2\text{H}_2\text{O}$ crystallizes as needle and rods [243-245], hydromagnesite phase i.e. $4\text{MgCO}_3\cdot\text{Mg}(\text{OH})_2\cdot 4\text{H}_2\text{O}$ crystallizes as sheet [246] and MgCO_3 forms rhombohedral crystals [247]. Recently, Sutradhar et al. have synthesized different MCH morphologies from clear solutions of $\text{Mg}(\text{NO}_3)_2(\text{NH}_4)_2\text{CO}_3$ and nesquehonite rods via hydrothermal, solvothermal and supercritical hydrothermal approaches [248]. They have found that CO_3^{2-} ion concentration have crucial role over the formation of different morphologies such as *cards*, *random nanoflakes*, *arranged nanoflakes*, *flowers* and *spherical* under hydrothermal method. The obtained morphologies have quite different basic properties and surface areas and high catalytic activity for Claisen-Schmidt condensation reaction. In another report, Ding et al. have shown the formation of rod, tube, needle and lamella like morphologies of $\text{Mg}(\text{OH})_2$ through hydrothermal route from different Mg sources namely Mg powder, MgSO_4 , and $\text{Mg}(\text{NO}_3)_2\cdot 6\text{H}_2\text{O}$ [249]. A good number of reports on

synthesis of MgO are found in the literature to obtain varied shapes and sizes through this method.

It is found that $\text{Mg}(\text{OH})_2$ is also an equally important starting material like the carbonate precursors for synthesis of MgO with controlled sizes and shapes [253]. Synthesis of $\text{Mg}(\text{OH})_2$ are generally prepared by different methods to get various shapes and sizes which after thermal treatment gives MgO structures with the retained shapes. Jeevanandam et al. have converted magnesium oxychloride nanorods i.e. $(\text{Mg}_x(\text{OH})_y\text{Cl}_z.n\text{H}_2\text{O})$ to $\text{Mg}(\text{OH})_2$ nanorods which were previously synthesized from $\text{MgCl}_2.6\text{H}_2\text{O}$ and MgO powder with NaOH solution of EtOH- H_2O or H_2O [250]. Li et al. also synthesized $\text{Mg}(\text{OH})_2$ nanorods from Mg powder and distilled water or ethylenediamine solvents under pressure in autoclave at 180 °C [251]. Similarly, Zhuo et al. synthesized $\text{Mg}(\text{OH})_2$ nanotubes in an autoclave taking 1:1 ratio of water: methanol (V/V) from MgCl_2 salt. They dissolved MgCl_2 in distilled water and added ammonia water to precipitate and transferred the mixture to autoclave containing water methanol to get the corresponding $\text{Mg}(\text{OH})_2$ [252]. Makhluף et al. reported the use of ethylene glycol as solvent to synthesize nanocrystalline MgO under microwave irradiation and calcination in air at 600 °C [253]. In another report, Aslani et al. synthesised ZnO-MgO mixed oxide nanoparticles with ethanol water solvent under solvothermal route in an autoclave [254].

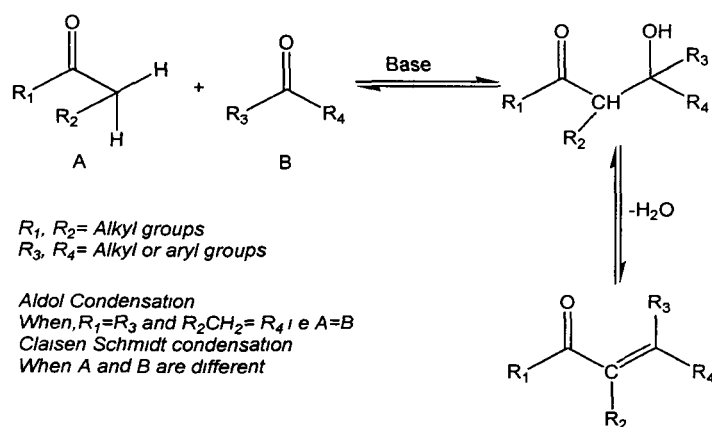
Thus, research on synthesis of MgO is centered on synthesis of its precursor salts via various synthetic strategies which in turn gives varieties of MgO shapes and sizes after thermal treatment.

1.9 Claisen-Schmidt condensation reaction

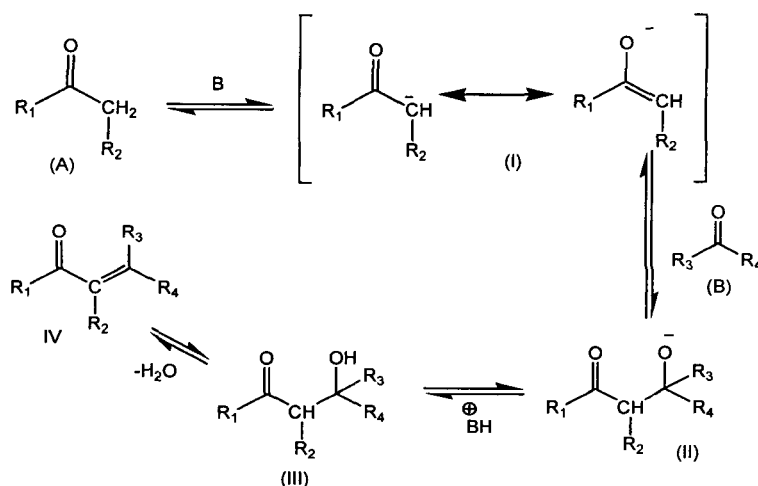
It is found that MgO exhibits excellent catalytic activities for a good number of base-catalyzed organic reactions such as Claisen-Schmidt condensation reaction [255], Nitroaldol reaction [256], Tishchenko reaction [257] and Aldol condensation reaction [258]. Claisen-Schmidt condensation reaction or cross-aldol condensation is an important C-C bond forming reaction in the domain of organic chemistry [259]. Aldol condensation is an acid or base catalyzed reaction between two molecules of carbonyl compounds, either identical or different and at least one of them containing α -H atom to give β -

hydroxy carbonyl compound (a dimer called aldol) or an α , β -unsaturated carbonyl compound (Scheme 1.6). The cross-aldol condensation reaction of an aromatic aldehyde with another carbonyl compound containing an α -H atoms to give α , β -unsaturated carbonyl compound is called as Claisen-Schmidt reaction.

Mechanism of this reaction involves abstraction of a proton by the base from the α -C atom of the carbonyl molecule (A) to form a resonance stabilized carbanion (I) in the first step followed by addition of the carbanion to the second carbonyl molecule (B) to form an alkoxide ion in the second step (II) (Scheme 1.7). The alkoxide ion takes a proton from water to form β -hydroxy carbonyl compound (III) which dehydrate to give α , β -unsaturated carbonyl compound (IV).



Scheme 1.6: General scheme of Aldol Condensation and cross-aldol reaction



Scheme 1.7: Mechanism of Claisen-Schmidt condensation reaction

Base catalyzed Claisen condensation is usually carried out in aqueous solutions of NaOH and KOH. It has been found that MgO catalyst under proper reaction conditions can effectively catalyze Claisen-Schmidt condensation reaction. Sutradhar et al. have shown that MgO catalyst calcined at 500 °C and sizes having 6-7 nm with different morphologies catalyzes the reaction between acetophenone and benzaldehyde to give high conversion (85%-99%) and selectivity (100%) within 2 hours. On the other hand bulk MgO shows low conversion (13%) under similar condition. Selvamani et al. found that calcination of rectangular hydromagnesite microsheet at 450 °C showed strong catalytic activity for solvent free Claisen-Schmidt condensation of benzaldehyde and acetophenone with 99% conversion within 4h [260]. The catalytic activity of regular microsheets were found higher than commercial MgO catalyst and the reaction was favoured by their small crystallite sizes due to the presence of large number of Lewis basic sites (O^{2-}) on the surface.

Thus, synthesis of size and shape controlled MgO through hydrothermal and solvothermal routes and their post synthesis modification would be quite interesting for improving the Claisen-Schmidt condensation reaction under different reaction conditions.

1.10 Objective of the present study

Having been gone through the literature reviews as described above, we have set the following objectives for the research work:

- (i) To prepare solid base zeolite catalysts by post synthesis modification of NaY and KL zeolites. i.e. by impregnating alkali or alkaline earth metal salts into zeolite structure.
- (ii) To prepare and modify solid base catalysts like metal oxides and mixed metal hydroxides by hydrothermal and solvothermal methods and to modify them via routes (a) impregnation of metal salts and (b) thermal treatment to observe their structural changes and change in basicity.

- (iii) To characterize the obtained basic materials by using techniques like FTIR, XRD, SEM, TEM, DSC, TGA, N₂-adsorption desorption method etc.

- (iv) To check the catalytic activity and selectivity of these materials in base catalyzed organic reactions i.e. Knoevenagel condensation, Henry reaction and Claisen-Schmidt condensation reaction.

1.11 References

- [1] Anastas, P.T., & Kirchhoff, M.M. *Acc. Chem. Res.* **35**, (9), 686-693, 2002.
- [2] Arends, I., Sheldon, R. & Hanefeld, U. *Green Chemistry and Catalysis*. WILEY-VCH Verlag GmbH & Co. KGaA, Weinheim, 2007.
- [3] Anastas, T. & Warner, J.C. *Green Chemistry: Theory and Practice*, Oxford University Press, Oxford, 1998.
- [4] Anastas, P.T., Heine, L.G. and Williamson T.C. Green Chemical Syntheses and Processes: Introduction, in *Green Chemical Syntheses and Processes*, Anastas, P.T.; Heine, L.G. and Williamson, T.C., Eds.; ACS Symposium Series 767, American Chemical Society: Washington, DC, 2000, 1-6.
- [5] Tundo, P., et al. *Pure Appl. Chem.* **72**, (7), 1207-1228, 2000.
- [6] Brundtland, C.G., *Our Common Future*, The World Commission on Environmental Development, Oxford University Press, Oxford, 1987.
- [7] Li, C.J. Water as Solvent for Organic and Material Synthesis, in *Green Chemical Syntheses and Processes*, Anastas, P.T et al., eds., American Chemical Society, 2000, 62-73.
- [8] Cornils, B., Herrmann, W.A., Schlögl, R. and Wong, C.H. *Catalysis from A to Z*, Wiley-VCH, 2003.
- [9] Bhaduri, S. & Mukesh, D. *Homogeneous Catalysis: Mechanisms and Industrial Applications*, 2nd ed., Wiley-VCH, 2000.
- [10] Farombi, E.O., et al. *Int. J. Environ. Res. Pulic Health* **4** (2), 158-165, 2007.
- [11] Barbaro, P. & Liguori, F., *Heterogenized Homogeneous Catalysts for Fine Chemicals Production*, Springer Dordrecht Heidelberg London New York, 2010.
- [12] Farnetti, E., Monte, D.R. and Kaspar, J. INORGANIC AND BIO-INORGANIC CHEMISTRY – Vol. II -Homogeneous and Heterogeneous Catalysis, in *Inorganic and Bioinorganic Chemistry, Volume I, ENCYCLOPEDIA OF LIFE SUPPORT SYSTEMS*, Bertin, I., eds.
- [13] Enberts, J.B.F.N., et al. *Recl. Trav. Chim. Pays-Bas* **115** (11-12), 457-463, 1996.
- [14] Hattori, H. *Stud. Surf. Sci. Catal.* **78**, 35-49, 1993.

- [15] Busca, G. *Chem. Rev.* **110**, (4), 2217-2249, 2010.
- [16] Tanabe, K. & Hölderich, W.F. *Appl. Catal. A* **181**, (2), 399-434, 1999.
- [17] Pines, H., et al. *J. Am. Chem. Soc.* **77** (23), 6314-6321, 6314, 1955.
- [18] Ono, Y., & Baba, T. *Catal. Today* **38** (3), 321-337, 1997.
- [19] Collis, A.E.C. & Horvath, I.T. *Catal. Sc. Technol.* **1** (6), 912-919, 2011.
- [20] Hattori, H., Solid Base Catalysts: Fundamentals and Applications, in 20th Annual Saudi-Japan Symposium Catalysts in Petroleum Refining & Petrochemicals, Dhahran, Saudi Arabia - December 2010.
- [21] Yamaguchi T., & Ookawa, M. *Catal. Today* **116**, (2), 191-195, 2006.
- [22] Wang, Y., et al. *Chem. Mater.* **13**, (2), 670-677, 2001.
- [23] Handa, H., et al. *Catal. Lett.* **59** (2-4), 195-200, 1999.
- [24] Baba, T., et al. *J. Catal.* **176**, (2), 488-494, 1998.
- [25] Baba, T., et al. *Catal. Lett.* **50** (1-2), 83-85, 1998.
- [26] Handa, H., et al. *Catal. Lett.* **44** (1-2), 119-121, 1997.
- [27] Sun, L. B., et al. *J. Phys. Chem. C* **112**, (13), 4978-4985, 2008.
- [28] Wang, Y., et al. *Chem. Mater.* **13**, (2), 670-677, 2001.
- [29] Lang, N., & Tuel, A. *Chem. Mater.* **16** (15), 2969- 2974, 2004.
- [30] Wu, Z.Y., et al. *Chem. Mater.* **18**, (19), 4600- 4608, 2006.
- [31] Lasperas, M., et al. *Micropor. Mater.* **1** (5) 345-351, 1993.
- [32] Hunger M. NMR Spectroscopy for the Characterization of Surface Acidity and Basicity, in Handbook of heterogeneous catalysis Volume 2, Ertl, G., et al. eds., Wiley-VCH, Weinheim, 2008, 1163-1178.
- [33] Knozinger, H. *Adv. Catal.* **25**, 185-201, 1976.
- [34] Huang, M., et al. *J. Catal.* **137**, (2), 322-332, 1992.
- [35] Sayed, Y.E. & Bandosz, T.Z. *Phys. Chem. Chem. Phys.* **5** (21), 4892-4898, 2003.
- [36] Tanabe, K., *Solid acids and bases*, Academic Press, NewYork, 1970.
- [37] Forni, L. *Cat. Rev.* **8**, (1), 65-115, 1974.

- [38] Tanabe, K. Misono, M. Hattori, H and Ono, Y. *New Solid Acids and Bases: Their Catalytic Properties*, Elsevier, Amsterdam, 1989.
- [39] Paul, M.A., & Long, F.A. *Chem. Rev.* **57** (1), 1-45, 1957.
- [40] Kappe, C.O. & Dallinger, D. *Mol. Divers.* **13** (2), 71-193, 2009.
- [41] Gedye, R., et al. *Tetrahedron Lett.* **27** (3), 279-282, 1986.
- [42] Giguere, R.J., et al. *Tetrahedron Lett.* **27**, (41) 4945-4948, 1986.
- [43] Surati, M.A., et al. *Arch. Appl. Sci. Res.*, **4** (1), 645-661, 2012.
- [44] Pal, A., et al. *Mater. Chem. Phys.* **114** (2-3), 530-532, 2009.
- [45] Hoogenboom, R. & Schubert, U.S. *Macromol. Rapid Commun.* **28** (4), 368-386, 2007.
- [46] Alcazar, J. & Oehlrich, D. *Future Med. Chem.* **2** (2) 169-176, 2010.
- [47] Zhu, Y. J. Microwave Heating: A Promising Method for Rapid Preparation of Inorganic Nanostructures, in *Nanotechnology Research: New Nanostructures, Nanotubes and Nanofibers*, Huang, X., eds., Nova Science publishers, 2008, 3-8.
- [48] Perreux, L., & Loupy, A. *Tetrahedron* **57** (45), 9199-9223, 2001
- [49] Gupta, M., et al. *Acta Chim. Slov.* **56** (4), 749-764, 2009.
- [50] Kingston, H.M. & Jassie L.B., in *Introduction to Microwave Sample Preparation, Theory and Practice*, Kingston H.M. & Jassie L.B. eds. American Chemical Society, Washington D. C., 1988, 110-122.
- [51] Baghurst, D. R., & Mingos, D. M. P. *J. Chem. Soc. Chem. Commun.* (9), 674-677, 1992.
- [52] Kappe, C.O. *Angew Chem. Int. Ed.* **43** (46), 6250-6284, 2004.
- [53] Laoupy, A. *C. R. Chim.* **7** (2), 103-112, 2004.
- [54] Li, C.J. & Chan, T.H. *Organic Reactions in Aqueous Media*, John Wiley & Sons, New York, 1997.
- [55] Li, C.J. *Chem. Rev.* **105** (8), 3095-3165, 2005.
- [56] Rideout, D.C. & Breslow, R., *J. Am. Chem. Soc.*, **102** (26), 7816-7817, 1980.
- [57] Breslow, R., et al., *Tetrahedron Lett.* **24** (18) 1901-1904, 1983.

- [58] Breslow, R., *Accounts Chem. Res.*, **24** (6) 159-170, 1991.
- [59] Blokzijl, W & Engberts, J.B.F.N., *Angew Chem. Int. Ed. Engl.*, **32** (11), 1545-1579, 1993.
- [60] A. Ben-Naim and J. Wilf, *J. Chem. Phys.* **70** (2), 771-777, 1979.
- [61] W. Kauzmann, *Adv. Protein Chem.* **14**, 1-63, 1959.
- [62] R. A. Pierotti, *Chem. Rev.* **76** (6), 717-726, 1976.
- [63] L. R. Pratt and D. Chandler, *J. Chem. Phys.* **67** (8), 3683-3704, 1977.
- [64] Strauss, C.R. et al., *Aust. J. Chem.*, **48** (11), 1665-1692, 1995.
- [65] Lidstrom, P., et al. *Tetrahedron* **57** (45), 9225-9283, 2001.
- [66] Weisz, P. B. & Frilette, *J. Phys. Chem.* **64** (3), 382, 1960.
- [67] Kogelbauer, A. & Prins, R. Zeolites, in *Encyclopedia of Chemical Physics and Physical Chemistry Volume III: Applications*, Moore, J.H. & Spencer, N.D. eds., Taylore and Francis, IOP Publishing, 2001.
- [68] Yang, S., et al. *J. Phys. Chem. Ref. Data* **39** (3), 033102-2-033102-45, 2010.
- [69] Flanigen, E.M., Broach, R.W. and Stephen T. Wilson Introduction, in *Zeolites in Industrial Separation and Catalysis*, Kulprathipanja, S. eds., Wiley-VCH, 2010.
- [70] Baerlocher C., Meier, W.M. and Olson, D.H., *Atlas of Zeolite Framework Types*, 5th ed., Elsevier Science, Amsterdam, 2001.
- [71] McCusker, L.B., et al., *Pure Appl. Chem.* **73** (2), 381-394, 2001.
- [72] Chakrabarty, D.K & Viswanathan, B. *Heterogeneous Catalysis*, New Age International (P) Ltd. Publishing, New Delhi, 2008.
- [73] Blauwhoff, P.M.M, Gosselink, J.W., Kieffer, E.P., Sie, S.T. and Stork W.H.J., Zeolites as Catalysts in Industrial Processes, in *Catalysis and zeolites Fundamentals and Applications*, Weitkamp, J & Puppe, L. eds., Springer, 1999.
- [74] Zhao, X. & Harding, R.H. *Ind. Eng. Chem. Res.* **48** (10), 3854-3859, 2009.
- [75] Weitkamp, J., et al. *Micropor. Mesopor. Mater.* **48** (1-3), 255-270, 2001.
- [76] Barthomeuf, D., *Stud. Surf. Sci. Catal.* **105**, 1677-1706, 1998.

- [77] Hung, M. & Kaliaguine, S. Catalytic behaviour of Lewis acid-base sites on alkali-exchanged zeolites, in *Heterogeneous Catalysis and Fine Chemicals III*, Guinset, M., et al., eds., Elsevier Science Publishers B.V., 1993, 559-566.
- [78] Barthomeuf, D., *Catal. Rev.-Sci. Eng.* **38** (4), 521-612, 1996.
- [79] Davis, R.J. *J. Catal.* **216** (1-2), 396-405, 2003.
- [80] Hathaway, P.E., & Davis, M.E. *J. Catal.* **116**, (1), 263-278, 1989.
- [81] Hathaway, P.E., & Davis, M.E. *J. Catal.* **116**, (1), 279-284, 1989.
- [82] Hathaway, P.E., & Davis, M.E. *J. Catal.* **119**, (2), 497-507, 1989.
- [83] Tsuji, H., et al. *Chem. Lett.* **20** (11), 1881-1884, 1991.
- [84] Yagi, F., et al. *Micropor. Mater.* **9**, (5-6), 237-245, 1997.
- [85] Wang, Y., et al. *Micropor. Mesopor. Mater.* **26**, (1-3), 175-184, 1998.
- [86] Arishtirova, K., et al. *Appl. Catal. A* **243**, (1), 191-196, 2003.
- [87] Lavalley, J.C. *Catal. Today* **27**, (3-4), 377-401, 1996.
- [88] Barthomeuf, D. *J. Phys. Chem.* **88** (1), 42-45, 1984.
- [89] Huang, M., & Kaliaguine, S. *J. Chem. Soc. Faraday Trans.* **88** (5), 751-758, 1992.
- [90] Xie, J., et al. *React. Kinet. Catal. Lett.* **58**, (4), 217-227, 1996.
- [91] Kim, J.C., et al. *Micropor. Mater.* **2**, (5), 413-423, 1994.
- [92] Okamoto, Y., et al. *J. Catal.* **112**, (2), 427-436, 1988.
- [93] Huang, M., et al. *J. Catal.* **137**, (2), 322-332, 1992.
- [94] Huang, M., et al. *J. Am. Chem. Soc.* **114**, (25), 10005-10010, 1992.
- [95] Choi, S.Y., et al. *J. Am. Chem. Soc.* **118**, (39), 9377-9386, 1996.
- [96] Doskocil, E.J., et al. *J. Phys. Chem. B* **103**, (30), 6277-6282, 1999.
- [97] Huang, M., et al. *J. Catal.* **157** (1), 266-269, 1995.
- [98] Bordawekar, S.V., & Davis, R.J. *J. Catal.* **189**, (1), 79-90, 2000.
- [99] Kheir, A.A., & Haw, J.F. *J. Am. Chem. Soc.* **116** (2), 817-818, 1994.
- [100] Sánchez-Sánchez, M., et al. *Phy. Chem. Chem. Phys.* **1** (18), 4529-4535, 1999.
- [101] Bosacek, V., et al. *Magn. Reson. Chem.* **37** (13), S135-S141, 1999.

- [102] Engelhardt, J., et al. *J. Catal.* **107** (2), 296-306, 1987.
- [103] Huang, M., et al. *J. Catal.* **157** (1), 266-269, 1995.
- [104] Hathaway, P.E. & Davis, M.E. *J. Catal.* **116** (1), 263-278, 1989.
- [105] Kim, J.C., et al. *Micropor. Mater.* **2** (5), 413-423, 1994.
- [106] Corma, A., et al. *J. Catal.* **126**, (1), 192-198, 1990.
- [107] Corma, A., et al. *Stud. Surf. Sci. Catal.* **59**, 503-511, 1991.
- [108] Ballini, R., et al. *J. Catal.* **191** (2), 348-353, 2000.
- [109] Wierzchowski, P.T., & Zatorski, L.W. *Catal. Lett.* **9**, (5-6), 411-414, 1991.
- [110] Kinage, A. K., et al. *Green Sust. Chem.* **1** (3), 76-84, 2011.
- [111] Khan, N.U.H., et al., *Tetrahedron Asymm.* **22** (1), 117-123, 2011.
- [112] Madhavi, G., et al. *J. Porous Mater.* **14** (4), 433-441, 2007.
- [113] Jianhua Z, Yuan C, Ying W, Qinhua X (1999) *Chinese Sci Bull* **44** (21), 1926-1934, 1999.
- [114] Murugan, C., et al. *Catal. Lett.* **137** (3-4), 224-231, 2010.
- [115] Khalilzadeh, M. A., et al. *Eur. J. Org. Chem.* **76** (6), 1587-1592, 2011.
- [116] Basudeb B, Das P, Das S (2008) *Curr Org Chem* **12** (2), 141-158, 2008.
- [117] Xie, W., & Huang X. *Catal Lett.* **107**, (1-2), 53-59, 2006.
- [118] Xie, W., et al. *Indust. Eng. Chem. Res.* **46**, (24), 7942-7949, 2007.
- [119] Xie W., et al. *Biores Technol* **98**, (4), 936-939, 2007.
- [120] Weinstock, L.M., et al. *Tetrahedron Lett.* **27**, (33), 3845-3848, 1986.
- [121] Ando, T., et al. *J. Chem. Soc. Perkin Trans.* **2** (8), 1133-1139, 1986.
- [122] Clerk, J.H., et al. *Chem. Lett.* **12** (8), 1145-1148, 1983.
- [123] Bergbreider, D.E., & Lalonde, J.J. *J. Org. Chem.* **52**, (8), 1601-1603, 1987.
- [124] Ando, T., *Stud. Surf. Sci. Catal.* **90**, 117-128, 1994.
- [125] Yamaguchi, T., et al. *Chem. Lett.* (10), 989-990, 1997.
- [126] Zhu, J.H., et al. *Micropor Mesopor Mater.* **24**, (1-3), 19-28, 1998.
- [127] Barthomeuf, D., et al. *Mat. Chem. Phys.* **18**, (5-6), 553-575, 1988.
- [128] Ono, Y. *Stud. Surf. Sci. Catal.* **5**, 19-27, 1980.
- [129] Clark, J.H. *Chem. Rev.* **80**, (5), 429-452, 1980.

- [130] Yamawaki, J., & Ando, T. *Chem. Lett.* **8** (7), 755-758, 1979.
- [131] Sun, L.B., et al. *Catal Lett* .**132** (1-2), 218-224, 2009.
- [132] Zianhua, Z. *Chem. Sci. Bull.* **42** (17), 1493-1494, 1997.
- [133] Zhu, J.H., et al. *Mater.Lett.* **33** (3-4), 207-210, 1997.
- [134] Chen, L., et al. *RSC Adv.* **3** (12), 3799-3814, 2013.
- [135] Jo, Y.B., et al. *Appl. Eng. Chem.* **23** (6), 604-607, 2012.
- [136] Luzzio, F.A. *Tetrahedron* **57** (6), 915-945, 2001.
- [137] Henry, L. C. R. *Acad. Sci. Ser. C.* **120**, 1265-1267, 1895.
- [138] Henry, L. *Bull. Soc. Chim. Fr.* **13**, 999, 1895.
- [139] Palomo, C., et al. *Eur. J. Org. Chem.* **72** (16), 2561-2574, 2007.
- [140] Ballini, R., & Bosica, G. *Eur. J. Org. Chem.* (2), 355-357, 1998.
- [141] Sasai, H., et al. *Tetrahedron Lett.* **35** (33), 6123-6126, 1994.
- [142] Kawabata, T., et al. *Tetrahedron Lett.* **34** (32), 5127-5130, 1993.
- [143] Kudyaba, I. et al., *Tetrahedron Lett.* **44** (48), 8685-8687, 2003.
- [144] Misumi, Y., & Matsumoto, K. *Angew. Chem. Int. Ed.* **41** (6), 1031-1033, 2002.
- [145] Grembecka, J., & Kafarski, P. *Mini Rev. Med. Chem.* **1** (2), 133, 2001.
- [146] Hanessian, S., & Rloss, J. *Tetrahedron Letters.* **26** (1), 1261-1264, 1985
- [147] Klein, G., et al. *Tetrahedron Lett.* **43** (42), 7503-7506, 2002.
- [148] Sohtome, Y., et al. *Synlett.* (1), 144-146, 2006.
- [149] Iseki, K., et al. *Tetrahedron Lett.* **37** (50), 9081-9084, 1996.
- [150] Fieser, L. F., & Fieser, M. *In Reagents for Organic Synthesis, Wiley: New York.* **1**, 739, 1967.
- [151] Forsyth, A.C. et al., *Tetrahedron Lett.* **30** (8), 993-996, 1989.
- [152] Simoni, D. et al., *Tetrahedron. Lett.* **38** (15), 2749-2752, 1997.
- [153] Luzzio, F.A., & Fitch, R.W. *Tetrahedron Lett.* **35** (33), 6013-6016, 1994.
- [154] Kisanga, P. B., & Verkade, J. G. *J. Org. Chem.* **64** (12), 4298-4303, 1999
- [155] Youn, S. W., & Kim, Y. H. *Synlett* (**6**), 880-882, 2000.
- [156] Ballini, R., & Bosica, G. *Tetrahedron* **52** (5), 1677-1684, 1996.
- [157] Majhi, A., et al. *Bull. Korean Chem. Soc.* **30** (8) 1767-1770, 2009.

- [158] Weeden, J.A., & Chisholm, J.D. *Tetrahedron Lett.* **47** (52), 9313-9316, 2006.
- [159] Desai, U.V., et al, *Synth. Commun.* **34** (1), 19-24, 2004.
- [160] Morao, L., & Cossio, F. P. *Tetrahedron Lett.* **38** (36), 6461-6466, 1997.
- [161] Yi W., et al. *Catal Commun* **8** (12), 1995-1998, 2007.
- [162] Ballini R., et al. *Green Chem* **9** (8), 823-838, 2007.
- [163] Li, C. *Chem Rev* **105** (8), 3095-3166, 2005.
- [164] Tang, R.C., et al. *J Mol Catal B: Enzym* **63** (1-2), 62-67, 2010.
- [165] Ballini, R., & Bosica, G. *J. Org. Chem.* **59** (18), 5466-5467, 1994.
- [166] Ballini, R., et al. *J. Org. Chem.* **73** (21), 8520-8528, 2008.
- [167] Choudary, B. M. *Green Chem.* **1** (4), 187-189, 1999.
- [168] Ballini, R., et al. *Tetrahedron* **52** (5), 1677-1684, 1996.
- [169] Wang, X., & Cheng, S. *Catal. Commun.* **7** (9), 689-695, 2006.
- [170] Bulbule, V.J., et al. *Tetrahedron* **55** (30), 9325-9332, 1999.
- [171] Mayani, V.J., et al. *J Org Chem* **75** (18), 6191-6195, 2010.
- [172] Keller, T.C. *Chem. Sci.* **5** (2), 677-684, 2014.
- [173] Jones, M. D., et al. *Angew. Chem., Int. Ed.* **42** (36), 4326-4331, 2003.
- [174] Corma, A., & Garcia, H. *Chem.Rev.* **103** (11), 4307-4365, 2003.
- [175] Anan, A., et al. *J. Mol. Catal. A: Gen.* **288**, (1-2), 1-13, 2008.
- [176] Huh, S., et al. *J. Am. Chem. Soc.* **126** (4), 1010-1011, 2004.
- [177] Varma, R.S., et al. *Tetrahedron Lett.* **38** (29), 5131-5134, 1997.
- [178] Gan, C., et al. *Synlett* (3), 387-390, 2006.
- [179] Ballini, R., et al. *Med. Chem. Lett.* **28** (10), 1105-1106, 1999.
- [180] Kumar, S., et al. *Chem. Lett.* **27** (7) 637—638, 1998.
- [181] Costantino, U., et al. *J. Mol. Catal. A: Chem.* **195** (1-2), 245-252, 2003.
- [182] Cavani, F., et al. *Catal. Today* **11** (2), 173-301, 1991.
- [183] Reichle, W. T. *Solid State Ionics* **22** (1), 135-141, 1986.
- [184] Zhang, F., et al. *Catal. Surv. Asia.* **12** (4), 253-265, 2008.
- [185] Suzuki, E., et al. *J. Mol. Catal.* **61** (3), 283-294, 1990.
- [186] Yun, O. et al. *Adv. Mater. Res.* **174**, 362-365, 2010.

- [187] Palomares, A. E., et al. *J. Catal.* **221** (1), 62-66, 2004.
- [188] Bulbule, V.J., et al. *Tetrahedron.* **55** (30), 9325-9332, 1999.
- [189] Kim, M.J., et al. *Fuel. Proc. Technol.* **91** (6), 618-624, 2010.
- [190] Corma, A., et al. *J. Catal.* **234** (2), 340-347, 2005.
- [191] Erickson, K.L., et al. *Mater. Lett.* **59** (2-3), 226-229, 2005.
- [192] Ebitani, K., et al. *J. Org. Chem.* **71** (15), 5440-5447, 2006.
- [193] Mokhtar, M., et al., *J. Mol. Cat. A: Chem.* **353-354**, 122-131, 2012.
- [194] Tichit, D., et al. *J. Catal.* **151** (1), 50-59, 1995.
- [195] Li, F. & Duan, X. Applications of Layered Double Hydroxides, in *Struct. Bond.* Springer, **119**, 193-223, 1996.
- [196] Sharma, Y. C., et al. *Fuel* **90** (4) 1309-1324, 2011.
- [198] Tietze, L.F. *Chem. Rev.* **96**, 329, 2006.
- [199] Jones G, The Knoevenagel condensation reaction. in *Organic Reactions*, Wiley: New York, 1967, 15, 204.
- [200] Knoevenagel, F. *Ber.*, **29**, 172, 1896.
- [201] Doebner, O. Synthese der Sorbinsäure. *Berichte der Deutschen Chemischen Gesellschaft*, **33** (2) 2140-2142, 1990.
- [202] Khan, F.A., et al., *Tetrahedron. Lett.* **45** (15), 3055-3058, 2004.
- [203] Tietze L. F., *Pure. Appl. Chem.* **76** (11), 1967-1983, 2004
- [204] Ono, Y. *J. Catal.* **216** (1-2), 406-415, 2003.
- [205] McCluskey, A., et al. *Tetrahedron Lett.* **43** (17), 3117-3120, 2002.
- [206] Gawande, M.B., et al. *Catal. Commun.* **7** (12), 931-935, 2006.
- [207] Corma, A., et al. *J. Catal.* **126** (1), 192-198, 1990.
- [208] Kloetstra, K.R., et al. *Catal. Lett.* **47**, (3-4), 235-242, 1997.
- [209] Kloetstra, K.R., et al. *Stud. Surf. Sci. Catal.* **105** 431-438, 1997.
- [210] Corma, A., & Martin-Aranda, R.M. *Appl. Catal. A: Gen.* **105** (2), 271-279, 1993.
- [211] Kerr, G.T., & Shipman, G.F. *J. Phys. Chem.* **72** (8), 3071-3071, 1968.
- [212] Zhang, X., et al. *Appl. Catal. A: Gen.* **261** (1), 109-118, 2004.
- [213] Bigi, F., et al. *Green Chem.* **2** (3), 101-103, 2000.

- [214] Wang, G. W. & Cheng, B. *ARKIVOC* (ix), 4-8, 2004.
- [215] Bonathu, V. et al., *J. Chem. Pharma. Res.* **5** (10), 97-101, 2013.
- [216] Ono, Y. & Baba, T. *Catal. Today* **38** (3), 321-337, 1997.
- [217] Busca, G. *Chem. Rev.* **110** (4), 2217-2249, 2010.
- [218] Kantam, M. L., et al. *Chem. Commun.* 1033-1034, 1998.
- [219] Ebitani, K., *J. Org. Chem.* **71** (15), 5440-5447, 2006.
- [220] Choudary, B. M., et al. *Tetrahedron* **56** (47), 9357-9364, 2000.
- [221] S. Coluccia, A. J. Tench, Proc. 7th Intern. Cong. Catal., Tokyo, 1980, p. 1160
- [222] H. Hattori, *Chem. Rev.*, **95** (3), 537-558, 1995.
- [223] Wang, W., et al. *Mater. Lett.* **61** (14-15), 3218-3220, 2007.
- [224] Zhao, J., et al. *J. Mater. Chem.* **22**, 19678-19683, 2012.
- [225] Llanos, M. E., & Lopez-Salinas, E. *J. Phys. Chem. B*, **101** (38), 7448-7451, 1997.
- [226] He, Y. *Mater. Lett.* **60** (29-30), 3511-3513, 2006.
- [227] Zhang, Y., et al. *J. Alloy Compounds* **590**, 73-79, 2014.
- [228] Fan, W., et al. *J. Solid State Chem.* **177** (7), 2329-2338, 2004.
- [229] K. Byrappa, M. Yoshimura, Handbook of Hydrothermal Technology, Noyes Publications, New Jersey, USA, 2001.
- [230] Morey, G. W., & Niggli, P. *J. Am. Chem. Soc.*, **35** (9), 1086-1130, 1913
- [231] Roy, R. *J. Solid State Chem.* **111** (1), 11-17, 1994.
- [232] A. Rabenau, The Role of Hydrothermal Synthesis in Preparative Chemistry, *Angew. Chem.*, **24**, 1026-1040, 1985.
- [233] M. Yoshimura and H. Suda, *Hydrothermal Processing of Hydroxyapatite: Past, Present, and Future*, in: *Hydroxyapatite and Related Materials*, CRC Press, 45-72, 1994.
- [234] K. Byrappa, *Hydrothermal Growth of Crystals*, pp., Pergamon Press, Oxford, UK, 1992, 1-365
- [235] Schäf, O.; Ghobarkar, H; Knauth, P. In; Knauth, P.; Schoonman, J. Ed., *Nanostructured Materials: Selected Synthesis Methods, Properties and Applications*, Kluwer Academic Publishers: Boston, 2002, 23-42.
- [236] Ghosh, M., et al, *J. Nanosc. Nanotechnol.* **4** (1-2), 136-140, 2004.

- [237] Pinna, N., et al, *J. Am. Chem. Soc.*, **127** (15), 5608-5612, 2005.
- [238] Rao, C.N.R., et al. *Dalton Trans.* 3728-3749, 2007.
- [239] Mastuli, M.S., et al. *APCBEE. Procedia* **3** (), 93-98, 2012.
- [240] Phillips, V.A., et al. *J. Cryst. Growth* **41** (2), 228-234, 1977.
- [241] Aramendia, M.A., et al., *J. Mater. Chem.* **6** (12), 1943-1949, 1996.
- [242] Stark, J.V. & Klabunde, K.J., *Chem. Mater.* **8** (8), 1913-1918, 1996.
- [243] Hao Z., & Du, F. *J. Phys. Chem. Solids* **70** (2), 401-404, 2009.
- [244] Yan X., et al. *Acta Mater.* **55** (17), 5747-5757, 2007.
- [245] Sutradhar, N., et al., *Mater. Res. Bull.* **46** (11), 2163-2167, 2011.
- [246] Yan, C., & Xue, D. *J. Phys. Chem. B* **209** (25), 12358-12361, 2005.
- [247] Sandengen, K., et al. *Ind. Eng. Chem. Res.* **47** (4), 1002-1004, 2008.
- [248] Sutradhar, N., et al., *J. Phys. Chem.* **115** (25), 12308-12316, 2011.
- [249] Ding, Y., et al. *Chem. Mater.*, **13** (2), 435-440, 2001.
- [250] Jeevanandam, P., et al, *Chem. mater.* **19** (22), 5395-5403, 2007.
- [251] Li, Y., et al. *Adv. Mater.* **12** (11), 818-821, 2000.
- [252] Zhuo, L., et al, *Cryst. Growth. Design.* **9** (1), 1-6, 2009.
- [253] Makhluif, B.S., et al., *Adv. Funct. Mater.* **15** (10), 1708-1715, 2005.
- [254] Aslani, A., et al., *Appl. Surf. Sc.*, **257** (11), 4885-4889, 2011.
- [255] Bain, S.W., et al. *J. Phys. Chem. C* **112** (30), 11340-11344, 2008.
- [256] Choudary, B.M., et al. *J. Am. Chem. Soc.* **127** (38), 13167-13171, 2005.
- [257] Seki, T. & Hattori, H. *Catal. Surv. Asia* **7** (2-3), 145-156, 2003.
- [258] Hathaway, B. A. *J. Chem. Educ.* **64** (4) 367, 1987.
- [259] Rajput, J.K. & Kaur, G. *Tetrahedron Lett.* **53** (6), 646-649, 2012.
- [260] Selvamani, T. et al., *Mater. Chem. Phy.* **129**, 853-886, 2011.

Chapter 2

Materials and details of experimental methods

This chapter covers the details of all chemicals and experimental techniques that have been used in the study. The procedures for chemical reactions, method of sample preparation along with their characterization techniques are described herein.

2.1 Materials used

The chemicals used in the present study and the suppliers are listed below

- (a) Chemicals: The important chemicals used in the study include NH₄Y zeolite, NaY zeolite, Mg(NO₃)₂·6H₂O, Al(NO₃)₂·9H₂O, KNO₃, KOH, K₂CO₃, KHCO₃, KF, organic reactants and reagents. All the chemicals and solvents used were analytical grade and purchased from Merck India, Sigma Aldrich (India), RANKEM India and Hi-media laboratories.

2.2 Preparation of catalysts

2.2.1 Preparation of KF loaded NaY and KL zeolites

At first NH₄⁺ ion of NH₄Y zeolite were exchanged with Na⁺ ion to get NaY zeolite. In the procedure, 5 g of NH₄Y zeolite was stirred with 100 mL of 1M NaNO₃ solution at 90 °C for 6 hours. The exchanged zeolites were then filtered and again stirred with fresh NaNO₃ solution. This procedure was repeated for 4 times. The zeolite was filtered, washed and dried in air for 48 h followed by drying in an oven at 110 °C for overnight. Similarly, KL zeolite was also dried at 110 °C prior to loading. The KF loaded NaY and KL basic zeolites were prepared by wet impregnation method from an aqueous solution of KF [1]. Here, 5 wt % (0.40 mmol) of KF was dissolved in 4 ml distilled water and added 500 mg of zeolite in it. The mixture was stirred for 24 h and the slurries obtained were dried in air followed by dried in an oven at 100° C for 14 h. After proper drying, the obtained zeolites were calcined at 450 °C for 6 h. The catalysts were named as KF/NaY and KF/KL. Different weight percentages (wt %) of KF was impregnated over sodium form of zeolite Y. In this procedure, KF amounts of 0.5, 1, 2, 3, 5, 10, 15 and 20 % KF (w/w) were impregnated over NaY zeolite by the same procedure as described above. Impregnation was carried out for 24 h and slurries were dried in air followed by drying in oven at 100 °C for overnight and finally calcined at 450 °C for 6 h.

2.2.2 Preparation of MgAl-Hydrotalcite

Magnesium aluminium carbonate (MgAl-CO₃) hydrotalcite was prepared according to the procedure reported by Nyambo et al. [2]. In the method, a solution containing 38.46 g Mg(NO₃)₂·6H₂O (0.15 mol) and 18.75 g Al(NO₃)₂·9H₂O (0.05 mol) in 125 ml distilled water was added drop wise to a solution containing 14 g NaOH (0.35 mol) and 15.9g Na₂CO₃ (0.1 mol) in 145 ml deionized water with vigorous stirring over 1 hour at pH 10-12. The solution was kept stirring vigorously for another 1 h. The white precipitate formed was aged for 24 h at 65 °C, cooled to room temperature, filtered and washed several times with distilled water until the filtrate becomes neutral. Finally, the precipitate was dried at 80 °C for 15 h to get MgAl-Hydrotalcite.

2.2.3 Preparation of MgAl-mixed oxides [MgAl(O)]

Hydrotalcites synthesized by the procedure described in Section 2.2.2 were calcined at 450 °C and 550 °C for 6 h in a muffle furnace to obtain MgAl-mixed oxides i.e. MgAl(O).

2.2.4 Preparation of potassium salt loaded MgAl-Hydrotalcites

The potassium salt modified hydrotalcites (HT) containing same amount of potassium ions were prepared by a wet impregnation method reported earlier. In the method, a solution of the metal salt containing 1mmol of the salt (except for K₂CO₃ where 0.5 mmol was taken) in 5 ml deionized water was stirred with 500 mg calcined hydrotalcite (450 °C) for 24 h and the slurries were dried at air followed by oven drying at 80 °C for 15 h to obtain the loaded catalysts. The loaded samples were denoted as KNO₃/HT, KOH/HT, K₂CO₃/HT, KHCO₃/HT and KF/HT. Following the same procedure, 15 %-40 % KOH /HT were prepared by taking appropriate quantity of KOH and the support.

2.2.5 Preparation of potassium salt loaded MgAl mixed oxides

Different potassium salt loaded MgAl mixed oxides were prepared by calcinations of hydrotalcites as described in Section 2.2.4. were calcined at 450 °C and 550 °C for 6h. The catalysts were named as KF/MgAl(O), KOH/MgAl(O), KNO₃/MgAl(O), K₂CO₃/MgAl(O) and KHCO₃/MgAl(O).

2.2.6 Synthesis of MgO by hydrothermal method

In a typical procedure, 40 mL of 1M NaOH in water (Solution B) was added dropwise to 40 mL of 0.1 M $\text{Mg}(\text{NO}_3)_2 \cdot 6\text{H}_2\text{O}$ solution in water (Solution A) with constant stirring. After addition, the solution mixture was kept stirring for half an hour and pH was recorded. The resultant solution was then transferred to a 250 mL stainless steel autoclave and kept in a preheated oven at 120 °C for 6 h. After completion of the treatment, the autoclave was cooled to room temperature, recovered the precipitate by centrifugation washed with distilled water and acetone for several times until the filtrate becomes neutral and finally dried at 50 °C overnight to get MgO precursors. Three bases namely urea, NaOH and Na_2CO_3 were used and three molar ratio of base versus $\text{Mg}(\text{NO}_3)_2 \cdot 6\text{H}_2\text{O}$ salt i.e. 0.1:1, 1:1 and 10:1 were used and the samples were in the text as MgO-U-0.1, MgO-U-1, MgO-U-10; MgO-OH-1, MgO-OH-10 and MgO-CO-1, MgO-CO-10 respectively according to their ratio with the salt used in the synthesis .

2.2.7 Synthesis of MgO by solvothermal method

In this procedure, 0.1 M $\text{Mg}(\text{NO}_3)_2 \cdot 6\text{H}_2\text{O}$ was dissolved in 20 ml water and added 20 ml solvent in it to get solution A. Solution B was containing 1M NaOH in 40 mL water was then added dropwise to solution A with constant stirring. The solution was kept stirring for half an hour and pH was recorded. The resultant solution was then transferred to a 250 mL stainless steel autoclave and kept in a preheated oven at 120 °C for 6 h. The autoclave was then cooled to room temperature, recovered the precipitate by centrifugation followed by washing with distilled water and acetone until the filtrate became neutral. The precipitate was finally dried at 50 °C overnight to get MgO precursors. Three solvents namely ethanol, ethylene glycol and glycerol were used with urea base and designated as MgO-U-Et, MgO-U-EG and MgO-U-Gly.

2.3. Details of equipments used for characterization of materials and organic compounds

2.3.1 X-ray diffraction (XRD) analysis

Powder X-ray diffraction analysis of all the prepared samples were done by a Rigaku (miniflex UK) X-ray diffractometer with $\text{Cu K}\alpha$ radiation of 1.5418 Å at a scan speed 7° min^{-1} and 2θ range from 5–70° at 30 kV and 15mA.

2.3.2 Fourier transformed infrared spectroscopy (FTIR) study

FTIR spectra of various catalysts were recorded on a Nicolet Impact Model-410 spectrometer with 1 cm^{-1} resolution and 32 scans in the mid IR ($400\text{--}4000\text{ cm}^{-1}$) region using the KBr pellet technique. The samples were finely ground before analysis.

2.3.3 Scanning electron microscopy (SEM)

The SEM measurements of the catalysts were carried out using a JEOL JSM-6390LV Scanning Electron Microscope at an accelerator voltage of 15 kV. The magnification of the micrographs ranges from $4000\times\text{--}10,000\times$. The surface of the catalyst samples were coated with Platinum prior to taking images.

2.3.4 Thermogravimetric analysis

Thermogravimetric analyses were performed by using Simadzu Thermogravimetric Analyser (TA-50) in the temperature range $25\text{--}600\text{ }^{\circ}\text{C}$ at a heating rate $10\text{ }^{\circ}\text{C}/\text{min}$. The analyses were performed under nitrogen atmosphere using $10\text{--}15\text{ mg}$ sample.

2.3.5 Differential Scanning Calorimetric analysis

Differential scanning calorimetric analyses were performed by Shimadzu Differential Scanning Calorimeter (DSC-60) in temperature range $25\text{--}300\text{ }^{\circ}\text{C}$ at a heating rate $10\text{ }^{\circ}\text{C}/\text{min}$. The analyses were performed under nitrogen atmosphere using $10\text{--}15\text{ mg}$ sample.

2.3.6 Surface area measurement

The specific surface areas, pore volume and pore sizes were determined from N_2 adsorption-desorption isotherms by Brunaur-Emmett-Teller method using a Quantachrome NOVA 1000e Surface area and Pore Size Analyzer at liquid N_2 temperature i.e. $-196\text{ }^{\circ}\text{C}$. Pore volume and pore size distributions were calculated by using Barrett-Joyner-Halenda (BJH) equation from the amount desorbed at a relative pressure of about $0.05\text{--}1$ by using N_2 desorption branches of the isotherm.

2.3.7 Nuclear Magnetic Resonance (NMR) spectroscopic study

Structural characterization of the organic compounds was carried out by taking ^1H NMR and ^{13}C NMR in a JEOL JNM-ECS400 NMR spectrometer taking Me_4Si as the internal standard and CDCl_3 and CD_3OD as solvents.

2.4 Procedures of physicochemical analyses

2.4.1 Relative Crystallinity (%) Study

The Relative Crystallinity (%) of the as synthesized and modified samples were determined by integrating the XRD peaks by using the following formula,

$$\text{Relative Crystallinity (\%)} = (A_S \times 100)/A_R,$$

Where,

A_R = Integrated area of the reference material under the peaks between a set of 2θ limits,

A_S = Integrated area of the sample under the peaks between the same set of 2θ limits as that of the reference.

2.4.2 Determination of crystallite size

The crystallite sizes were determined by X-ray line broadening method considering particular reflection planes and using the Debye-Scherrer equation [3],

$$t = 0.89 \lambda / \beta \cos\theta,$$

where, t is the crystallite size, λ is the X-ray wavelength, β is the full width at half maximum (FWHM) in radian and θ is the angle of diffraction or Bragg's angle.

2.4.3 Measurement of Basic properties

Measurement of basic nature of the catalyst samples were measured both qualitatively and quantitatively by Hammett indicator method and acid-base titration method as described below.

(a) Hammett indicator method

Qualitative determination of strength of basic sites of all catalysts was done by Hammett indicator method reported by a standard literature method [4]. The Hammett indicators used were: neutral red ($H_L = 6.8-8.0$), phenolphthalein ($H_L = 8.0-9.6$), Nile blue ($H_L =$

10.1–11.1), Tropaeolin-O ($H_L = 11.1–12.7$), 2, 4-dinitroaniline ($H_L = 15$) and 4-chloro-2-nitroaniline ($H_L = 17.2$). In the procedure, 1 mL indicator solution (0.1 % in methanol) was added to 25 mg of catalyst at first. The mixture was shaken well, allowed to equilibrate for 2 h and then the color of the catalysts was noted. The base strengths have been reported as stronger than the weakest indicator which exhibits a colour change and weaker than the strongest indicator which exhibit no colour change [5].

(b) Acid-base titration method

The total basicities of the catalysts were determined by titration with benzoic acid. In this method, a suspension of calcined solid (0.15 g) in a toluene solution of phenolphthalein (2 ml, 0.1mg/ml) was stirred for 30 minutes and titrated with a toluene solution of benzoic acid (0.01M).

The leachable basicities were determined by two different methods. In the first method [6, 7] (for parent and modified zeolites), 100 mg of calcined sample was shaken in 10 mL water at room temperature for 24 h and the catalyst was separated by centrifuge. The filtrate containing soluble basicities was neutralized with 10 ml aqueous HCL (0.05M). The remaining acid in the filtrate was titrated with 0.01 M standard aqueous NaOH. Oxalic acid dihydrate was used for standardization of NaOH and a methanol solution of phenolphthalein (1 mL, 0.1mg/mL) was taken as indicator. In the second method (for hydrotalcites), 100 mg of calcined catalyst was added to 10 mL water and the mixture was shaken well at room temperature for 1h. The catalyst was filtered off; a methanol solution of phenolphthalein (1 mL, 0.1 mg/mL) was added to the filtrate and titrated with a methanol solution of benzoic acid (0.01 M).

2.5 Typical procedures of catalytic reactions

2.5.1 Henry (Nitroaldol) reaction under classical condition

In the procedure, 1 mmol of aldehyde and 2 mmol nitroalkane was stirred with 2 ml solvent and 20 mg KF/NaY in a beaker at room temperature. The progress was monitored via thin layer chromatography technique, extracted the organic portions with ethyl acetate, dried over Na_2SO_4 and concentrated over vacuum to get the crude product. Conversions were obtained from 1H NMR analyses of the crude reaction mixture. The

yields were purified through preparative column chromatography and thin layer chromatography technique.

2.5.2 Henry (Nitroaldol) reaction under microwave irradiation condition

All catalytic reactions were performed in “Catalyst system Scientific Microwave systems” scientific microwave reactor having power output 700 Watt (2450 MHz), power levels from 140-700 Watt and automatic temperature sensors with flexible probe upto 600 °C. In a typical procedure of synthesis of β -nitroalcohols, 0.015 g of calcined catalyst (450 °C) was added to a mixture of 1 equivalent aldehyde, 4 equivalent nitromethane and 3 mL solvent in a long necked special microwave flask fitted with a reflux condenser at 280 watt (40 % of 700 watt) microwave power and at 50 °C. The progress was monitored by thin layer chromatography, stopped after completion and cooled to room temperature. Organic portion was then extracted with ethyl acetate, dried over anhydrous sodium sulphate (Na_2SO_4) and concentrated under vacuum to obtain the crude product. The product was then purified by thin layer chromatographic technique and analyzed by ^1H and ^{13}C NMR techniques. The conversions and selectivity were calculated on the basis of integration of ^1H NMR signals of the reactants and products from crude reaction mixture. Catalysts were recovered by centrifuge, dried at 100 °C for overnight calcined and reused. Catalytic activities of the recovered catalysts were then checked under similar reaction conditions.

2.5.3 Knoevenagel condensation under classical condition

Knoevenagel condensation reaction was carried out in a 50 ml round bottomed flask at room temperature. In the procedure, 0.025 g catalyst was added to a mixture of 1 mmol aldehyde, 1 mmol active methylene compound and 3 ml DMF at room temperature, stirred for the required time and monitored by thin layer chromatography. The catalysts were oven dried at 80 °C for 12 h before using. After completion of reaction, the product was extracted with ethyl acetate, dried over anhydrous Na_2SO_4 , evaporated, purified and finally analyzed by ^1H NMR and ^{13}C NMR (JEOL JNM-ECS 400) taking Me_4Si as the internal standard and CDCl_3 as solvent. The used catalysts were washed several times

with acetone, dried and then reused. The conversions (%) were determined from integration of ^1H NMR signal of the crude reaction mixtures.

2.5.4 Knoevenagel condensation under microwave irradiation condition

In the procedure, Knoevenagel reaction was carried out in the microwave vessel (given specifications in 2.5.2) fitted with a water condenser by adding 1 mmol aldehyde, 1 mmol malononitrile, 3 ml DMF and 0.030 g $\text{KNO}_3/\text{MgAl}(\text{O})$. The mixture was stirred vigorously under microwave irradiation at 350 Watt and 50 °C for the required time and the progress was monitored by TLC. After completion of the reaction, DMF was evaporated, diluted the mixture with ethyl acetate and catalysts was separated by centrifugation. Ethyl acetate was then evaporated to get the crude product. The purity was checked by ^1H NMR, ^{13}C NMR and FTIR techniques. The separated catalysts were washed several times with acetone, dried, calcined again at 723 K and reused.

2.5.5 Claisen-Schmidt condensation under classical condition

The reaction was carried out in a two neck round bottomed flask taking 1mmol aromatic aldehyde, 1 mmol acetophenone and 35 mg MgO . The mixture was stirred at 130 °C in an oil bath for the required time and the progress was monitored by TLC (8:1 hexane/ethyl acetate). After completion of the reaction, the catalyst was separated from the mixture, washed several times with acetone, dried, calcined again at 500 °C and then reused. The mixture was extracted with ethyl acetate, dried, evaporated and purified by thin layer chromatography technique with hexane/ ethyl acetate as moving phase. The purity was and then checked by ^1H NMR, ^{13}C NMR and FTIR techniques.

2.5.6 Claisen-Schmidt condensation under microwave irradiation condition

The reaction was carried out in a special microwave flask by taking 1mmol aromatic aldehyde, 1 mmol acetophenone and 35 mg MgO . The mixture was stirred at 80 °C under 490 Watt microwave power for the required time and the progress was monitored by TLC (hexane/ethyl acetate). After completion of the reaction, the catalyst was separated from the mixture, washed several times with acetone, dried, calcined again at 500 °C and then reused. The mixture was extracted with ethyl acetate, dried, evaporated and purified by

thin layer chromatography technique with hexane/ethyl acetate as moving phase. The purity was then checked by ^1H NMR, ^{13}C NMR and FTIR techniques.

2.6 Theoretical Calculations

For the theoretical part, Density functional calculations were performed using DMol³ program package [8,9] as implemented in the Materials Studio program system. Geometry optimization was done by treating the exchange-correlation interaction with generalized gradient approximation (GGA) using the Perdew, Burke, and Ernzerhof (PBE) functional [10]. We have used the double numerical with polarization (DNP)¹ basis set for our calculations. The PBE functional has demonstrated reliable for predicting structures of inorganic oxides and it is one of the most universally applied GGA functional [11].

2.5 References

- [1] Zhu, J. H., et al. *Chem. Commun.* (16),1889-1890, 1996.
- [2] C. Nyambo, et al., *J. Mater. Chem.* **18** (40) , 4827-4838, 2008.
- [3] Rodrigues, E., et al., *Mater. Lett.* **78** , 195-198, 2012.
- [4] Fraile, J.M. et al., *Appl. Catal. A: Gen* **364** (1-2), 87-94, 2009.
- [5] Cantrell, D. G. et al., *Appl. Catal. A: Gen.* **287** (2), 183-190, 2005.
- [6] Sun, L. B., et al. *Catal. Lett.* **132** (1-2), 218-224, 2009.
- [7] Sun, L. B., et al. *Micropor. Mesopor. Mater.* **116** (1-3), 498-503, 2008.
- [8] Delley, B., *J. Chem. Phys.* **92** (1), 508-517, 1990.
- [9] Delley, B., *J. Chem. Phys.* **113** (18), 7756-7764, 2000.
- [10] Perdew, J.P., et el. *Phys. Rev. Lett.* **77** (18), 3865-3868, 1996.
- [11] Bleken, F., et al. *J. Phys. Chem. A* **114** (15), 7391-7397, 2010.

Chapter 3

Design of Zeolite catalysts for Henry reaction

Section 3A: Modification of NaY and KL zeolites by potassium fluoride and their application for Henry reaction under mild condition

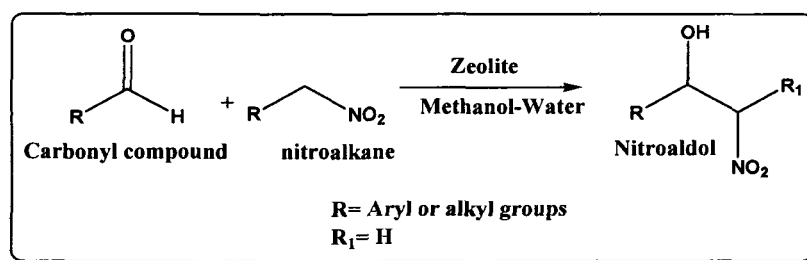
Zeolites possessing aluminosilicate compositions and varieties of pore architecture are considered as exciting materials in the industry due to their peculiar shape selectivity, thermal stability and catalytic properties [1-4]. Porous nature, large surface area and porous channels with different dimensions are additional advantages in their structures which can accommodate different guest species over their structures and thus play important role in benign catalytic processes [5-10]. It is found that zeolites and modified zeolites can efficiently catalyze a good number of acid and base catalyzed organic reactions [11,12]. However, base catalyzed reactions are not widely studied in comparison to acid catalyzed reactions. Moreover, zeolites as solid bases have got limitations due to their weak base strengths and difficulty in generating strong basic sites owing to the presence of Si-components, for which modification of zeolites to generate strong basicity is important in the area of base catalysis [13-15]. Success in this field has been achieved through exchanging extra-framework cations of zeolites by other metal cations or introducing various basic precursors like alkali or alkaline earth salts into their structures and subsequent activation at high temperatures [16-20]. However, the common problem encountered during this process is the collapse of zeolite framework structure during loading and activation process [21,22]. Therefore, increase of basic character along with perseverance of zeolite framework structure is challenging in the field of catalysis.

Henry reaction offers β -nitroaldol as the condensation product which can be transformed into compounds like aminoalcohols, aminoketones, nitoalkenes etc. and thus act as versatile intermediates for synthesis of various biological, pharmaceutical and fine chemical products [23-29]. Selectivity of Henry reactions have been found successful in the previous studies by single site or multiple site functionalization of mesoporous silica based materials such as SBA-15 or MCM-41 [30-33] and use of varied reaction conditions like supercritical CO₂ [34,35] as solvent and application of ultrasound to

[Chapter 3]

promote reactions [36]. Zeolite, due to its peculiar shape selectivity and mild basicity are expected to catalyze Henry reaction selectively. Therefore, we aimed to study Henry reaction with these modified zeolites by varying different reaction parameters to understand their catalytic activities.

This part of the thesis describes the modification of NaY and KL zeolites from aqueous solution of KF, change of structural and basic properties after modification and their catalytic activities towards Henry reaction under mild conditions. The results of XRD, FTIR, N₂ adsorption-desorption, Hammett indicator method and acid base titration methods have also been described herein. We have also included the results of optimization of reaction parameters such as temperature, solvents, amount of catalysts and ratio of substrates versus reagents for this reaction. Complete characterization of the catalysts along with their analyses have been well correlated to the catalytic activities of the catalysts and thus described herein. The procedure of the characterization techniques were described in Chapter 2.



Scheme 3A.1: Henry reaction catalyzed by KF/NaY and KF/KL zeolites

3A.1 Results and discussion

3A.1.1 Characterization of KF loaded NaY and KL zeolites

Initial investigation of zeolite framework stability was made by performing powder X-ray diffraction analyses of both parent and KF modified zeolites as shown in Figure 3A.1 (a-e). Peak positions of parent KL zeolite and NaY zeolite corroborate well with standard literature pattern [37,38]. Interestingly, both zeolites exhibit identical XRD patterns as that of their parent counterparts after loading with KF and calcination at 450 °C. Besides, no additional diffraction peaks corresponding to KF are observed in both the cases which in turn suggest that 5 wt % of KF is well dispersed over both KL and NaY zeolites.

However, it is obvious from the diminished peak intensities of the modified samples that crystallinity decreases after modification with KF. The comparison of intensity ratio of some high intensity peaks of the parent zeolites with that of the modified zeolites are presented in Figure 3A.2 (a-b).

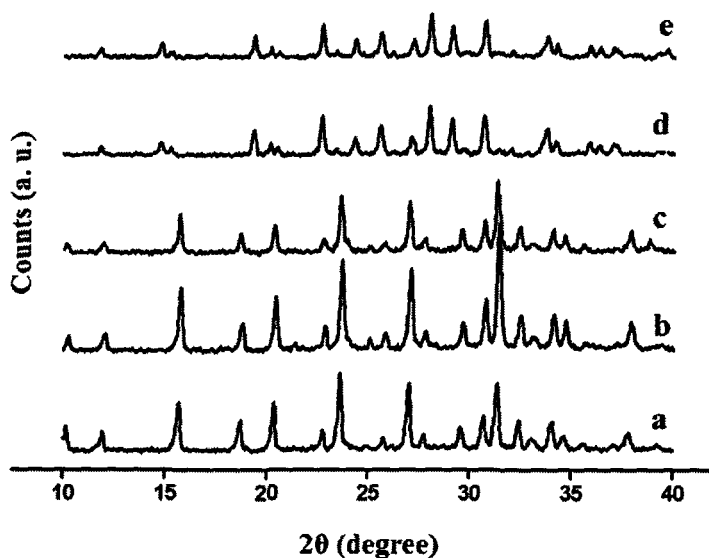


Figure 3A.1: XRD pattern of (a) NH_4Y (b) NaY zeolite (c) KF/NaY (d) KL zeolite (e) KF/KL after calcinations at $450\text{ }^\circ\text{C}$

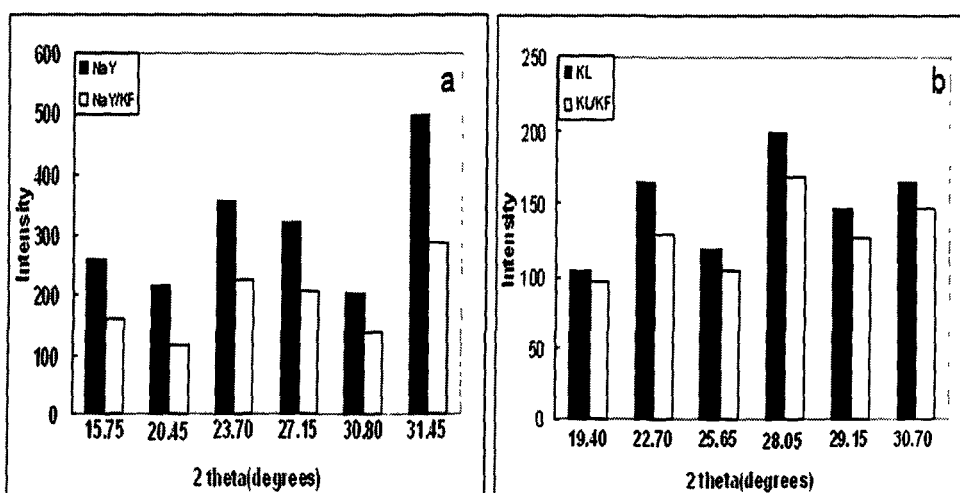


Figure 3A.2: The intensity ratio of the modified zeolites with parent zeolites at some 2θ points for (a) NaY zeolites (b) KL zeolites.

It is observed from the figure that the intensity of KL zeolite is less affected than NaY zeolite due to 5 wt % (0.40 mmol) KF loading. Moreover, relative crystallinity (%) obtained by comparing peak areas of some high intensity peaks shown in Figure 3A.3(a-b) reveal that crystallinity (%) of KF/NaY and KF/KL decrease up to 40% and 15% respectively than their parent counterparts. Thus, modification only changes the crystallinity of zeolites and does not affect the framework structures.

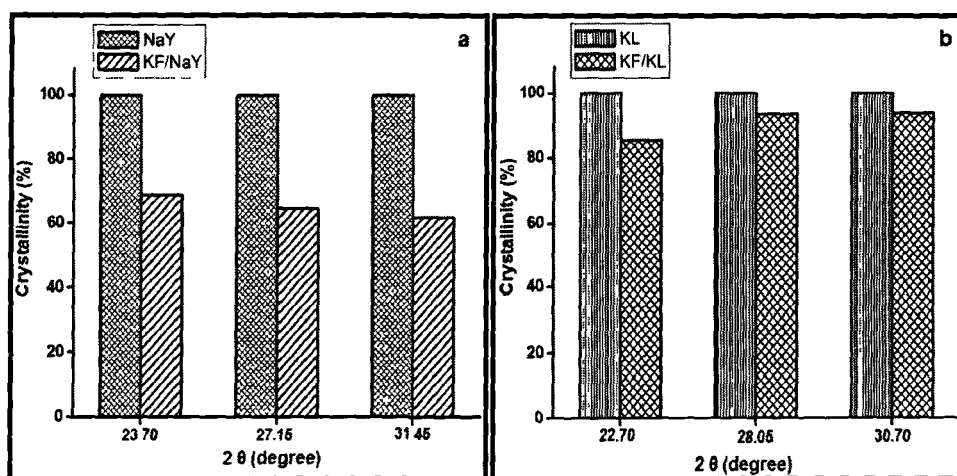


Figure 3A.3: The relative crystallinity (%) of modified zeolites with parent zeolites (a) NaY, KF/NaY zeolites (b) KL, KF/KL zeolites

Following XRD analysis, FTIR patterns were recorded after drying the samples in an oven at 100 °C for overnight. Figure 3A.4 shows FTIR spectra of NH₄Y, NaY, KF/NaY, KL and KF/KL zeolites. Infrared bands obtained from the original NH₄Y, NaY and KL zeolites in the region from 400–1600 cm⁻¹ gave information about the structural features of zeolite framework [39] which did not alter after loading with KF. Strong vibrations at ~950–1050 cm⁻¹ and vibration at ~650–700 cm⁻¹ are due to asymmetric and symmetric T–O (Si or Al) stretching mode, respectively in TO₄ tetrahedra and these both arise due to internal tetrahedral vibrations. These stretching modes are responsible for Si/Al composition of the zeolite framework and may shift to higher or lower frequency depending on increase or decrease of Si to Al ratio [40]. Again band at ~500–600 cm⁻¹ is due to double ring and bands at ~1100–1200 cm⁻¹ and 750–800 cm⁻¹ are, respectively

due to asymmetrical and symmetrical stretching vibrations of T–O in external linkages. Bands at around 1640 cm^{-1} is due to bending mode of adsorbed water molecules while band at around 1400 cm^{-1} for NH_4^+Y , NaY and KF/NaY are due to the N-H bending mode of NH_4^+ ions. As reported earlier there is a possibility of dealumination in case of KF/NaY and KF/KL due to reaction of KF with aluminium ions in zeolites [41,42] which can alter the framework band at $\sim 950\text{--}1050\text{ cm}^{-1}$ and $\sim 650\text{--}700\text{ cm}^{-1}$. However, we have not observed any distinct shifting of IR bands in this study i.e. no dealumination occurs in this study (Figure 3A.4). This may be due to low amount of KF loading (5 wt %) in this study. This is in good agreement with XRD observation that KF is well dispersed in zeolite NaY and KL and their framework structures are not affected after modification.

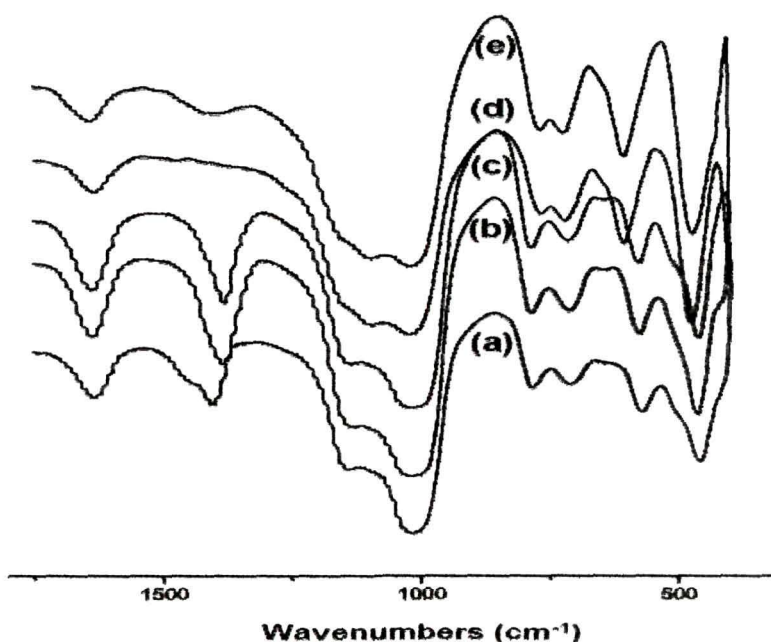


Figure 3A.4: FTIR spectra of (a) NH_4Y (b) NaY (c) KF/NaY (d) KL and (e) KF/KL zeolites after activation at $450\text{ }^\circ\text{C}$.

Morphological study was carried out through scanning electron microscopy. The micrographs of NaY, KF/NaY, KL and KF/KL zeolites are shown in Figure 3A.5 (a-d). Magnification of micrographs at X 10,000 and X 5,500 clearly shows homogeneity in shapes and highly crystalline nature of all samples. From the micrographs no aggregation of salt particles on support is detected i.e. KF is highly dispersed on support.

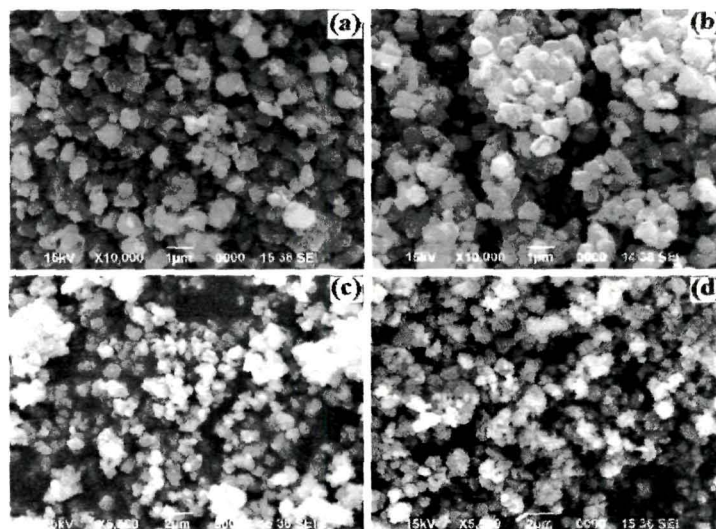


Figure 3A.5: SEM images of (a) NaY (b) KF/NaY (c) KL (d) KF/KL

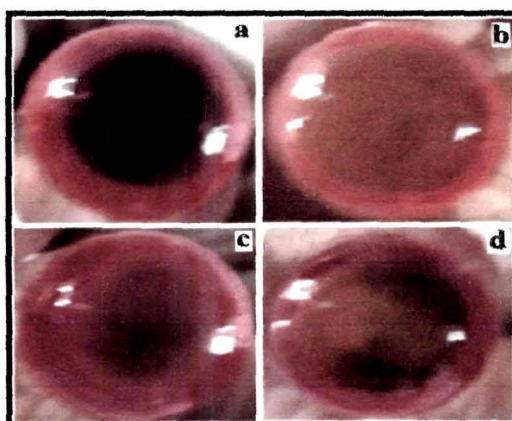


Image 3A.1: Image of base strengths of (a) NaY, (b) KF/NaY, (c) KL and (d) KF/KL

Table 3A.1: Basic properties of zeolite NaY and KL before and after loading with KF

Catalysts ^a	Base strength
NaY	6.8 < H _L < 8.0
KL	6.8 < H _L < 8.0
KF/NaY	8.0 < H _L < 10.0
KF/KL	8.0 < H _L < 10.0

^a Calcined at 450 °C.

To understand the basic properties of the materials, Hammett indicator method were employed. The base strengths and total basic sites of the prepared zeolites are presented in Table 3A.1. As expected from our catalytic experiment, the strength of basic sites of potassium modified NaY and KL zeolites are found to be higher ($8.0 < pK_{BH^+} < 10.0$) than parent zeolites ($6.8 < H_L < 8.0$). In neutral red solution, NaY becomes red in colour while KL shows reddish yellow colour. Thus, the base strengths of the parent zeolites lies in the range of $6.8 < H_L < 8.0$. On the other hand, KF/KL becomes pale yellow in colour and KF/NaY shows the brightest yellow colour in neutral red (Image 3A.1). This indicates that KF/NaY possesses the highest base strength amongst the four catalysts. Moreover, no change of colour was observed in phenolphthalein solution. This indicates that base strengths of all the catalysts are less than 10.0 (H_L). Therefore, it can be concluded from the results that base strengths of zeolites increases after modification which follow the trend $NaY < KL < KF/KL < KF/NaY$. It is noteworthy to mention that the framework structure is preserved even after loading and activation at 450 °C and simultaneous increase of base strengths occurs. This is the important observation in contrary to previous reports [43] where the structure of KF loaded NaY completely collapsed after activation at 600 °C.

3A.1.2 Catalytic reaction

In our attempt to study the catalytic activities of prepared catalysts towards Henry reaction and to investigate environmentally benign reaction conditions, initially we chose KF/NaY as catalyst to check whether the reaction proceeds without solvent or not. For this purpose, 1 equivalent of p-nitrobenzaldehyde and 1 equivalent of nitromethane were grounded with 20 mg catalyst using mortar and pestle for 10 minutes. No conversion was observed for both solid and liquid substrates after monitoring through thin layer chromatography technique (Table 3A.2, entries 1 & 2). It may be due to inadequate contact between catalyst and reactants in absence of a medium which could not facilitated the abstraction a proton from nitromethane and thus could not precede the reaction further. Therefore, the reaction was performed in presence of a variety of organic solvents. Accordingly, p-nitrobenzaldehyde and nitromethane was taken as model reactants and performed the reaction at room temperature with different organic solvents

[Chapter 3]

and 50 % aqueous solution of organic solvents. Both polar aprotic and protic solvents, less polar organic solvents and mixture of organic solvents and water were screened to understand the effects. As observed from Table 3A.2, dichloromethane (CH_2Cl_2) and chloroform (CHCl_3) having similar polarity gives comparable conversion of 71% -78%. Aprotic polar solvents like DMF, acetonitrile, THF have similar effects on reaction rate and gives moderate yield and selectivity (64%-78%) within 48 h.

Table 3A.2: Effect of solvents on Henry reaction of 4-nitrobenzaldehyde and Nitromethane catalyzed by KF/NaY

Entry	Solvents	Time (h)	Conversion (%) ^a	Selectivity (%) ^b
1	No	10 min ^c	0	0
2	No	10 min ^d	0	0
3	MeOH	48	92	73
4	EtOH	48	90	85
5	(Me) ₂ CHCH ₂ OH	48	90	86
6	CH ₂ Cl ₂	48	71	66
7	CHCl ₃	48	78	78
8	THF	48	64	80
9	DMF	48	78	67
10	CH ₃ CN	48	71	57
11	H ₂ O–MeOH	12	98	88
12	H ₂ O–CHCl ₃	48	98	76
13	H ₂ O–EtOH	48	88	60
14	H ₂ O– (Me) ₂ CHCH ₂ OH	48	82	80
15	H ₂ O	48	15	-

^aReactions were carried out with 1 mmol scale with molar ratio 1: 1 of 4-nitrobenzaldehyde/Nitromethane, 2 mL solvent and 0.020g KF/NaY at room temperature.

^bYields and selectivities were obtained from ¹H NMR data of the crude reaction mixture.

(byproducts formed are dehydrated product and polymerized product 1,3-dinitro-2-(4-nitrophenyl)-propane.)

^cReaction with p-nitrobenzaldehyde, ^dReaction with 1-naphthaldehyde

[Chapter 3]

On the other hand, both conversion and selectivity increases (entries 3, 4, & 5; Table 3A.2) when protic polar solvents were used. We have also found that further enhancement of conversion and selectivity when the reaction was carried out with 50 % aqueous solution of protic and aprotic solvents (entries 11-14, Table 3A.2). This indicates that the reaction proceeds smoothly in presence of water in the reaction medium. The decreasing order of conversions in presence of water in the medium follow the trend MeOH-H₂O > EtOH-H₂O > isobutanol-H₂O. It may be due to increase of steric effect of alkyl groups from MeOH to isobutanol which affects the activation of catalysts through solvation process. The reaction in H₂O was very slow (entry 15, Table 3A.2). This is due to the fact that the hydrophobic nature of the reactant molecules places them in heterogeneous phases from the reaction medium. Among all the studied solvents, MeOH-H₂O (1:1 ratio) shows the highest percentage of conversion and selectivity. Therefore, MeOH-H₂O pair has been chosen as the best solvent in this study. Subsequently, all other reactions were carried out with MeOH-H₂O solvent.

Table 3A.3: Effect of temperature on Henry reaction of 4-nitrobenzaldehyde and nitromethane catalyzed by KF/NaY.

Entry	Temperature (°C)	Time (h)	Conversion (%) ^a	Selectivity (%) ^a
1	RT	12	98	88
2	40	5	98	80
3	50	2.5	99	77
4	60	1	97	63

^aReactions were carried out in 1mmol scale with molar ratio 1:1 of 4-nitrobenzaldehyde/nitromethane. 2 mL solvent (MeOH-H₂O) and 0.02 g KF/NaY. ^bYields and selectivities were obtained from ¹H NMR data of crude reaction mixture.

Having been found the best solvent in this study, the reaction was attempted with nitromethane, p-nitrobenzaldehyde and MeOH-H₂O (1:1) solvent at temperature range of 25 °C- 60 °C to understand the crucial role of temperature over yield and selectivity of the desired product. The results are summarized in Table 3A.3. The reaction time

decreases noticeably from 12 h at room temperature to 1 h at 60 °C (entries 1 & 4, Table 3A.3) and selectivity decreases gradually on increasing temperature. Formation of side products of similar nature was observed both at room temperature and at higher temperatures. This illustrates that both speed of reaction and formation of side products become faster on increasing temperature. On the other hand, formation of side products reduced significantly when the reaction was performed with higher amount of nitromethane at room temperature. Therefore, study of molar equivalent of nitromethane at room temperature would be interesting for better understanding of the reaction. Hence, further studies were continued at room temperature.

Table 3A.4: Effect of amount of nitromethane on conversion (%) and selectivity (%) on Henry reaction

Entry	4-nitrobenzaldehyde (mmol)	Nitromethane (mmol)	Time (h)	Conversion (%) ^a	Selectivity (%) ^b
1	1	1	12	98	88
2	1	2	4	99	91
3	1	3	3	99	93
4	1	5	3	99	91
5	1	10	45 min	99	93

^aReactions were carried out in 1mmol 4-nitrobenzaldehyde with different molar amount of Nitromethane, 2 mL solvent (MeOH–H₂O) and 0.02g KF/NaY at room temperature. ^bYields and selectivities were obtained from ¹H NMR data of crude reaction mixture.

Subsequently, the reaction was performed with 0.02 g catalyst and MeOH–H₂O (1:1) solvent at room temperature to observe the effect of molar equivalent of nitromethane on yield of Henry reaction. We observed that the reaction time gradually decreases with increasing the amount of nitromethane. As shown in Table 3A.4, increasing nitromethane amount from 1 mmol to 2 mmol, reaction time reduced from 12h to 4h, respectively (entry 2, table 3A.4), showing similar conversions and selectivities. Further improvement of reaction speed was watched from 1:5 and 1:10 ratio of aldehyde and nitromethane (entries 4 & 5, Table 3A.4). We also observed comparable selectivities

in every attempt. Hence, it has been understood that the increasing amount of nitromethane would be a possible approach to reduce the formation of side products in this study. However, use of excess nitromethane is not acknowledged from the green chemistry principles which thus led us to select 2 mmol nitromethane as the optimum amount for further studies.

Table 3A.5: Effect of the amount of catalyst on Henry reaction

Entry	Catalyst (mg)	Time (h)	Conversion (%) ^a	Selectivity (%) ^b
1	10	15	91	78
2	15	13	94	82
3	20	12	98	88
4	25	12	99	92

^aReactions were carried out in 1mmol scale with molar ratio 1:1 of 4-nitrobenzaldehyde/ nitromethane and 2 mL solvent (MeOH-H₂O) and 0.02 g KF/NaY at room temperature. ^bYields and selectivities were obtained from ¹H NMR data of crude reaction mixture.

Table 3A.6: Effect of catalysts on Henry reaction

Entry	Zeolite	Time (h)	Conversion (%) ^a	Selectivity (%) ^a
1	KL	12	87	63
2	NaY	12	90	75
3	KF/KL	7	95	67
4	KF/NaY	4	99	91

^aReactions were carried out in 1mmol scale with molar ratio 1:2 of 4-nitrobenzaldehyde/nitromethane, 2 mL solvent (MeOH-H₂O) and with different catalysts at room temperature.

^bYields and selectivities were obtained from ¹H NMR data of crude reaction mixture.

We next examined the effect of amount of catalyst on reaction time and percentage conversions to optimize the reaction conditions. The results are summarized in Table 3A.5. We have noticed that the amount of catalyst does not have huge effect over conversions (entries 1 & 4, Table 3A.5). However, slow and gradual increase of

conversions was observed on increasing catalysts amount from 10 mg to 25 mg. Conversely, selectivity increases satisfactorily upon increasing catalyst amount (entries 1 & 4, Table 3A.5). We have observed 92 % selectivity of nitroladol product with 25 mg KF/NaY in comparison to 78% of that from 10 mg catalyst. We have selected 20 mg catalyst as optimum amount for further studies.

In order to study the effect of catalysts as well as basicities over the reaction, the reaction was studied with fauzasite and zeolite-L having supercage and straightly channel, respectively. The basicity of both the zeolites was enhanced by impregnating KF. It was found that KF/NaY has the highest base strengths amongst the four. We have also found that KF/NaY shows superior conversion and selectivity amongst the four and gives 99 % conversion and 91 % selectivity within 4 hours at room temperature (entry 4, table 3A.6). This may be due to the presence of supercages in NaY which allow bulkier transition states to form during the reaction. The effect of different catalysts on Henry reaction is presented in Table 3A.6. Further studies with different substrates were carried out with KF/NaY. We have observed formation of some dehydrated product from nitroaldol and corresponding addition product i.e. 1,3-dinitro-2-(4-nitrophenyl)-propane) as by products in our study.

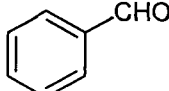
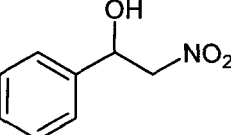
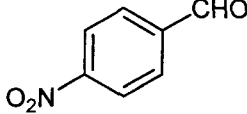
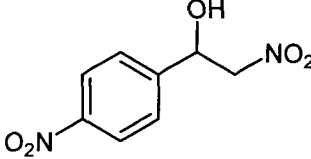
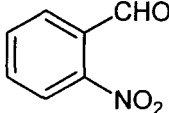
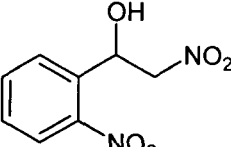
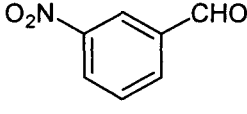
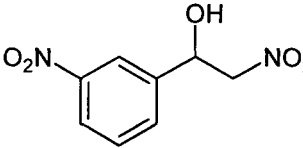
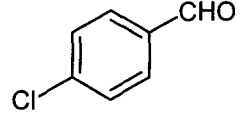
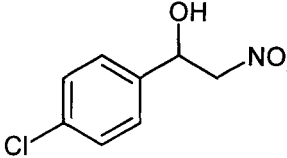
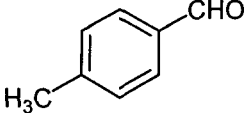
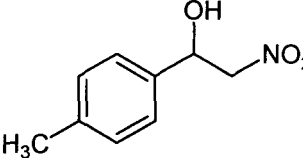
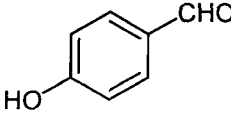
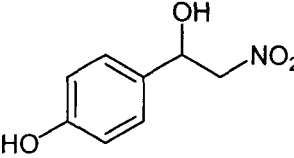
To further extend the scope of the reaction, it was performed with variety of aldehydes such as simple aromatic aldehydes, heterocyclic aldehydes and polycyclic aromatic aldehydes. The results are summarized in Table 3A.7. It is found that substrates having electron withdrawing groups (entry 1-3, Table 3A.7) reacted faster to give 84-92 % yield within 4 hours while reaction with substrates having electron donating groups (entry 6-8, Table 3.1.7) were comparatively slow and gave moderate yields within 48 hours. Reactions for 1-naphthaldehyde and 2-furaldehyde are somewhat faster than substrates with electron withdrawing groups giving 72-78 % yields within 24 hours. It can be conferred from Table 3A.7 that the reaction goes smoothly with different aldehydes under mild conditions with good selectivity of the nitroaldol product.

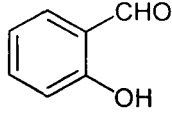
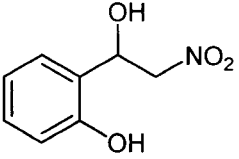
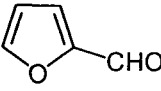
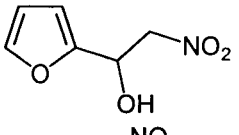
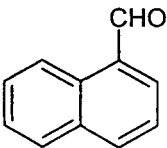
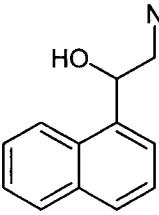
Having been found results for various meta- and para- substituted benzaldehydes, it would be interesting to see whether there is a linear relationship between the percentage yield and the Hammett's substituent constant (σ). As observed from Figure 3A.6, Henry

[Chapter 3]

reaction with these modified zeolites shows a linear relationship between the percentage yield and the Hammett's substituent constants (σ).

Table 3A.7: Henry reaction of nitromethane with different aldehydes

Entry	Substrate	Product	Time (h) ^a	Yield (%) ^b
1			4	81
2			4	92
3			7	90
4			7	84
5			48	70
6			48	63
7			48	53

8			48	47
9			24	72
10			24	78

^aReactions were carried out in 1mmol scale with molar ratio 1:2 of 4-nitrobenzaldehyde/nitromethane, 2mL solvent (MeOH-H₂O) and 0.02 g KF/NaY at room temperature. ^bIsolated yields after TLC purification. All products were characterized by FT-IR, ¹H NMR and ¹³C NMR. ^cbyproducts formed were not isolated.

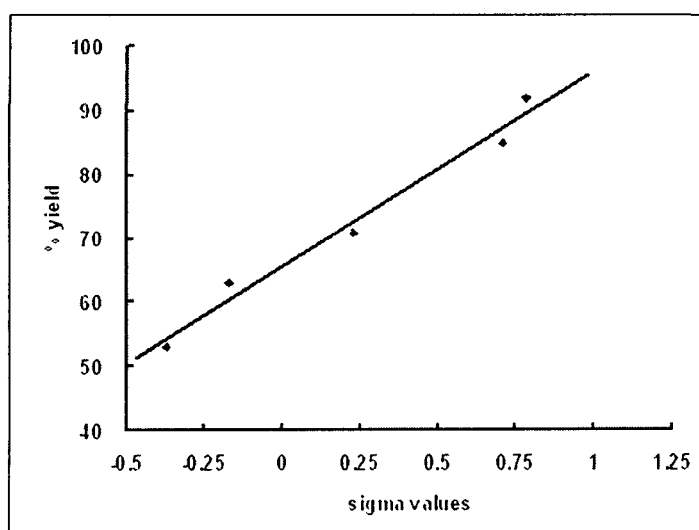


Figure 3A.6 Plot of yield (%) against Hammett substituent constant (σ).

The reusability of catalysts is important in the field of catalysis. We have investigated reusability of KF/NaY upto four times and performed the reaction with 4-nitrobenzaldehyde and nitromethane (1:2 ratio), MeOH-H₂O solvent and 50 mg KF/NaY at room temperature (Table 3A.8). After the first run, the catalyst was recovered by

centrifugation, washed with acetone and water and finally dried for 24 h at 150 °C to remove adsorbed water molecules on the surface before performing the next run. Excellent conversions were observed in each cycle. However, reaction time gradually increases after each run.

Table 3A.8 Reusability study of KF/NaY for Henry reaction

Entry	Run	Catalyst amount (mg)	Time (h)	Conversion (%)
1	First	50	1.5	99
2	Second	46	1.5	99
3	Third	40	2	99
4	Fourth	28	3	99

^aReactions were carried out in mmol scale with molar ratio 1:2 of 4-nitrobenzaldehyde/nitromethane, 2mL solvent (MeOH–H₂O) and 0.02 g KF/NaY at room temperature

It may be due to decrease of catalyst amount after each run and slight leaching or deactivation of active sites of zeolite through adsorption of polar solvent molecules on the surface. To investigate the leaching phenomena we performed flame photometry study for K⁺ ion. Negligible amount of K⁺ leaching (0.001 g/L) was detected and it does not hamper the reaction. Thus, the catalyst is active up to fourth run showing excellent conversions in each run.

Thus, we have obtained KF/NaY as the optimum catalyst in presence of MeOH-H₂O solvent for efficient synthesis of nitroaldol product at room temperature.

3A. 2 References

- [1] Weitkamp, J. *Solid State Ionics* **131** (1-2), 175-188, 2000.
- [2] Smit, B. & Maesen T.L.M. *Nature* **451** (7179), 671-678, 2008.
- [3] Nabera, J.E., et al. *Stud. Surf. Sci. Catal.* **84**, 2197-2219, 1994.
- [4] Csicsery, S.M. *Zeolites* **4** (3), 202-213, 1984.
- [5] Zhang, C., et al. *J. Phys. Chem. C.* **112** (37), 14501-14507, 2008.
- [6] Jongpatiwuta, S., et al. *Catal. Lett.* **100** (1-2), 7-15, 2005.
- [7] Gates, B.C. *Chem. Rev.* **95** (3), 511-522, 1995.
- [8] Martens, J.A., et al. *Appl. Catal. A: Gen.* **45** (1), 85-101, 1988.
- [9] Davis, M.E. *Accounts. Chem. Res.* **26** (3), 111-115, 1993.
- [10] Dartt, C.B. & Davis, M.E. *Ind. Eng. Chem. Res.* **33** (12) 2887-2899, 1994.
- [11] Venuto, P.B. *Microporous. Mater.* **2** (5), 297-411, 1994.
- [12] Holderich, B.W., et al. *Angew. Chem. Int. Ed. Engl.* **27** (2), 226-246, 1988.
- [13] Zhu, J., et al. *Catal. Today* **51** (1), 103-111, 1999.
- [14] Corma, A. *J. Catal.* **216** (1-2), 298-312, 2003.
- [15] Jeong, M.S., et al. *J. Phys. Chem.* **97** (39), 10139-10143, 1993.
- [16] Suppes, G.J., et al. *Appl. Catal. A: Gen.* **257** (2), 213-223, 2004.
- [17] Corma, A., et al. *Appl. Catal. A: Gen.* **59** (1), 237-248, 1990.
- [18] Corma, A., et al. *J. Catal.* **126** (1), 192-198, 1990.
- [19] Martins, L., et al. *J. Catal.* **258** (1), 14-24, 2008.
- [20] Pena, R., et al. *Fuel* **110**, 63-69, 2013.
- [21] Intarapong, P., et al. *Int. J. Ren. Energ. Res.* **1** (4), 271-280, 2011.
- [22] Romero, M.D., et al. *Micropor. Mesopor. Mater.* **81** (1-3), 313-320, 2005.
- [23] Brittain, R.T., et al. *Adv. Drug Res.* **5**, 197-253, 1970.
- [24] Ballini, R. *J. Chem. Soc., Perkin Trans.* **1** (6), 1419-1421, 1991.
- [25] Bandini, M., *Chem. Commun.* (6), 616-618, 2007.
- [26] Ballini, R. & Bosica, G. *J. Org. Chem.* **59** (18), 5466-5467, 1994.

[Chapter 3]

- [27] Zou, W., et al. *J. Org. Chem.* **72** (7), 2686-2689, 2007.
- [28] Sasai, H., et al. *J. Org. Chem.* **60** (23), 7388-7389, 1995.
- [29] Nikalje, M. D., et al. *Tetrahedron Lett.* **41** (6), 959-961, 2000.
- [30] Huh, S., et al. *J. Am. Chem. Soc.* **126** (4), 1010-1011, 2004.
- [31] Anan, A., et al. *Catal. Lett.* **126** (1-2), 142-148, 2008.
- [32] Demicheli, G., et al. *Tetrahedron Lett.* **42** (12), 2401-2403, 2001.
- [33] Anan, A., et al. *J. Mol. Catal. A Chem.* **288** (1-2), 1-13, 2008.
- [34] Ballini, R., et al. *J. Org. Chem.* **73** (21), 8520-8528, 2008.
- [35] Parratt, A.J. et al. *Chem. Commun.* (23), 2720-2721, 2004.
- [36] Nulty, J.M., et al. *Tetrahedron Lett.* **39** (44), 8013-8016, 1998.
- [37] Zhu, J.H., et al. *Micropor. Mesopor. Mater.* **24** (1-3), 19-28, 1998.
- [38] Trakarnroek, S., et al. *Chem. Eng. Commun.* **194** (7), 946-961, 2007.
- [39] Garcia, F.A.C., et al. *J. Braz. Chem. Soc.* **22** (10), 1894-1902, 2011.
- [40] Gupta, N.M. Catalyst Characterization Using Infra Red Spectroscopy, in *Catalysis Principles and Applications*, B. Viswanathan et al., eds., Narosa Publishing House Pvt. Ltd., New Delhi, 2006, 127-144.
- [41] Ando, T., et al. *J. Chem. Soc., Perkin Trans.2* **(8)**, 1133-1138, 1986.
- [42] Weinstock, L.M., et al. *Tetrahedron Lett.* **27** (33) 3845-3848, 1986.
- [43] Sun, L.B. *Catal Lett* **132** (1-2), 218-224, 2009.

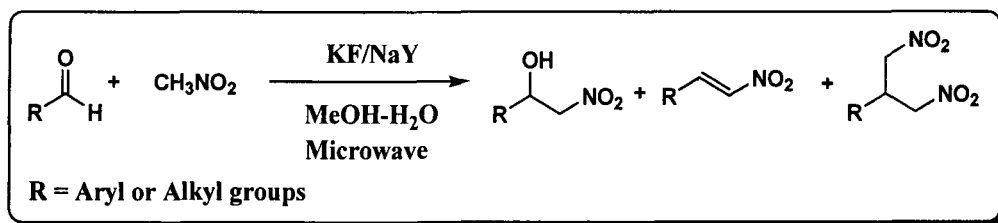
Section 3B: Study of structural change and basicity of KF loaded NaY zeolite and its application for Henry reaction under microwave irradiation condition

Microwave irradiation technique as alternating heating source occupies an important position in every area of science now a days [1-5]. It has become a key practice to accelerate organic synthesis by microwave irradiation due to its core heating mechanism, energy saving mode and possibility to carry out reactions under solvent less conditions [6-10]. Solventless organic synthesis is the most commonly employed route under microwave to get high yield and selectivities [11-14]. However, coupling benign reaction media with microwave technologies are often advantageous for processes where requirement of solvents is necessary and the solventless route does not effectively work [15-17]. In organic synthesis, optimization of reaction parameters such as solvents, temperatures and reaction time have been commonly investigated to get maximum yield and selectivity within short reaction time and low consumption of energy. Utilization of microwave irradiation technique has proven to be superior to conventional heating in many reactions and thus meet these above requirement upto a greater extent [18-21]. Henry nitroaldol reaction is an interesting example of getting various side products during the course of the reaction due to simultaneous progress of competitive reactions [22,23]. Therefore, optimization of reaction conditions to control the selectivity is an essential step for this reaction with almost all catalytic conditions. Zeolites and modified zeolites are found to be effective basic catalysts for various reactions including Henry reaction [24,25]. Zeolites have recently been modified by exchanging their cations with other metal ions and loading varieties of basic guests such as alkali or alkali metal oxides and hydroxides to generate strong basicity [26-30]. These modified zeolites have proven to be potential catalysts for biodiesel synthesis [31,32]. However, conventional organic reactions are not well studied with zeolite catalysts. This has motivated us to study Henry nitroaldol reaction with NaY zeolite under optimum conditions. The mild basicity of zeolites, possibility to tune their basicity and environmentally benign nature drive us to

[Chapter 3]

modify these materials and use them for Henry nitroaldol reaction under microwave irradiation.

In this section, we have found that potassium salt modified NaY zeolite along with methanol-water mixture as solvent under microwave irradiation offers an environmentally benign way to synthesize β -nitroalcohols rapidly with excellent yield and selectivities. Here, NaY zeolite was modified with 0.5% - 20 % KF (w/w) by a wet impregnation method and characterized by X-ray diffraction, FT-IR and Hammett base strength measurement methods. It was observed that framework structure preserved even after 20 % loading of KF and crystallinity diminished from lower to higher loading. The obtained materials showed quite different base strengths according to varied percentage of the salt over the support and change of their activation temperatures. The effects of different reaction parameters such as amount of solvents, nature of solvents, microwave power and microwave irradiation time were studied and explained herein. We have found that 10 wt % KF loaded NaY is the best catalyst and gives 97 % yield under optimized reaction conditions. Again, recoverability of the catalysts was tested and explained herein. The detailed experimental methods and reaction procedures are given in Chapter 2.



Scheme 3B.1: Henry reaction catalyzed by KF/NaY under microwave

3B.2 Results and discussion

3B.2.1 Characterization of KF loaded NaY zeolite

Powder X-ray diffraction analyses were performed on both parent NaY zeolite and 0.5 % - 20 % KF (w/w) loaded NaY zeolite after calcinations at 450 °C. Figure 3B.1 illustrates the presence of fauzasite zeolite structural peaks [33] in all loaded samples which thus suggests the perseverance of zeolite framework structure even after loading of 20 % KF.

Conversely, peak intensities decrease gradually from lower to higher loading (Figure 3B.2). The relative crystallinity (%) calculation of three high intensity peaks at 2θ values 24.05° , 27.20° and 30° reveals that crystallinity (%) follows the same trend as that of intensities and goes on decreasing on increasing amount of KF loading (Figure 3B.3).

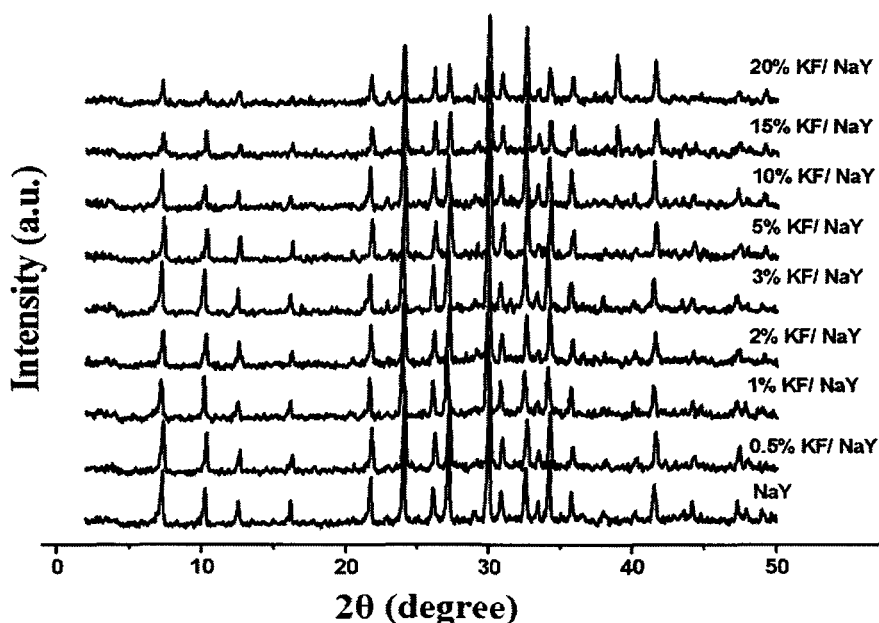


Figure 3B.1: XRD patterns of NaY and KF/NaY zeolites calcined at 450°C

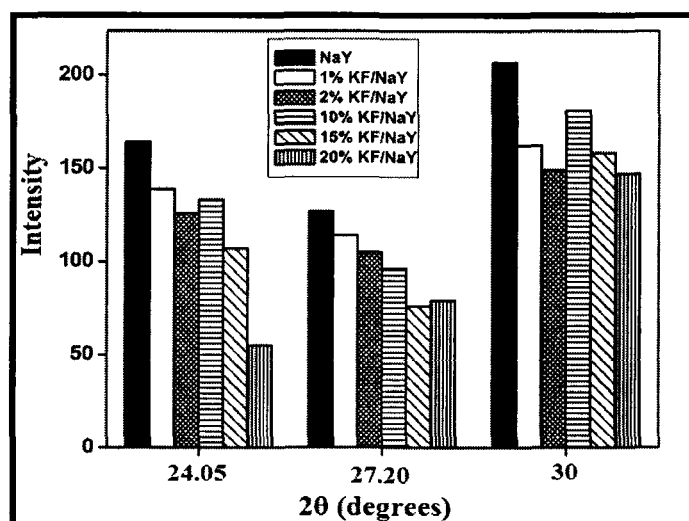


Figure 3B.2: Intensity differences of crystallinity of NaY and different KF/NaY zeolites calcined at 450°C

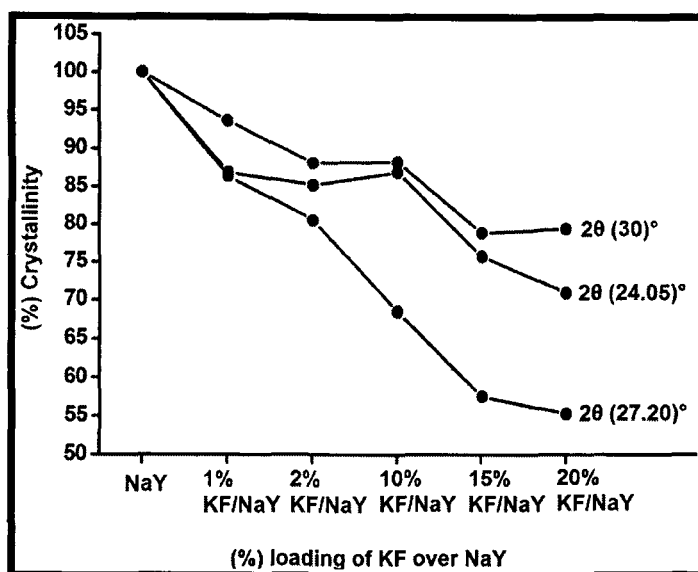


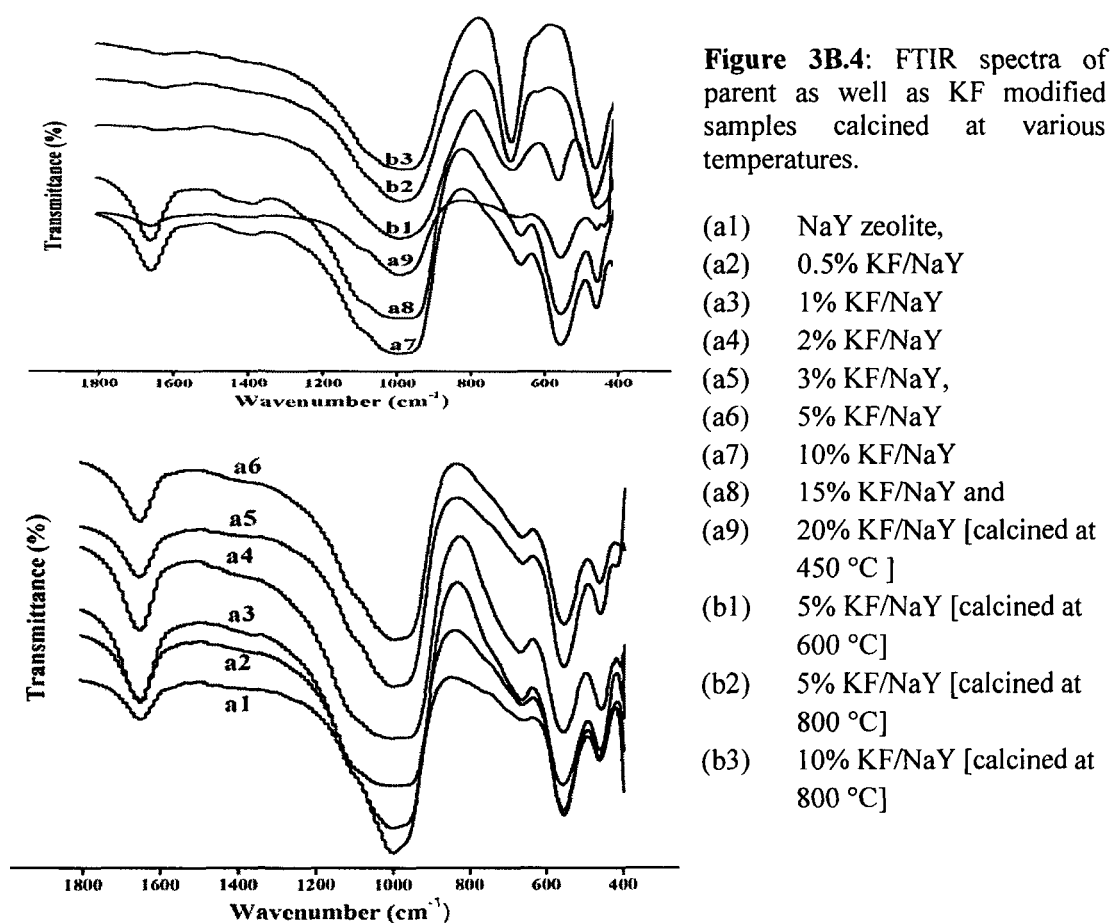
Figure 3B.3: Differences of (%) crystallinity of NaY and different KF/NaY zeolites calcined at 450 °C

Table 3B.1: Surface properties and particle size of zeolites

Sample	Crystallite size (nm)		
	7.25 (2θ)	24.05 (2θ)	30 (2θ)
NaY	63	52	45
10 % KF/NaY	73	48	46

However, we have observed high dispersion of KF over NaY zeolite upto 10 % loading of KF. It can be evidenced from figure 3B.1 that no emergence of additional peaks corresponding to KF or other phases occurs up to 10 % KF/NaY. On the other hand, emergence of an additional peak at 2θ position 39.95° for 15 % and 20 % KF loaded zeolites can be attributed to the formation of $KAlF_4$ phase (JCPDS card number 84-1009). Thus, KF loading beyond 10 % is strictly prohibited over NaY zeolite. Calculation of crystallite sizes from XRD peaks of NaY zeolite and 10 % KF/NaY shows that crystallite sizes of both zeolites are comparable to each other (Table 3B.1). This further confirms that KF loading up to 10 % is not harmful over zeolite structure.

FTIR spectra of parent as well as modified zeolites were recorded after calcinations at 450 °C, 600 °C and 800 °C. Figure 3B.4 shows vibrations in the region 400-1800 cm^{-1} which is a clear evidence of the presence of zeolite framework structure in the parent as well as modified zeolites [34]. Band at around 1650-1700 cm^{-1} can be ascribed to bending vibration of water molecules attached to zeolite structure which remain intact in all samples activated at 450 °C [35,36]. On the other hand, it disappeared after calcinations at 600 °C (b1) and 800 °C (b2, b3). This clearly indicates that high activation temperature is not recommended for zeolite structure in presence of KF. Distinct bands for internal tetrahedral vibrations i.e. in the ranges 1050-1000 cm^{-1} and 700-650 cm^{-1} are assigned for asymmetric and symmetric T-O (Si or Al) stretching mode respectively in tetrahedral co-ordination while band in the range 650-500 cm^{-1} is for tetrahedral T-O-T bending mode. Vibration in the range 500-410 cm^{-1} is for external linkages between tetrahedra and is assigned for double ring [37].



[Chapter 3]

As can be seen from figure 3B.4, no alteration of all these bands takes place up to 15 % loading of KF. On the contrary, 20 % loaded sample (a9) shows very weak vibrations for these bands. This is in good agreement with XRD observation that KF loading beyond 10 % is restricted for NaY zeolite structure. We have also observed from the FTIR pattern of the calcined samples that both internal and external zeolite structure exists for 5 % loaded sample activated at 600 °C (b1) while the band for double ring is absent in samples activated at 800 °C (b2, b3). It shows that both high activation temperature and higher loading of KF have harmful effect over the support. Therefore, 10 % KF loaded catalyst calcined at 450 °C can be considered as optimum in this study. Slight dealumination was reported [38] earlier in case of KF loaded NaY zeolite due to reaction of KF with aluminium at high temperature. In this study, no dealumination was detected from the obtained results.

Table 3B.2: Base strength of zeolites modified with KF

Sample	Base strength (H_-)	Amount of soluble basic sites (mmol g^{-1})
NaY	$8.0 < H_- < 10.0$	0.292
0.5% KF/NaY	$8.0 < H_- < 10.0$	
1% KF/NaY	$8.0 < H_- < 10.0$	
2% KF/NaY	$8.0 < H_- < 10.0$	0.419
3% KF/NaY	$8.0 < H_- < 10.0$	
5% KF/NaY	$10.0 < H_- < 11.1$	0.475
10% KF/NaY	$10.0 < H_- < 11.1$	0.507
15% KF/NaY	$10.0 < H_- < 11.1$	
20% KF/NaY	$10.0 < H_- < 11.1$	0.797
0.5%–5% KF/NaY ^a	$8.0 < H_- < 10.0$	
10% KF/NaY ^a	$10.0 < H_- < 11.1$	
15% KF/NaY ^a	$10.0 < H_- < 11.1$	
3–10% KF/NaY ^b	$8.0 < H_- < 10.0$	
15% KF/NaY ^b	$10.0 < H_- < 11.1$	

^aThe activation temperature was 600 °C, ^bThe activation temperature was 800 °C

Basic property investigation shows quite different basicities for parent NaY and modified NaY zeolites. The results are depicted in Table 3B.2. Base strengths of parent NaY and 0.5-3 % KF loaded NaY zeolites are the same and lies in the range of $8.0 < H_- < 10$, which

shows that no detectable change of basic properties take place upon loading low amount of KF. On the other hand, base strength of 5 % - 20 % KF loaded zeolites are higher than the parent NaY and lies in the range of $10 < H_- < 11.1$. This illustrates that basicity increases on increasing KF loading. It is again interesting to note that the framework structure remain preserved even after loading of 20 % KF and simultaneous activation at 450 °C. This signifies that activation of KF loading up to 20 % does not have negative effect on NaY zeolite structure at activation temperature 450 °C. However, XRD study prohibited the possibility to load KF beyond 10%. Therefore, 10 % loading has been conceded as the optimum amount in this study. This study furnishes concomitant result with previous reports confirming that activation temperature and amount of loading both have their role on basic properties [39,40]. Consequently, 5 % and 10 % loaded catalysts were further activated at 600 °C and 800 °C and basicities were checked (Table 3B.2). Surprisingly, base strength of 10 % KF/NaY lowered upon increasing activation temperature. It can be attributed to the interaction of KF with zeolite structure at high temperature and thus reducing some basic sites. Conversely, base strength of 5 % KF/NaY does not change even after calcination at 800 °C and lies in range $8.0 < pK_{BH^+} < 10$ which confirms that loading low amount of KF does not have detectable effect over structure as well as basic properties even after calcination at high temperature. The result of titrimetric analysis shows some amount of soluble basicities in the parent NaY zeolite and it goes on increasing after loading KF. The soluble basicities of parent NaY may be due to the presence of impurities in the structure during its formation.

3B.2.2 Catalytic reaction

To check the catalytic activity of 10 % KF/NaY catalyst towards Henry niroaldol reaction under microwave irradiation condition, we chose to optimize the reaction conditions at the beginning by varying reaction parameters such as solvents, microwave power as well as microwave irradiation time. For this purpose, the reaction was initially carried out under solvent free conditions and then in presence of a variety of solvents. The results are summarized in Table 3B.3. Thin layer chromatography monitoring showed no detectable conversion (entries 1 & 2, Table 3B.3) in case of solvent free conditions. This may be due to poor mixing of the reactants and catalyst which hinders the catalyst to abstract a

proton in the absence of a reaction medium. In section 3A of this thesis, it has been found that methanol is the best solvent among a variety of polar and non-polar solvents for this reaction at room temperature. Therefore, a variety of alcohols and alcohol-H₂O mixtures as solvents have been screened at this time under microwave irradiation to understand the role of reaction medium over the conversions and selectivities. Inspection of table 3B.3 shows that the reaction is comparatively faster for alcohols containing small alkyl groups than with alcohols containing bulky alkyl groups. Octanol gives only 12 % conversion in comparison to methanol which gives 95 % conversion within 2 minutes. This can be attributed to decrease of polarity of alcohols on increasing bulky nature of alkyl groups. The conversions for pure alcohols decrease in the order MeOH ~ EtOH > n-butanol > isopropanol > octanol > isobutanol. Thus, straight chain alcohols with smaller alkyl groups are more favourable than alcohols containing bulky alkyl groups under microwave irradiation condition. Subsequently, the reaction was carried out with water-alcohol mixtures (1:1) to understand their polar effect. With 50 % aqueous alcoholic solution, the reaction becomes rapid and conversions are higher than the pure alcohols. The reaction with aqueous alcoholic mixture bearing small alkyl groups gives excellent conversions and selectivities within 1 minute irradiation time (entries 10 & 11, Table 3B.3). It confers that water miscible alcohols offer a reaction medium suitable for both reactant and catalysts making the conditions favourable for the reaction. On the other hand bulky alcohols are less soluble in water and place the reactants and catalysts in different phases thus lowering the feasibility of the reaction. In this case, conversions decrease in the trend H₂O - MeOH ~ H₂O - EtOH ~ H₂O - isopropanol > H₂O isbutanol > H₂O - butanol > H₂O - octanol. Feasibility of the reaction in water miscible alcohols can be suggested that the tendency of intermolecular H-bonding of alcohols makes the alkoxide ions to interact with acidic protons of nitromethane. This further increase the acidity of acidic protons of nitromethane and thus basic sites of zeolites can easily abstracts a proton from it. We have also observed that the catalytic activity of used zeolite decreases in the next run which may be due to blockage of some active sites of zeolite by the adsorbed solvent molecules during the reaction. Thus, activation of zeolite at proper temperature is crucial for their catalytic activities.

[Chapter 3]

Table 3B.3: Henry reaction of 4-nitrobenzaldehyde and nitromethane catalyzed by 10% KF/NaY in different solvents under microwave ^a

Entry	Solvents	% Conversion (time in min)	Selectivity (%) ^d		
			A	B	C
1	Solvent free ^b	No (5)	–	–	–
2	Solvent free ^c	No (5)	–	–	–
3	MeOH	95 (2)	92	8	
4	EtOH	97 (2)	98		2
5	n-Butanol	86 (2)	94	3	3
6	Octanol	12 (2)	88	2	
7	Isopropanol	51 (2)	93	5	2
8	Isobutanol	6 (2)	100		
9	H ₂ O	71 (1)	97		3
10	MeOH–H ₂ O	97 (1)	95		5
11	EtOH– H ₂ O	94 (1)	97		3
12	Butanol– H ₂ O	21 (1)	100		
13	Octanol – H ₂ O	21 (1)	100		
14	Isopropanol – H ₂ O	96 (1)	98		2
15	Isobutanol – H ₂ O	40 (1)	97		3
16	Ethylene glycol	50 (30)	77	1	16
17	Ethylene glycol– H ₂ O	58 (30)	76	6	18

^aAll reactions were carried out with aldehyde (0.5 mmol), nitromethane (2 mmol), 10% KF/NaY (10 mg), solvent (3ml), MW power (40%), Temperature (50 °C), ^bSolvent free condition between p-nitrobenzaldehyde and nitromethane, ^cSolvent free condition between benzaldehyde and nitromethane, ^dConversions and selectivities of the products were obtained from ¹H NMR data of crude reaction mixture [[A: 1-(4-nitrophenyl)-2-nitroethanol, B: 1-(4-nitrophenyl)-2-nitroethene and C: 1,3- dinitro-2-(4-nitrophenyl)-propane]]

The feasibility of the reaction in aqueous alcoholic mixture has been further confirmed by observing the absorbed microwave energy by a series of polar solvents when irradiated with 40 % microwave power for 10 minutes by keeping the amount of solvents fixed (Figure 3B. 5). It has been observed that the highest microwave energy is absorbed by H₂O-MeOH (1:1 ratio) pair among all the screened solvents. We have also observed a gradual increase of absorbed energy in terms of temperature for the same solvent and fixed amount of solvent on increasing microwave irradiation time. Increasing irradiation time up to 10 minutes, rate of increase of temperature becomes faster for first 4 minutes, steady up to 7 minutes and then again increases slightly up to 10 minutes. Irradiating 20 % MW power for 1 minute, MeOH - H₂O pair shows temperature rise of 50 °C and increases gradually up to 72 °C at 8 minutes, remain constant beyond that. This confers that microwave irradiation for longer time is not necessary.

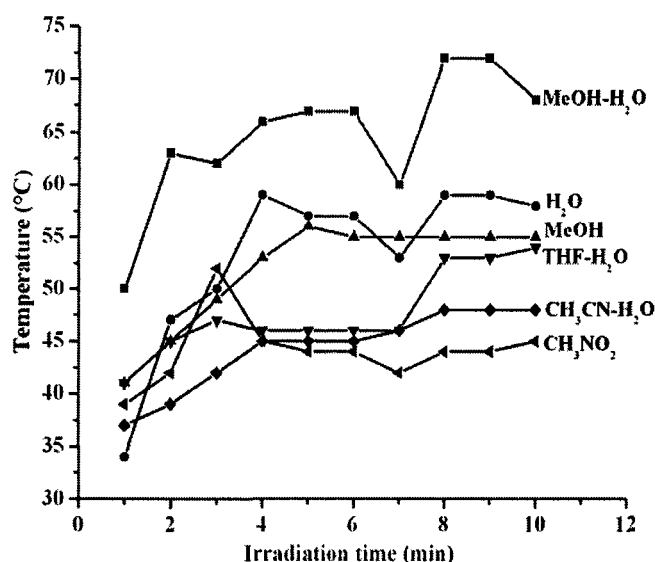


Figure 3B. 5: Effect of microwave irradiation time on different polar solvents

The investigation of effect of microwave power on amount of solvent is important to minimize solvent and energy used in the process. The results are depicted in figure 3B.6. This was studied at constant irradiation time where the microwave power was changed first by keeping amount of solvent fixed and then changed the amount of solvent by keeping microwave power fixed. In both cases temperature rises on increasing

amount of solvent as well as MW power. However, no significant effect was observed upon changing MW power for small amount of solvents.

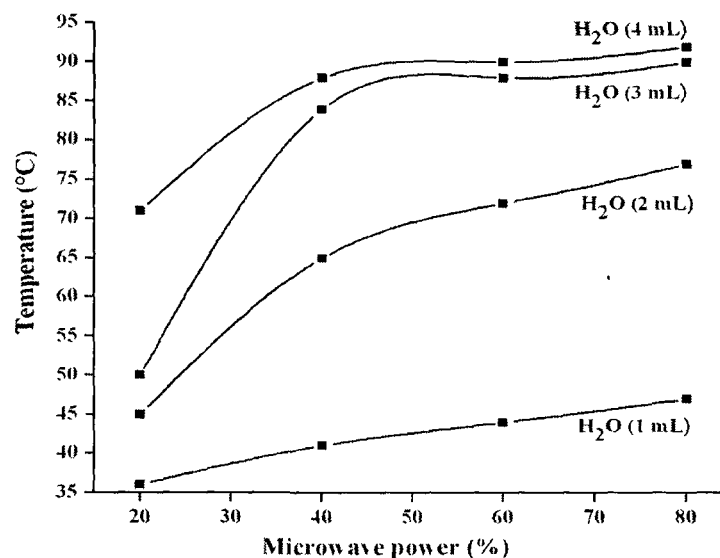


Figure 3B.6: Effect of microwave irradiation power on amount of solvent.

On increasing MW power from 140 watt to 560 watt, temperature rise for 1 mL H₂O was from 36 °C to 47 °C i.e. a rise of 11 °C, while temperature rise of 20 °C (71°C -91°C) was observed for 4 ml H₂O under same conditions. It shows that MW power does not have vast effect for small amount of solvents. Hence, 40 % power and 3 ml MeOH-H₂O solvent has been chosen as optimum amount in this study.

Following this step, Henry reaction with variety of aldehydes have been carried out by taking 3 mL H₂O-MeOH, 1 mmol aldehyde, 4 mmol nitromethane and 40 % microwave power at 50 °C to understand the effect of specific heating of microwave on formation of the desired product. The results are summarized in Table 3B.4. In comparison to room temperature methodology as described in section 3A, the reaction time greatly reduces from hours to minute (Table 3B.4) under microwave irradiation giving moderate to excellent yields (64-92%) within 2-15 minutes. The improved conversions and selectivities are not only the effect of rise of temperature of MeOH-H₂O solvent under microwave, can be suggested by heating the reaction mixture at 50 °C in oil bath. Table 3B.4 shows that the reaction complete within 2.5 hours [41] and less

[Chapter 3]

selective in comparison to microwave condition which takes only 1 minute with superior selectivities. The usefulness of MeOH-H₂O as reaction media under microwave can again be noted by comparing the obtained results with previous reports where nitroaldol reaction in ionic liquid medium [42] and supercritical CO₂ medium [43] at 50-60 °C gives inferior results in comparison to the present system. We have found that the reaction goes well with aromatic, heterocyclic and polycyclic aromatic aldehydes to afford the desired nitroaldol product in good yields. Reaction of aromatic aldehydes containing electron withdrawing groups like -NO₂ and -Cl (entries 3-6, Table 3B.4) are comparatively faster than aldehydes containing electron donating groups (entries 7-8, Table 3B.4) and gives 76-92 % yields within 1 minute. Besides, reaction with substituted nitrobenzaldehyde at para position (entry 3, Table 3B.4) is faster than that at ortho and meta positions (entries 4 & 5, Table 3B.4). Unsubstituted aldehyde like benzaldehyde smoothly proceed the reaction to give 75 % yield within 5 minutes. Heterocyclic and polycyclic aromatic aldehydes (entries 9&10, Table 3B.4) react slowly to give moderate yields within 15 minutes. Therefore, our strategy can be understood as efficient in terms of reaction time, conversions and selectivities which is tolerable to a varied substrates and gives respectable yields with all substrates.

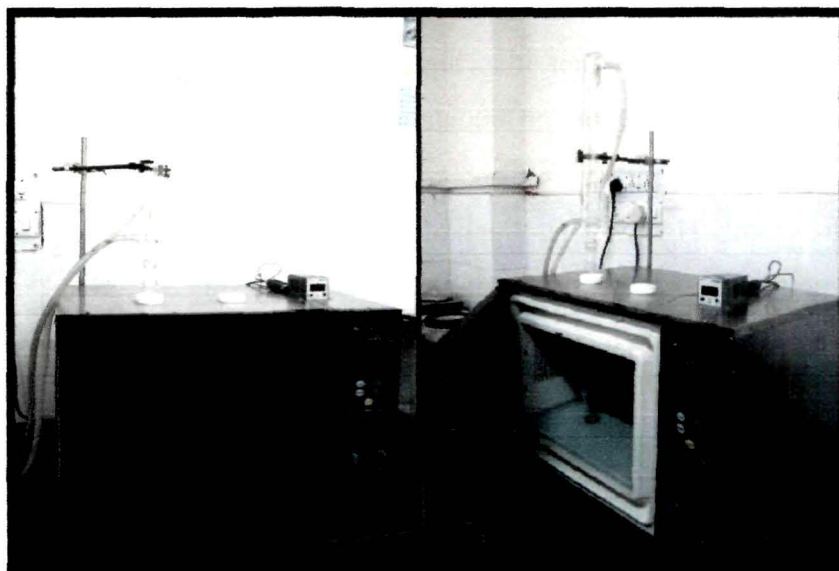
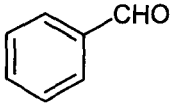
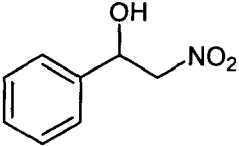
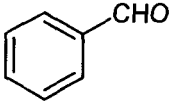
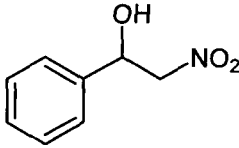
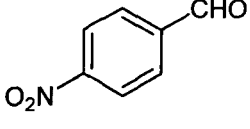
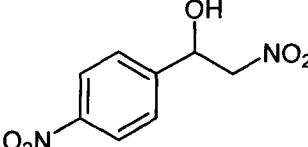
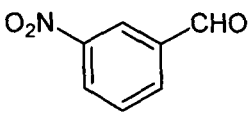
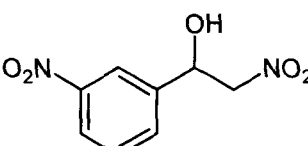
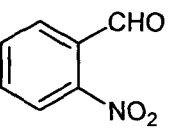
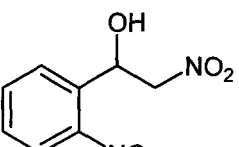
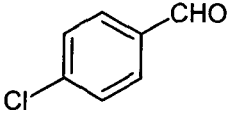
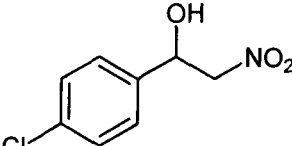
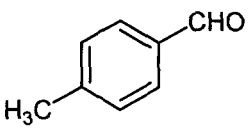
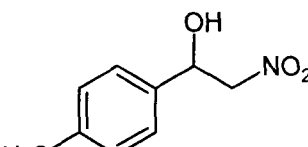
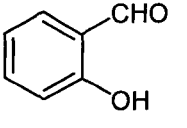
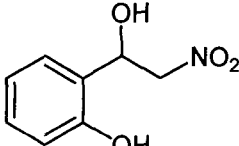
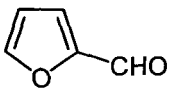
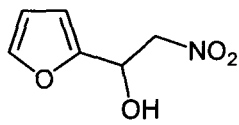
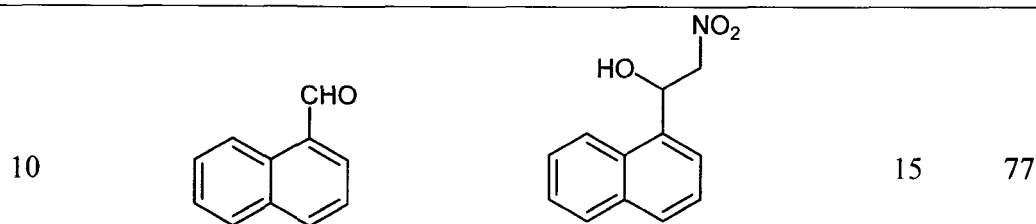


Image 1: Catalyst System Scientific Microwave

Table 3B.4: Henry reactions with various aldehydes under MW^a

Entry	Substrate	Product	Time (min)	Yield (%) ^b
(No catalyst)				
1			5	0
2			5	75
3			1 4 h 2.5 h 7 h	92 92 ^c 72 ^d 81 ^e
4			2	88
5			2	84
6			10	76
7			15	73
8			15	64
9			10	70



^a Reaction conditions: aldehyde (1 mmol), nitromethane (4 mmol), 10% KF/NaY (15 mg, calcined at 450 °C), MeOH-H₂O (3 ml), MW power (40%) at 50°C. ^b Isolated yields. ^c with of 4-nitrobenzaldehyde/nitromethane (1:2), 2mL solvent (MeOH-H₂O) and 0.02 g NaY/KF at room temperature, ^d Reaction with 1:1 of 4-nitrobenzaldehyde/nitromethane, 2mL solvent (MeOH-H₂O) and 0.02 g NaY/KF at 50 °C in oil bath, ^e Reactions 0.5mmol of aldehyde, 0.75mmol of nitromethane, 19–30mg Mg–Al HT in 1mL of ionic liquid.

The reusability of the catalyst was tested up to fourth cycle under similar reaction conditions to further enhance the scope of the catalyst. The catalyst was recovered from the reaction mixture through centrifugation, washed properly with distilled water and acetone and dried in an air oven at 150 °C for 24 h to clean the surface from adsorbed water and solvent molecules prior to the next run. The results are summarized in Table 3B.5. We have observed that the catalyst is active up to fourth run giving excellent conversions within 3 minutes. To confirm the effect of aqueous wash basicity upon conversion, we have stirred the catalyst with 3 ml water-methanol mixture for 24 h at room temperature, separated the catalyst by centrifugation and then performed the reaction with the filtrate under same reaction conditions. No conversion was detected through thin layer chromatography observation which proves that the basicity was imparted by the catalyst itself and the reaction was heterogeneously catalyzed.

Table 3B.5: Reusability study of KF/NaY for Henry reaction under MW

Entry	Run	Catalyst amount (mg)	Time (min) ^a	Conversion (%)
1	First	30	1	99
2	Second	26	1	99
3	Third	20	3	99
4	Fourth	13	3	88

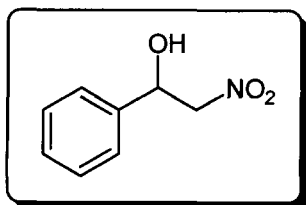
^aReactions were carried out in mmol scale with molar ratio 1:4 of 4-nitrobenzaldehyde/nitromethane, 3mL solvent (MeOH-H₂O) and KF/NaY at room temperature.

[Chapter 3]

Thus, we have we have described an efficient method of synthesis of β -nitro alcohols catalyzed by KF modified NaY zeolite under microwave irradiation condition which can be a good alternative to conventional synthesis. The method is fast and selective and superior to many literature methods. The reaction rate greatly enhances due to the combined effect of microwave and aqueous alcoholic reaction medium and the catalyst is recoverable up to fourth cycle to afford good yield in short time.

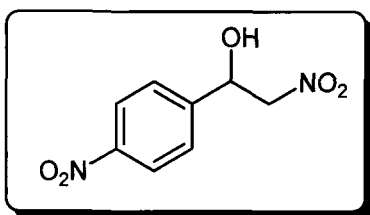
3B.4 Spectral data

(a) 2-Nitro-1-phenyl-ethan-1-ol (entry 1, Table 3B.4)



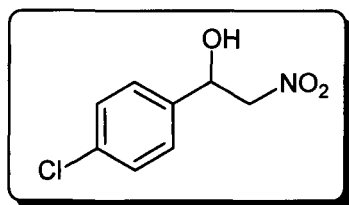
¹H NMR (400 MHz, CDCl₃): δ 7.46-7.33 (m, 5H, ArH), 5.48-5.41(m, 1H, -CH₂), 4.57-4.49 (m, 1H, -CH₂), 4.45-4.42 (m, 1H, -CH), 2.93 (brs, 1H, -OH) ;
¹³C NMR (100MHz, CDCl₃): δ 138.3, 132.3, 125.1, 125.8, 80.9 & 70.4; FTIR (KBr, ν = cm⁻¹): 3542, 3040, 1688, 1554, 1499 & 1378.

(b) 2-Nitro-1-(4-nitrophenyl) ethan-1-ol (entry 3, Table 3B.4)



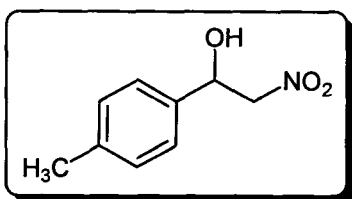
¹H NMR (400 MHz, CDCl₃): δ 8.22 (d, *J* = 8Hz, 2H, ArH), 7.62 (d, *J* = 8Hz, 2H, ArH), 5.59-5.61 (m, 1H, -CH), 4.48-4.60 (m, 2H, -CH₂), 3.52 (s, 1H, -OH); ¹³C NMR (100MHz, CDCl₃): δ 147.7, 144.9, 126.7, 123.8, 80.3 & 69.7; FTIR (KBr, ν = cm⁻¹): 3444, 3110, 2921, 1604, 1536 & 1338.

(c) 2-Nitro-1-(4-chlorophenyl) ethan-1-ol (entry 6, Table 3B.4)



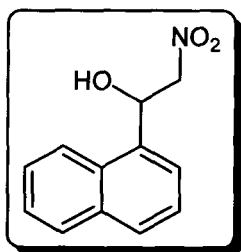
¹H NMR (400 MHz, CDCl₃): δ 7.40-7.35 (m, 4H, ArH), 5.47-5.43 (m, 1H, -CH), 4.46-4.46 (m, 2H, -CH₂), 3.92 (s, 1H, -OH); ¹³C NMR (100MHz, CDCl₃): δ 140.1, 134.8, 129.8, 126.1, 80.7 & 70.3; FTIR (KBr, ν = cm⁻¹): 3515, 2925, 1608, 1560, 1487 & 1382.

(d) 2-Nitro-1-(4-methylphenyl) ethan-1-ol (entry 7, Table 3B.4)



¹H NMR (400 MHz, CDCl₃): δ 7.35-7.26 (m, 4H, ArH), 5.47-5.40 (m, 1H, -CH), 4.62-4.54 (m, 1H, -CH₂), 4.46-4.54 (m, 1H), 2.88 (brs, 1H), 2.39 (s, 3H); FTIR (KBr, ν = cm⁻¹): 3441, 2928 & 1558.

(e) 2-Nitro-1-naphthyl-ethan-1-ol (entry 10, Table 3B.4)



¹H NMR (400 MHz, CDCl₃): δ 8.0-7.98 (m, 1H, ArH), 7.90-7.88 (m, 1H, ArH), 7.86-7.85 (m, 1H, ArH), 7.74-7.70 (m, 1H, ArH), 7.60-7.51 (m, 3H, ArH), 6.28-6.27 (m, 1H, -CH), 4.68-4.66 (m, 2H, -CH₂), 2.93 (brs, 1H, -OH); ¹³C NMR (100MHz, CDCl₃): δ 133.6, 133.5, 130.7, 130.2, 129.6, 129.5, 126.2, 124.6, 123.8, 121.9, 80.8 & 68.3.

3B.5 Spectral Images

Image 3B.5 (a-b): ¹H NMR spectra of crude reaction mixtures with various solvents

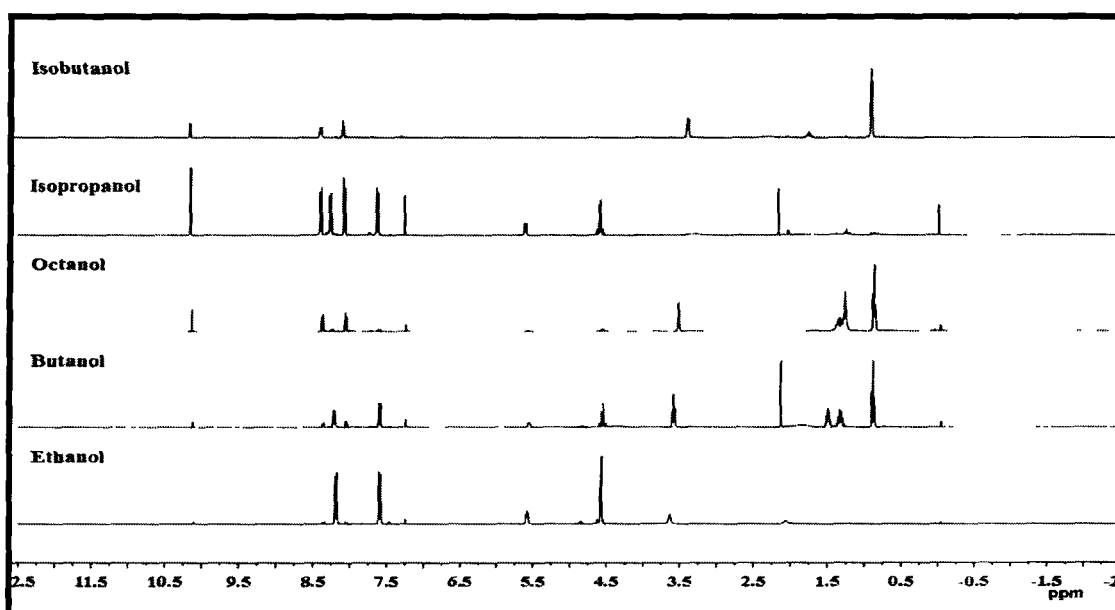


(Image 3B. 5a)

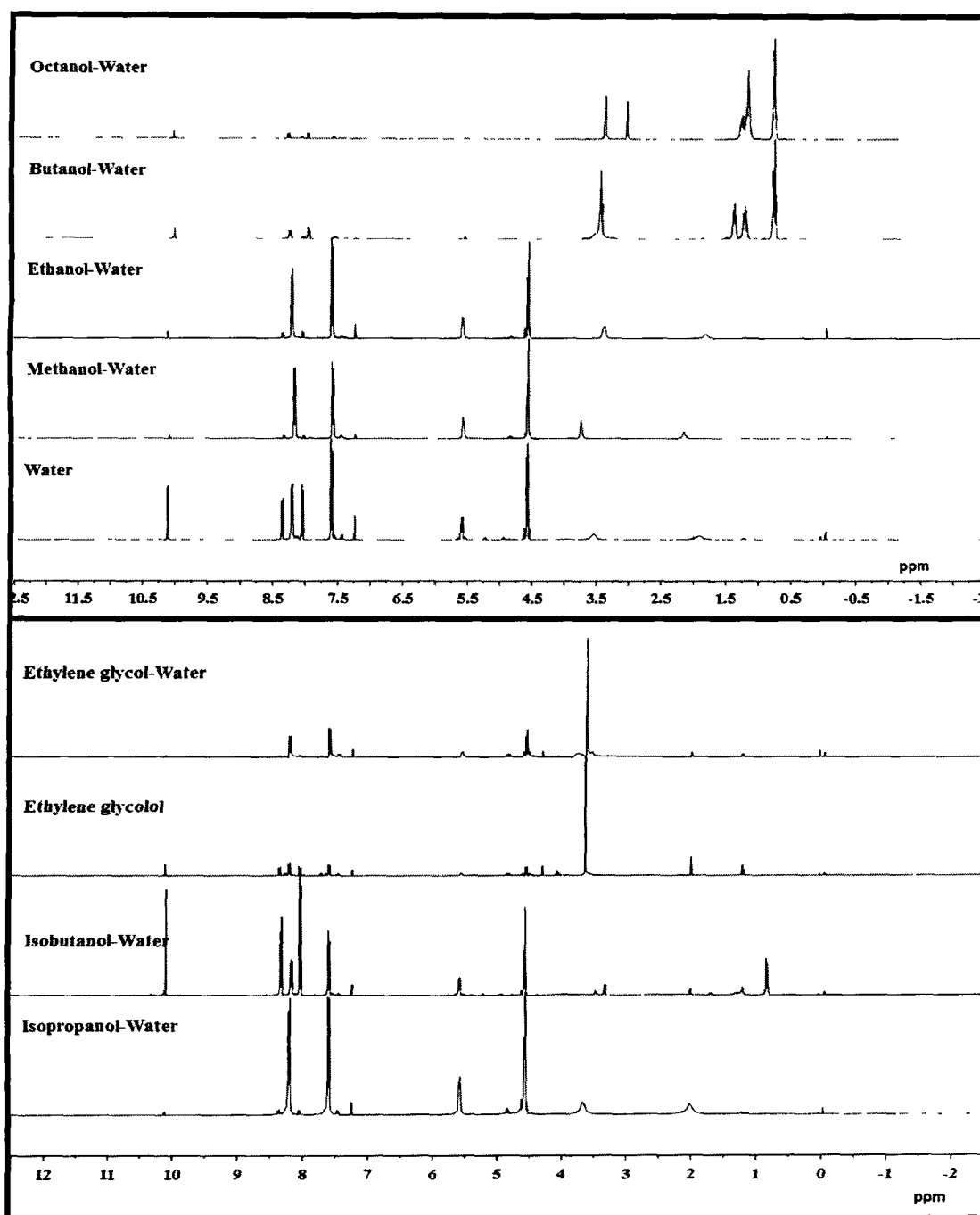


(Image 3B. 5b)

3B.6 References

- [1] Perreux, L. & Loupy, A. *Tetrahedron* **57** (45), 9199-9223, 2001.
- [2] Hayes, B.L. *Aldrichim. ACTA* **37** (2), 66-76, 2004.
- [3] Caddick, S. *Tetrahedron* **51** (38), 10403-10432, 1995.
- [4] Puligundla, P., et al. *J. Food Process. Technol.* **4** (11), 2013.
- [5] Sridhar, V. *Curr. Sci.* **74** (5) 446-450, 1998.
- [6] Hoz, A.D.L., et al. *Chem. Soc. Rev.* **34** (2), 164-178, 2005.
- [7] Roberts, B.A. & Strauss, C.R. *Accounts Chem. Res.* **38** (8), 653-661, 2005.
- [8] Trost, B.M. *Angew Chem. Int. Edit. Engl.* **34** (3), 259-281, 1995.
- [9] Gabriel, C., et al. *Chem. Soc. Rev.* **27** (3), 213-224, 1998
- [10] Varma, R.S. *Green Chem.* **1** (1), 43-55, 1999.
- [11] Varma, R.S. *Pure Appl. Chem.* **73** (1), 193-198, 2001.
- [12] Loupy, A., et al. *Synthesis* (9), 1213-1234, 1998.
- [13] Kabalka, G.W., et al. *Tetrahedron Lett.* **41** (27), 5151-5154, 2000.
- [14] Whittaker, A.G. & Mingos, D. M. P. *J. Microwave Power E. E.* **29** (4), 195-219, 1994.
- [15] Polshettiwar, V. & Varma, R.S. *Accounts. Chem. Res.* **41** (5), 629-639, 2008.
- [16] Chen, J., et al. *Green Chem.* **7** (2), 64-82, 2005.
- [17] Dallinger, D.; Kappe, C.O. *Chem. Rev.* **107** (7), 2563-2591, 2007.
- [18] Camacho, R.C., et al. *C. R. Chim.* **16** (5), 427-432, 2013.
- [19] Shankaraiah, N. *Synthesis* (13) 2163-2190, 2009.
- [20] Dahal, N., et al. *ACS Nano* **6** (11), 9433-9446, 2012.
- [21] Algul, O., et al. *Molecules* **13** (4), 736-748, 2008.
- [22] Ballini, R. & Bosica, G. *J. Org. Chem.* **62** (2), 425-427, 1997.
- [23] Rosini, G. & Ballini, R. *Synthesis* (11), 833-847, 1988.
- [24] Hattori, H. *Appl. Catal. A: Gen.* **222** (1-2), 247-259, 2001.
- [25] Sheldon, S.H. & Bekkum, H.V. *Fine Chemicals through Heterogeneous Catalysis*, Wiley, New York, 2001.
- [26] Martens, L.R.M., et al. *Stud. Surf. Sci. Catal.* **28**, 935-941, 1986.

[Chapter 3]

- [27] Martens, L.R.M., et al. *Nature* **315** (6020), 568-570, 1985.
- [28] Supamathanon, N., et al. *Quim. Nova* **35** (9), 1719-1723, 2012.
- [29] Davis, R.J. *J. Catal.* **216** (1-2), 396-405, 2003.
- [30] Refaat, A.A. *Int. J. Environ. Sc. Technol.* **8** (1), 203-221, 2011.
- [31] Ramos, M.J., et al. *Appl. Catal. A: Gen.* **346** (1-2), 79-85, 2008.
- [32] Brito, A., et al. *Energ. Fuel* **21** (6), 3280-3283, 2007.
- [33] Xu, Y., et al. *New J. Chem.* **28** (2), 244-252, 2004.
- [34] Yuan, X., et al. *Lat. Am. Appl. Res.* **37** (2), 151-156, 2007.
- [35] Garcia, F.A.C, et al. *J. Brazil. Chem. Soc.* **22** (10), 1894-1902, 2011.
- [36] Alwash, A.H., et al. *Adv. Chem. Eng. Sci.* **3** (2), 113-122, 2013.
- [37] B. Viswanathan, S. Sivasanker, A. V. Ramaswamy, *Catalysis Principles and Applications*, Daryaganj, New Delhi, 2006.
- [38] Zhu, J.H., et al. *Micropor. Mesopor. Mat.* **24** (1-3), 19-28, 1998.
- [39] Xue, W., et al. *Nat. Sci.* **1** (1), 55-62, 2009.
- [40] Noiroj, K., et al. *Renew. Energ.* **34** (4), 1145-1150, 2009.
- [41] Devi, R., et al. *Appl. Catal. A: Gen.* **433-434**, 122-127, 2012.
- [42] Khan, F.A., et al. *Tetrahedron. Lett.* **45** (15), 3055-3058, 2004.
- [43] Ballini R., et al. *J. Org. Chem.* **73** (21), 8520-8528, 2008.

Chapter 4

**MgAl-Hydrotalcite as solid base catalysts
for Knoevenagel condensation reaction**

Section 4A: Comparative study of structure and basicity of potassium salt modified MgAl hydrotalcite and their application for Knoevenagel condensation reaction

The Knoevenagel condensation reaction furnishes important intermediates of chemical and biological significance such as α -cyanocinnamates, α , β -unsaturated esters, α,β -unsaturated nitriles and α,β -unsaturated acids [1-4]. Various synthetic strategies have been continuously investigated to carry out this reaction by efficient and benign ways among which the use of heterogeneous catalysts in place of homogeneous ones and room temperature synthesis are worth mentioning [5-9]. Hydrotalcites and hydrotalcite like compounds are considered as important solid base materials for a good number of organic reactions such as Aldol condensation reaction [10], Knoevenagel reaction [11], Claisen-Schmidt reaction [12], Michael addition [13] etc. What makes these layered material more attractive in the field of catalysis is that the synthetic procedure is simple, their basic properties can be tuned by loading other basic guest materials in the structure and replacing the interlayer anions with various counter-anions by simple exchange method, getting different properties at various calcination temperatures and possibility to reconstruct the structure after activation [14,15]. Impregnation of basic guests is a common strategy to increase basic properties of solid bases including hydrotalcites [16-18]. Hydrotalcites after calcination above 400-450 °C gives mixed metal oxides and generally exhibits high surface area and strong basic strengths which can be used either as catalysts or catalyst supports [19]. However, it has been reported that uncalcined hydrotalcites are more preferred for base catalyzed organic reactions due to the presence of Brønsted basic sites i.e. the surface -OH groups [20,21]. Therefore, increasing basic properties of uncalcined hydrotalcites would be more interesting for catalysis of Knoevenagel condensation reaction. Among various basic guests, potassium salt has proved to be effective for a number of supports [22]. However, effect of guest over structure and basicity are not well studied for hydrotalcite like compounds.

Therefore, this section focuses on investigation of structural and basic properties of hydrotalcites and their catalytic performances for Knoevenagel condensation reaction.

[Chapter 4]

This section describes the preparation of a series of potassium salt loaded hydrotalcites by impregnation of KF, K₂CO₃, KHCO₃, KNO₃ and KOH salts over calcined Mg-Al hydrotalcite (3:1 ratio) and the effect of these base precursors on structure and basicity of the loaded and reconstructed hydrotalcite. The results of catalytic activities for Knoevenagel condensation reaction of aldehydes and active methylene compounds have also been presented herein. The detailed methods of synthesis and characterization techniques were given in the experimental section (Chapter 2).

4A.1. Results and discussion

4A.1.1. Characterization of Mg-Al hydrotalcites loaded with potassium salts

Having prepared the parent hydrotalcite and potassium salt loaded hydrotalcites according to the procedure described in 2.2.4, initial investigation of structural parameters was done through powder X-ray diffraction analysis (XRD). The XRD patterns of parent hydrotalcite and potassium salt loaded hydrotalcites are presented in Figure 4A.1.

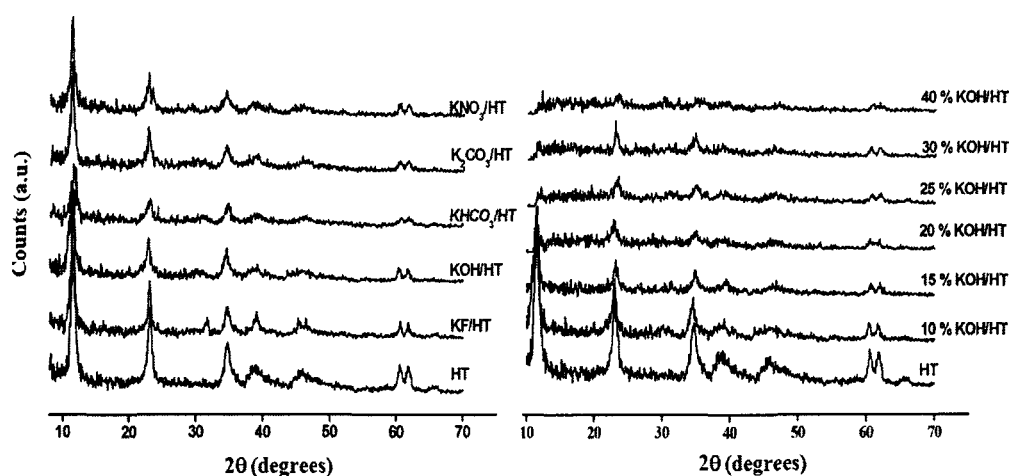


Figure 4A.1: Powder x-ray diffraction pattern of potassium loaded hydrotalcites

Reflections of parent hydrotalcite (HT) at 2θ values 11.5, 23.05, 34.7, 38.35, 45.95, 60.5 and 61.75° corresponding to (003), (006), (102), (105), (108), (110) and (113) planes, respectively indicates the formation of highly crystalline hydrotalcite layered structure which corroborate well with literature reports [23,24]. Besides, presence of strong peaks for (003) and (006) reflections of all potassium salt loaded samples confirms the

rehydration and reconstruction of hydrotalcite phase after loading. However, shifting of 2θ position to slightly higher or lower values and diminished intensity of loaded samples can be attributed to the presence of potassium salts on hydrotalcite structure. It has been observed from figure 4A.1 that the salts KOH, KHCO_3 and K_2CO_3 are well dispersed over the support while KF and KNO_3 loaded hydrotalcites showed some additional diffraction lines in the XRD pattern. Therefore, KOH, KHCO_3 and K_2CO_3 can be considered as more preferred than KF and KNO_3 . To understand the effect of loading, relative crystallinity (%) of the loaded hydrotalcites were investigated. Comparison of relative crystallinity (%) calculated from three high intensity peaks at 2θ values 11.50 (003), 23.05 (006) and 34.70 (102) has been presented in figure 4A.2. The highest recovery of hydrotalcite structure after loading was achieved for KOH/HT and the lowest recovery was found for KHCO_3 /HT. Besides, crystallinity loss is greater for hydrotalcites loaded with salts having larger anions i.e. CO_3^{2-} , HCO_3^- and NO_3^- , while it is minimum for KOH/HT. This shows that KOH is more preferred over the other salts.

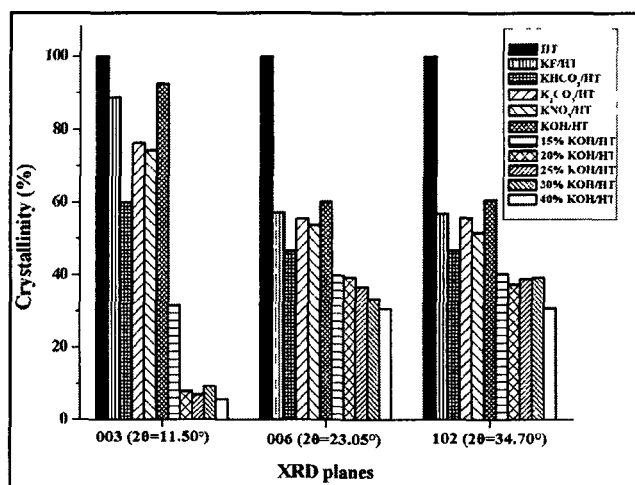


Figure 4A.2: Crystallinity (%) of different potassium loaded hydrotalcites

Following this, the structural parameters such as crystallite sizes, unit cell parameters 'a' (cation-cation distance in the brucite like layer), 'd' (basal spacing between the layers) and 'c' (thickness of one brucite like layer and one interlayer) were calculated and summarized in Table 4A.1. Peaks corresponding to (003) reflection was considered to calculate basal spacing (d) between the layers and cell parameter 'c' ($c = 3d_{003}$) and

[Chapter 4]

(110) reflection was used to calculate unit cell parameter 'a' ($a = 2d_{110}$) [25,26]. Comparing the parameters of original hydrotalcite to the loaded ones, we have observed that no considerable change of 'a' occurs after loading. This suggests that loading of salts does not have considerable effect over metal-metal distances in the brucite layers [27]. On the contrary, basal spacing 'd' and cell parameter 'c' increases after loading. This again supports reconstruction of hydrotalcite structure with well-defined layers after loading. We have observed that the increase of c and d are larger for KOH/HT ($d_{003}=7.93$; $c=23.79$) in comparison to the other samples ($d_{003}= 7.70-7.80$; $c= 23.10-23.40$) which again shows highest recovery of layered structure after loading. Therefore, a stability order of the support in presence of the salts can be understood from the overall findings of X-ray diffraction results which follows the trend as KOH/HT ~ K₂CO₃/HT > KF/HT > KHCO₃/HT ~ KNO₃/HT. This confers that among the studied salts KOH is the preferred salt over hydrotalcite support. Smaller crystallite size of KOH/HT (Table 4A.1) in comparison to others is again in favour of its selection as preferred catalyst in our study [28]. Following this, KOH amount of 15-40% (w/w) was loaded by the impregnation method to have a better understanding of its effect over the support.

Table 4A.1: Calculation of lattice parameter and basal spacing of potassium salt loaded hydrotalcites

Sample	(003) reflection, 2θ (°)	d ₀₀₃ (Å)	(110) reflection, 2θ (°)	d ₁₁₀ (Å)	a (Å)	c (Å)	Crystallite size (003)
HT	11.5	7.70	60.50	1.53	3.06	23.10	128.09
KF/ HT	11.50	7.70	60.60	1.52	3.05	23.10	135.56
KHCO ₃ /HT	11.45	7.73	60.55	1.52	3.05	23.19	153.65
K ₂ CO ₃ /HT	11.35	7.80	60.35	1.53	3.06	23.40	135.70
KNO ₃ / HT	11.35	7.80	60.20	1.53	3.07	23.40	164.93
KOH/ HT	11.15	7.93	60.35	1.53	3.06	23.79	82.31

Figure 4A.1 shows that the layered structures remain preserved up to 20 % loading of KOH while the structure collapsed above it and reflection for (003) plane was completely destroyed for 25-40 % loaded samples. However, loading of 15 % and 20 % KOH cannot

[Chapter 4]

be encouraged in our study due to high loss of crystallinity. Loading 15 % KOH over the support shows the loss of crystallinity more than six times than that of 10 % loaded sample. This has validates that loading of KOH beyond 10 % is not effective over hydrotalcite support. Hence, 10 % KOH/HT has been conceded as the best catalyst in this study.

Thermogravimetric analysis (TGA) and Differential thermal analysis (DTA) pattern of uncalcined samples recorded between temperature range of 20-500 °C are shown in figure 4A.3. Presence of four decomposition steps corresponding to typical hydrotalcite structure have been observed for all the samples [29]. The first weight loss step in the temperature range 20 °C - 90 °C corresponds to the loss of physically adsorbed water on the surface and loss of 1-12 % weight occur in the process. In the second step, 12-15 % weight loss takes place in the range of 80 °C - 250 °C due to the loss of interlayer water molecules. In the third step i.e. 250 °C - 415 °C, dehydroxylation and partial loss of carbon dioxide takes place showing 13-22 % weight loss while the fourth step corresponds to the loss of carbon dioxide from the samples in temperature range of 395 °C-518 °C showing a weight loss of 2-4 %. The heat flow steps, temperature ranges and amount of weight loss in the samples are depicted in Table 4A.2. All the weight loss steps other than the step for interlayer water loss of all loaded samples are similar to the parent hydrotalcite. In case of interlayer water loss, it takes place only in single step for HT, KF/HT and KNO₃/HT. On the other hand, it takes place in several steps for KOH/HT, KHCO₃/HT and K₂CO₃/HT. This shows that the water molecules may be linked in different environment in presence of different guest molecules. It is noteworthy to mention that the collapse of brucite layers of the loaded samples start at lower temperatures in comparison to the parent hydrotalcite and dehydroxylation becomes slower in presence of the salts. We have observed that dehydroxylation is the fastest in case of KNO₃/HT and slowest in case of KOH/HT which in turn confers that the hydrotalcite phase is less stable in presence of KNO₃ salt and more stable in presence of KOH. Thus, TGA and DTA analyses reveal that hydrotalcite layer collapse earlier for KNO₃/HT and KF/HT in comparison to the other three i.e. KOH/HT, KHCO₃/HT and K₂CO₃/HT. Hence, a stability order of hydrotalcite layered structure can be presented in order as KNO₃/HT < KF/HT < KHCO₃/HT < K₂CO₃/HT < KOH/HT. This result is in

[Chapter 4]

good evidence with XRD observations that KOH/HT is the most stable catalyst and the preferred catalyst in this study.

Table 4A.2 Thermo gravimetric and Differential thermal analysis results of the potassium salt loaded hydrotalcites.

Sample	Heat flow step (°C)	Temperature (°C)	Weight loss (%)	Total weight loss (%)
HT	23-88	73	1.5	42.8
	88-253	197	15.3	
	253-412	382	22.5	
	412-518	470	3.5	
KF/HT	21- 82	33	5	38
	82-236	192	12.4	
	236-414	353	16.6	
	414-506	445	4	
KOH/HT	20-86	47	7.2	43.1
	86-224	103, 141, 199	12.5	
	224-415	360	19.5	
	415-500	458	3.9	
KHCO ₃ /HT	20-91	53	12.4	44.5
	91-228	111 and 191	12	
	228-401	353	15.8	
	401-500	478	4.3	
K ₂ CO ₃ /HT	20-77	49	5.7	42.1
	77-245	101, 166 and 195	14.2	
	245-409	359	17.5	
	409-505	463	4.7	
KNO ₃ /HT	28-72	55	3.2	35.3
	72-232	91 and 190	11	
	232-395	341	18.4	
	395-500	447	2.6	

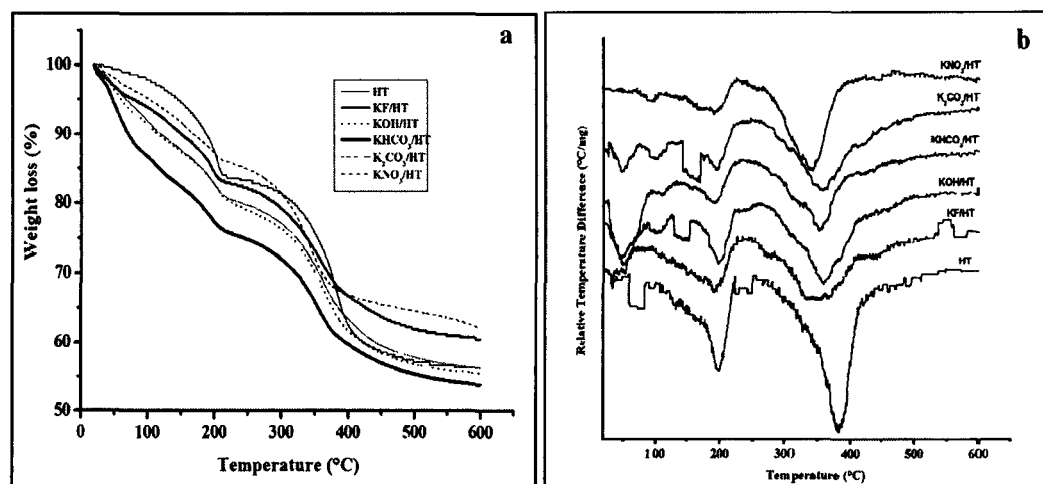


Figure 4A.3: Thermogravimetric analysis (a) and differential thermal analysis (b) patterns of different hydrotalcites

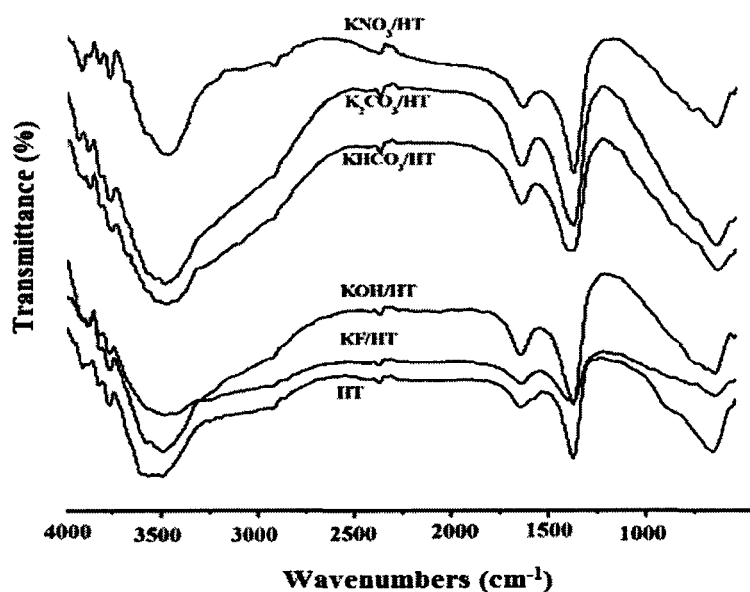


Figure 4A. 4: FTIR patterns of hydrotalcites loaded with potassium salts

The FTIR spectra of prepared hydrotalcites are presented in Figure 4A.4. The structural vibrational pattern of hydrotalcites are observed in both the parent hydrotalcite and all loaded hydrotalcites [30]. Absorption at $3450\text{--}3600\text{ cm}^{-1}$ in all hydrotalcites is attributed to the stretching vibration of --OH groups in the brucite like layers as well as interlayer water molecules. On the other hand, weak band at around $1640\text{--}1650\text{ cm}^{-1}$ is

due to bending vibration of interlayer water molecules. Both these vibrations of KNO_3/HT and KF/HT are weaker than KHCO_3/HT , $\text{K}_2\text{CO}_3/\text{HT}$ and KOH/HT confirming the low water content of these materials which in turn agree well with previous findings of TGA, DTA and XRD analyses. Band at about 1380 cm^{-1} is due to the presence of CO_3^{2-} anions in interlayer while vibration at 860 cm^{-1} can be assigned for covalent carbonate. Absorption in the low frequency range 661 and 510 cm^{-1} are due to Mg-O and Al-O bonds in all samples. Besides, broad absorption bands at around $3600\text{-}2800\text{ cm}^{-1}$ for KOH/HT , $\text{K}_2\text{CO}_3/\text{HT}$ and KHCO_3/HT samples indicate large water content in the surface as well as in the interlayer spacing. This again correlates well with thermogravimetric analysis of the samples confirming high interlayer water content of these samples.

Nitrogen adsorption-desorption measurements were carried out to get information about specific surface area, pore sizes and pore volumes of the materials. The textural properties of parent hydrotalcite and potassium salt loaded hydrotalcites are given in Table 4A. 3. The parent hydrotalcite exhibits BET surface area $207\text{ m}^2\text{g}^{-1}$. Introduction of potassium species decreases the BET surface area of all the samples. It is observed that surface area of K_2CO_3 loaded hydrotalcite is lost to the greater extent in comparison to the other four salts and decrease upto $90\text{ m}^2\text{g}^{-1}$. We have also observed that the pore volume of $\text{K}_2\text{CO}_3/\text{HT}$ is the smallest among the five and decreases from $0.23\text{ cm}^3\text{g}^{-1}$ of parent hydrotalcite to $0.19\text{ cm}^3\text{g}^{-1}$ of the loaded one. This may be due to the blockage of pores and interlayer spaces by the large CO_3^{2-} anions of K_2CO_3 , thus preventing N_2 molecules to adsorb onto the surface. Conversely, surface areas of KNO_3/HT and KF/HT are $201\text{ m}^2\text{g}^{-1}$ and $197\text{ m}^2\text{g}^{-1}$ respectively which can be expected in accordance with the low water content of these materials as described earlier. We have found intermediate values of surface areas for the samples KOH/HT and KHCO_3/HT . This can be attributed to the high water content in these samples. It is also observed from Table 4A.3 that KOH/HT sample shows the largest pore volume and pore diameter with comparable surface area as that of the parent hydrotalcite. Thus, surface areas and pore sizes of loaded hydrotalcites, other than K_2CO_3 salt, are not abruptly affected after loading the salts. Figure 4A.5 (a-e) shows N_2 adsorption-desorption isotherms and pore size distribution curves of the parent HT and loaded hydrotalcites. All hydrotalcites exhibit

type II isotherm and H3 hysteresis loops characteristics of both monolayer and multilayer adsorption and typical for aggregated powders like clays or cements having no uniform pore structures [31,32]. Type H3 hysteresis loops are generally found for non-rigid aggregates of plate-like particles or assemblages of slit-shaped pores in the sample. It has again been confirmed from the pore size distribution curves of the samples which shows broad range of pore sizes in the samples. However, narrow pore size distribution centered at pore radius of 20 Å and large pore volume of KOH/HT has led us to select it as the optimum sample in this study.

The SEM images of parent hydrotalcite and KOH/HT in magnification of X4000 and X5500 are shown in Figure 4A.6 (a1-b2). The parent hydrotalcite has crystal sizes in nanometer ranges with homogeneous shapes of the crystals. On loading KOH onto it, particle size decreases showing layers of agglomerated sheets in the ranges of 1-2 micrometer.

The qualitative and quantitative basic properties of all hydrotalcites measured by Hammett indicator method and titration method are summarized in Table 4A.3. Hydrotalcites loaded with KF, K₂CO₃, KNO₃ and KOH after drying at 80 °C for 15 h showed colour change in presence of 2,4-dinitroaniline (H_L = 15) indicator, while could not change the colour of 4-chloro-2-nitroaniline (H_L = 17.2). Hence, their base strengths lie in the range i.e. 15 < H_L < 17.2. On the other hand, the unloaded parent hydrotalcite and KHCO₃/HT showed colour change with Tropaeolin-O (H_L = 11.1–12.7) but could not change the colour with 2,4-dinitroaniline (H_L = 11.1–12.7) indicator. Thus their base strengths lies in the range 12.7 < pK_{BH+} < 15. Total basicity measurement of the samples shows that the number of total basic sites for K₂CO₃/HT and KOH/HT are higher than the other samples. This is reflected in the catalytic activities shown in Table 4A.5 that the conversions for KOH/HT and K₂CO₃/HT are higher than the other catalysts. Soluble basicities of the samples are quite low. It is observed that the total number of basic sites of all the catalysts are relatively low as compared to calcined hydrotalcites reported in literature [33]. Hence, calcination of hydrotalcites is important to increase the strength of basic sites as well as to total number of basic sites. However, it is quite obvious from Table 4A.5 that although the number of total basic sites is not very high, uncalcined hydrotalcites also can fairly catalyze Knoevenagel condensation reaction with its

moderate base strengths. Thus, loading of alkali metal compounds over hydrotalcites would be acknowledged to catalyze some base catalyzed organic reactions such as Knoevenagel reaction, Nitroaldol condensation reaction etc.

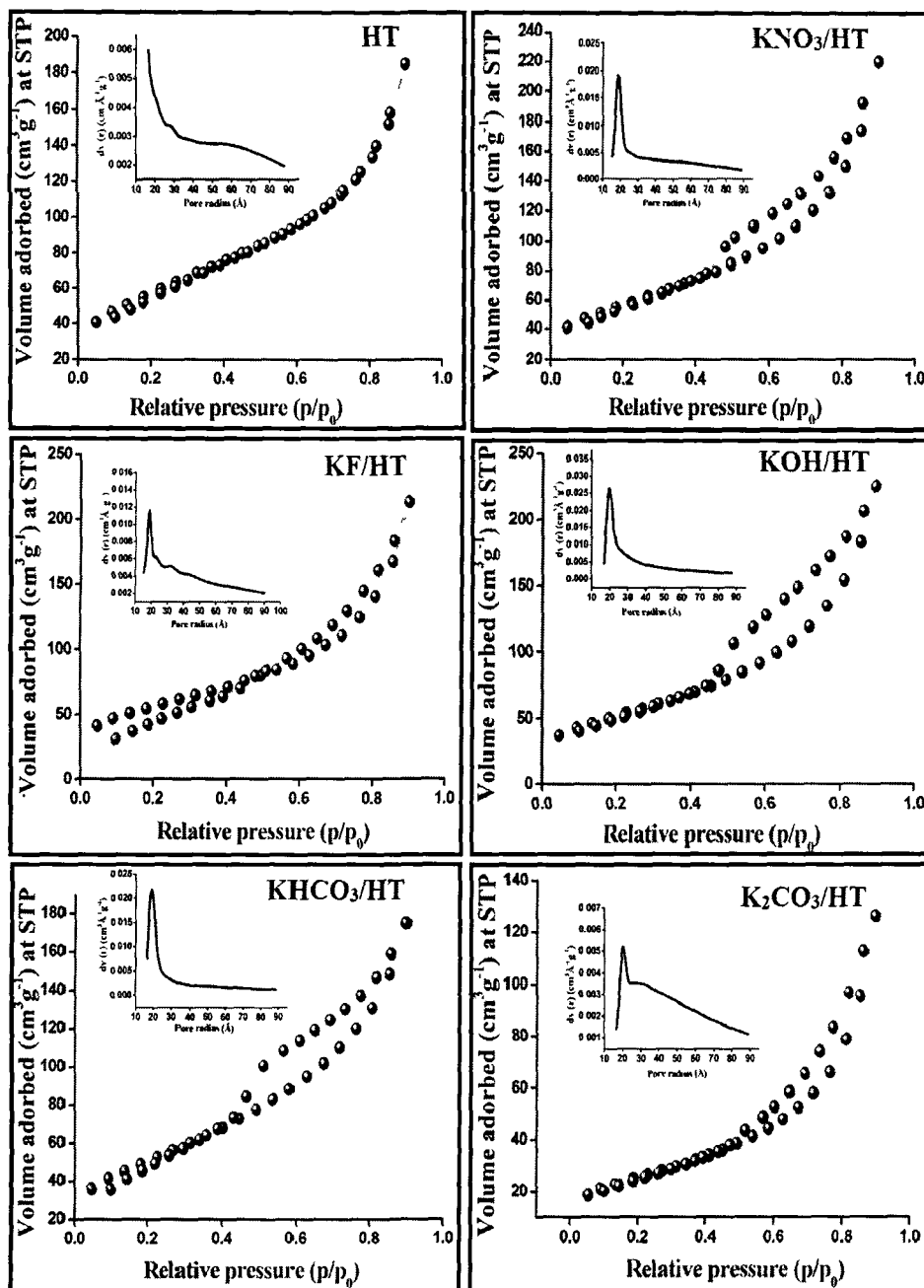


Figure 4A.5: Nitrogen adsorption/desorption isotherms and corresponding pore size distribution curves of HT and loaded HT dried at 80 °C for 15 h

[Chapter 4]

Table 4A.3 Textural properties of potassium salt loaded hydrotalcites

Sample	BET Area (m^2g^{-1})	Pore volume (cm^3g^{-1})	Pore diameter (nm)	Base Strength Of unc (H _L)	Total basicity (mmolg^{-1})	Soluble basicity (mmolg^{-1})
HT	207	0.23	3.30	12.7 < H _L < 15	0.12	0.00 ^a 0.00 ^b
KF /HT	197	0.32	3.38	15 < H _L < 17.2	0.18	0.02
KHCO ₃ /HT	184	0.25	3.95	12.7 < H _L < 15	0.18	0.03
K ₂ CO ₃ /HT	90	0.19	3.99	15 < H _L < 17.2	0.23	0.05
KNO ₃ / HT	201	0.32	3.66	15 < H _L < 17.2	0.19	0.00
KOH /HT	185	0.36	4.00	15 < H _L < 17.2	0.22	0.03

^aUncalcined hydrotalcite, ^bReconstructed hydrtalcite

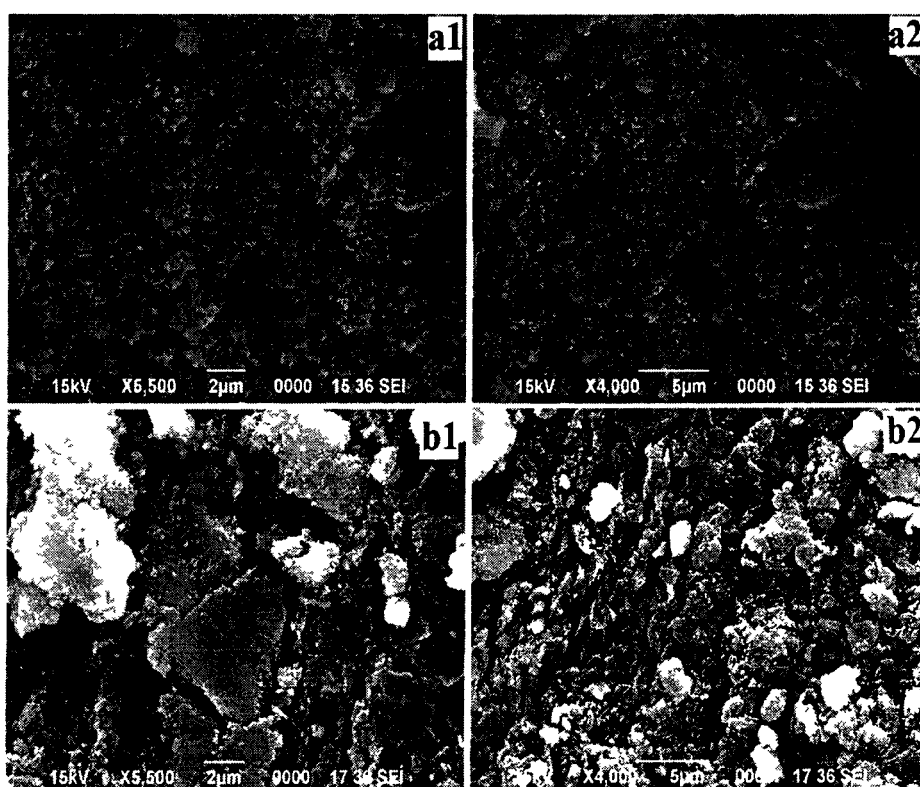


Figure 4A.6: Scanning electron micrographs of (a) HT and (b) KOH/HT at two different resolutions

Following this, we have also calculated reactivity of the O-atoms using density functional based reactivity descriptor, Fukui function. Fukui functions, f_o^+ and f_o^- , are evaluated using Hirshfeld population analysis (HPA) and Mulliken population analysis (MPA) schemes to locate the nucleophilic and electrophilic sites, respectively. Though an analytical expression for the Fukui function is not available, it is usually calculated using finite difference approximation which is called condensed Fukui function. The condensed Fukui function of an atom 'O' in a molecule with N electrons at constant external potential, $v(\vec{r})$ can be expressed as:

$$f_o^+ = \frac{1}{\Delta N} [\rho_o(N_o + \Delta N) - \rho_o(N_o)] \quad (\text{for nucleophilic attack})$$

(1a)

$$f_o^- = \frac{1}{\Delta N} [\rho_o(N_o) - \rho_o(N_o - \Delta N)] \quad (\text{for electrophilic attack})$$

(1b)

where, $\rho_o(N_o)$, $\rho_o(N_o + \Delta N)$ and $\rho_o(N_o - \Delta N)$ are charge densities on atom O of the system with N_o , $N_o + \Delta N$ and $N_o - \Delta N$ electron systems, respectively. In conventional Fukui function computations, a value of 1.0 is used for ΔN . In the present calculation, we have used a value of 0.1 for ΔN . The values of Fukui functions are given in Table 4A.4.

We have calculated the fukui functions (f_o^+ and f_o^-), relative electrophilicity (f_o^+/f_o^-) and relative nucleophilicity (f_o^-/f_o^+) for those oxygen atoms in the hydrotalcite system having higher values of these reactivity parameters. In general, it is observed that for a particular atom in a molecule, the increase in f_o^- values is the indication of high basicity. From Table 4A.4, it has been seen that the highest f_o^- value is obtained for the oxygen atom number 38, which is the one attached to the Potassium atom. Relative electrophilicity, (f_o^+/f_o^-) and relative nucleophilicity, (f_o^-/f_o^+) are better reactivity parameters to locate the preferable site for nucleophilic and electrophilic attacks, respectively in a chemical system [34]. The basicity of a system increases with the increase of (f_o^-/f_o^+) ratio.

Table 4A. 4: The values of Fukui functions with respect to Mulliken and Hirshfeld charges of the basic oxygen atoms of the metal oxide

Atom	Fukui function (f_o^+)		Fukui function (f_o^-)		Relative electrophilicity (f_o^+/f_o^-)		Relative nucleophilicity (f_o^-/f_o^+)	
	MPA	HPA	MPA	HPA	MPA	HPA	MPA	HPA
O 38	0.026	0.025	0.019	0.027	1.37	0.93	0.73	1.08
O 65	-0.001	0.006	0.002	0.005	-0.50	1.20	-2.00	0.83
O 69	0.021	0.022	0.021	0.022	1.00	1.00	1.00	1.00
O 80	0.004	0.006	0.002	0.006	2.00	1.00	0.50	1.00
O 83	0.017	0.019	0.017	0.020	1.00	0.95	1.00	1.05

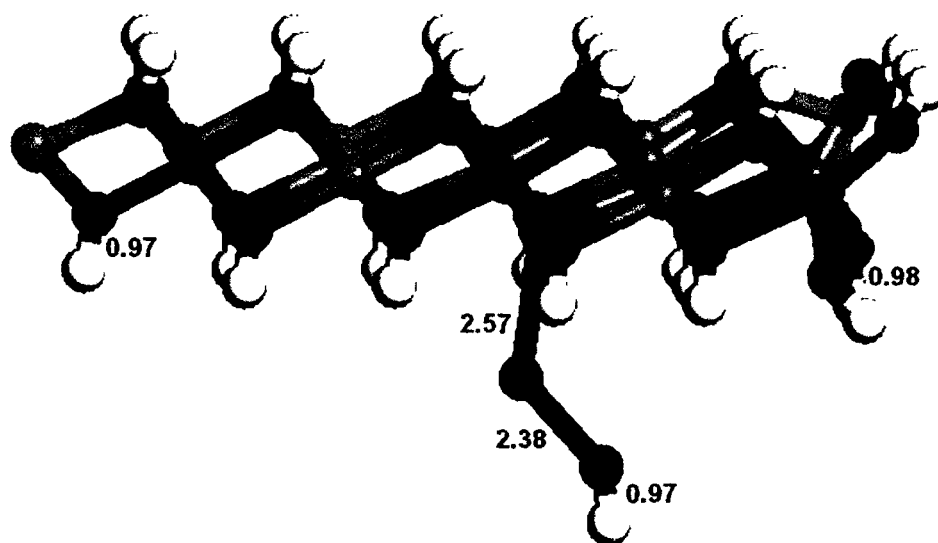
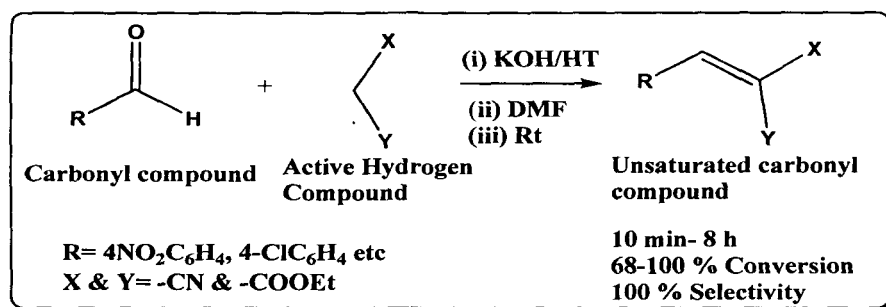


Figure 4A. 7: Optimized structure for most stable geometry of Mg₃Al(OH)₈KOH. The green balls represent Magnesium, pink represent Aluminium, purple represent Potassium, red represent oxygen and the grey balls represent Hydrogen atoms in the optimized geometry. The Oxygen atoms having larger values of $f(-)$ (higher basicity) are numbered and the bond lengths are in Å

Thus, the oxygen attached to the potassium having highest value of relative nucleophilicity (f_o^-/f_o^+) will be the most basic site. From this calculation we have inferred that the O-atom attached to the K-atom have highest values of f_o^- as well as f_o^-/f_o^+ . Therefore, we can conclude O38 is the most basic site in the hydrotalcite system. The optimized structure of the hydrotalcite is shown in Figure 4A.7. The oxygen atoms for which the reactivity parameters have been evaluated are marked, and these are the atoms having higher basic character in the system.

4A.1.2 Catalytic reaction

The catalytic activities of the parent and potassium salt loaded hydrotalcites were evaluated for liquid phase Knoevenagel condensation reaction at room temperature (Scheme 4A.1).



Scheme 4A.1: Knoevenagel condensation reaction catalyzed by KOH/HT

It is well known that the conversion of an organic reaction is mainly influenced by parameters such as solvent, temperature, effect of substituted groups in the substrates, amount of catalysts etc. Taking these points in to consideration, we have first performed the reaction at room temperature without any catalyst by taking malononitrile and p-nitrobenzaldehyde as model reactants and methanol as solvent at room temperature. The reaction does not progress without catalyst. Therefore, the reaction was carried out with all modified hydrotalcites as well as rehydrated hydrotalcite under the same reaction conditions. The results are summarized in Table 4A.5. Reaction with rehydrated hydrotalcite is comparatively slower than the loaded hydrotalcite (entry 2, Table 4A.5). It

has been observed that the reaction in methanol is not selective for all the catalysts. Among the studied catalysts, KNO₃/HT and KF/HT catalysts give better results in terms of selectivity which can be correlated to their larger surface areas than the other loaded catalysts.

Table 4A. 5 Knoevenagel condensation reaction with different potassium salt loaded hydrotalcites at room temperature.

Entry	Sample	Time (min)	% Conversion ^a	% Selectivity ^a
1	No catalyst	30	0	-
2	HT ^b	30	41	90
3	KNO ₃ /HT	30	57	91
4	KF /HT	30	42	90
5	K ₂ CO ₃ /HT	30	63	69
6	KOH /HT	30	66	81
7	KHCO ₃ /HT	30	61	76
8	KOH	30	-	-

Conditions: p-nitrobenzaldehyde (1 mmol), malononitrile (1 mmol), methanol (3 mL), catalyst (25 mg), reaction temperature: r t

^a Obtained from ¹H NMR analysis of the crude reaction mixture

^b Reconstructed hydrotalcite obtained by immersion of the mixed oxide MgAl in water for 24 h

In addition, it can be conferred from TGA results described above that due to low water content (physically adsorbed water and interlayer water) in KNO₃/HT and KF/HT, aprotic environment of the catalyst makes the aldol type intermediate to dehydrate easily thus showing better selectivity of the Knoevenagel product in comparison to KOH/HT, KHCO₃/HT and K₂CO₃/HT. However, comparatively low conversions with KNO₃/HT and KF/HT catalysts can be attributed to the interaction of the salts with the support forming new phases and thus reducing some active sites of the catalysts (XRD). Again, KHCO₃/HT and K₂CO₃/HT shows low selectivities in comparison to KNO₃/HT and KF/HT (entries 5 & 7, Table 4A.5) which can also be related to the low surface area and high water content of these catalysts. On the other hand, the preferred catalyst of this

[Chapter 4]

study i.e. KOH/HT (entry 6, Table 4A.5) showed the highest conversion, largest pore volume, longest pore diameter and good selectivity within 30 minutes which drive us to carry out the reaction further with this catalyst to optimize the reaction conditions. High conversion of KOH/HT is also supported by its small crystallite sizes (Table 4A.1) which may favour the active hydroxyl groups to take part in the reaction. It is notable that the selectivity of the reaction is mainly dominated by solvent methanol which requires screening of the reaction with different solvents.

Table 4A.6: Effect of various solvents on Knoevenagel condensation reaction at room temperature

Entry	Solvent	Time (min)	% Conversion ^a	% Selectivity ^a
1	Toluene	40	99	100
2	DMF	15	99	100
3	MeOH	30	66	81
4	Acetonitrile	15	81	100
5	DCM	15	99	100
6	Diethyl ether	4h	61	100

Conditions: p-nitrobenzaldehyde (1 mmol), malononitrile (1 mmol), solvent (3 mL), catalyst (25 mg);

Catalyst: 10 % KOH/HT, ^aObtained from ¹H NMR yield of the crude reaction mixture.

To understand the effect of solvents over conversions and selectivity, the reaction was investigated with six different solvents having varying polarity with 10 % KOH/HT at room temperature. The results are depicted in Table 4A.6. It is observed that solvents play a significant role on both conversions as well as selectivities. When aprotic polar solvents were used (entries 2, 4 and 5, Table 4A.6), the reaction was faster giving 81-99 % conversion and 100 % selectivity within 15 minutes. On the other hand, polar protic solvents like methanol react comparatively show and gives moderate conversion and selectivity within 30 minutes (entry 3, Table 4A.6). Non-polar solvents like toluene and diethyl ether (entries 1, 6) takes longer reaction time than polar solvents giving 61-99 % conversion and 100 % selectivities within hours. It is noteworthy to mention that in this study DMF is superior to the most commonly used solvent toluene for Knoevenagel

condensation reaction with hydrotalcite catalysts. It can be attributed that the reactants are miscible well in a polar environment and forms a homogeneous mixture with the catalyst during vigorous stirring condition. Thus interaction of the catalyst with reactants becomes feasible in DMF in comparison to non-polar solvents toluene and diethyl ether. Hence, it can be suggested from Table 4A. 6 that DMF is the best choice in terms of conversion, selectivity and reaction time.

We then next used 10 % KOH/HT and DMF solvent for Knoevenagel condensation reaction of various aromatic aldehydes and active methylene compounds (malononitrile and diethyl malonate) at room temperature. The results are summarized in Table 4A.7. Knoevenagel condensation reaction was reported previously with hydrotalcite like catalysts such as rehydrated Mg-Al hydrotalcite, metal loaded Mg-Al hydrotalcite in different reaction media and optimized reaction conditions [36,37]. In our attempt, the rehydration of hydrotalcites and loading have been done in the same step and found them as efficient catalysts for this reaction. We have observed that the result goes hand in hand with previous literature results where 21wt %/MgO-ZrO₂ [38] and 10.3 wt % K-MgAl(O) [39] in DMF medium showed comparable conversion to the present study. As seen from the Table 4A.7, aldehydes with both electron donating and electron withdrawing groups reacted efficiently with malononitrile under similar reaction condition to give 99 % conversions and 100 % selectivity of the corresponding olefins (entries 5, 7). Aldehydes containing electron withdrawing groups (entries 2, 5; Table 4A.7) reacted faster than aldehydes bearing electron donating groups (entry 8; Table 4A.7). We have observed that the substrates having electron withdrawing groups in the ortho-, meta- and para- positions do not have much effect over the reaction time. Polycyclic aromatic aldehyde such as naphthaldehyde also reacted efficiently giving 99 % conversion within 1 hour. On the other hand, rehydrated catalyst takes comparatively longer reaction time than the loaded catalysts and gives 99 % conversion and 100 % selectivity within 40 minutes (entry 3, Table 4A.7). It can be attributed to the higher basicity of the loaded catalysts thus completing the reaction within short time. The as prepared hydrotalcite took longer reaction time than the rehydrated hydrotalcite to complete the reaction and gives 99 % conversion within 90 minutes (entry 4, Table 4A.7). With diethyl malonate as active

Table 4A. 7 Knoevenagel condensation reaction of different aldehydes and active methylene compounds with 10 % KOH/HT.

Entry	R	X	Time	% Conversion ^a	% Selectivity ^a
1	Ph	CN	30 min	99	100
2	4-NO ₂ C ₆ H ₄	CN	15 min	99	100
			15 min	97 ^b	
			10 min	99 ^c	
3	4-NO ₂ C ₆ H ₄	CN	40 min	99 ^d	100
4	4-NO ₂ C ₆ H ₄	CN	90 min	99 ^e	100
5	2-NO ₂ C ₆ H ₄	CN	15 min	99	100
6	4-ClC ₆ H ₄	CN	10 min	99	100
7	4-CH ₃ C ₆ H ₄	CN	1 h	99	100
8	4-OHC ₆ H ₄	CN	1 h	99	100
9	1-Naphthyl	CN	1 h	99	100
10	4-NO ₂ C ₆ H ₄	COOEt	4 h	99	100
11	2-NO ₂ C ₆ H ₄	COOEt	4 h	99	100
12	4-ClC ₆ H ₄	COOEt	4 h	99	100
13	4-CH ₃ C ₆ H ₄	COOEt	8 h	82	100
14	4-OHC ₆ H ₄	COOEt	8 h	77	100
15	1-Naphthyl	COOEt	8 h	68	100
16	4-ClC ₆ H ₄	CN	15 min	99 ^f	100

Conditions aldehyde (1 mmol), malononitrile (1 mmol), DMF (3 mL), 10 % KOH/HT (25 mg),

^a Obtained from ¹H NMR yield of the crude reaction mixture

^b Aldehyde (2 mmol), malononitrile (2 mmol), 21 wt %/MgO-ZrO₂ (20 mg), DMF (1 mL)[39]

^c Aldehyde (2 mmol), malononitrile (2 mmol), 10.3 wt % K-MgAl(O) (20 mg), DMF (1 mL)[40]

^d Reaction with rehydrated hydrotalcite

^e Reaction with as prepared hydrotalcite after drying at 80 °C for 15 h,

^f 4th run with recovered catalyst

[Chapter 4]

methylene compound, all the substrates reacted slowly giving 70-90 % conversion and 100 % selectivity within 4-8 hours. This is due to decrease of acidity of the acidic protons of the active methylene compound in presence of two ester groups. We have also evaluated the efficiency of the catalyst by performing the reaction between malononitrile and 4-chlorobenzaldehyde for four repetitive cycles. The catalyst has been found active upto fourth cycle and gives 99 % conversion and 100 % selectivity within 15 minutes (entry 16, Table 4A.7). On the whole, potassium hydroxide loaded MgAl-hydrotalcite acts as an efficient solid base catalyst for Knoevenagel condensation reaction at room temperature.

Thus, we have found that KOH loaded MgAl-hydrotalcite acts as an efficient catalyst for Knoevenagel condensation reaction in presence DMF at room temperature to afford 99 % conversion and 100 % selectivity within 10 minutes.

4A.3 References

- [1] Perin, G., et al. *J. Braz. Chem. Soc.* **16** (4) 857-862, 2005.
- [2] Peng, Y. & Song, G. *Green Chem.* **5** (6), 704-706, 2003.
- [3] Freeman, F. *Chem. Rev.* **80** (4), 329-350, 1980.
- [4] Mosaddegh, E. & Hassankhani, A. *Catal. Commun.* **33**, 70-75, 2013.
- [5] Zhu, D.J., et al. *Green Chem.* **12** (3), 514-517, 2010.
- [6] Gawande, M.B., et al. *Chem. Soc. Rev.* **42** (12), 5522-5551, 2013.
- [7] Knoevenagel, E. *Chem. Ber.* **27**, 2345, 1894.
- [8] Islam, S.K., et al. *J. Mol. Catal. A: Chem.* **394**, 66-73, 2014.
- [9] Prida, K.M. & Rath, D. *J. Mol. Catal. A: Chem.* **310** (1-2), 93-100, 2009.
- [10] Roelofs, J.C.A.A., et al. *J. Catal.* **203** (1) 184-191, 2001.
- [11] Costantino, U., et al. *J. Mol. Catal. A: Chem.* **195** (1-2), 245-252, 2003.
- [12] Guida, A., et al. *Appl. Catal. A: Gen.* **164** (1-2) 251-264, 1997.
- [13] Choudhary, B.M., et al. *J. Mol. Catal. A: Chem.* **146** (1-2), 279-284, 1999.
- [14] Kannan, S. *Catal. Surv. Asia* **10** (3-4), 117-137, 2007.
- [15] Nalwade, P., et al. *J. Sci. Industr. Res.* **68** (4), 267-272, 2009.
- [16] Gao, L., et al. *Biomass Bioenerg.* **34** (9), 1283-1288, 2010.
- [17] Martens, L.R., et al. *Stud. Sulf. Sci. Catal.* **28**, 935-941, 1986.
- [18] Gao, L., et al. *Energ. Fuels* **24** (1), 646-651, 2010.
- [19] Kutalek, P., et al. *Fuel. Process. Technol.* **122**, 176-181, 2014.
- [20] Wang, Z., et al. *J. Catal.* **318**, 108-118, 2014.
- [21] Kumbhar, P.S., et al. *Chem. Commun.* (10), 1091-1092, 1998.
- [22] Wang, Y., et al. *Micropor. Mesopor. Mater.* **77** (2-3), 139-145, 2005.
- [23] Millange, F., et al. *J. Mater. Chem.* **10** (7), 1713-1720, 2000.
- [24] Corma, A., et al. *J. Catal.* **148** (1), 205-212, 1994.
- [25] Obadiah, A., et al. *Dig. J. Nanomater. Bios.* **7**, 321-327, 2012.
- [26] Zeng, H.Y., et al. *Fuel* **87** (13-14), 3071-3076, 2008.
- [27] Silva, C.C.C.M., et al. *Fuel Process. Technol.* **91** (2), 205-210, 2010.
- [28] Abello, S., et al. *Chem. Eur. J.* **11** (2), 728-739, 2005.

[Chapter 4]

- [29] Kloprogge, J.T. & Frost, R. L. *Appl. Catal. A: Gen.* **184** (1), 61-71, 1999.
- [30] Moreno, M.J.H., et al. *Phys. Chem. Minerals* **12** (1), 34-38, 1985.
- [31] Rouquerol, F., Rouquerol, J., and Sing, K. *Adsorption by powders and porous solids*; Academic Press, San Diego, USA, 1999.
- [32] Triantafyllidis, K.S., et al. *J. Colloid Interf. Sci.* **342** (2), 427-436, 2010.
- [33] Sahu, P.K., et al. *J. Mol Catal. A: Chem.* **395**, 251-260, 2014.
- [34] Deka, R.C., et al. *Chem. Phys. Lett.* **389** (1-3), 186-190, 2004.
- [35] Deka, R.C., et al. *Bull. Catal. Soc. India* **8**, 140-155, 2009.
- [36] Debeker, D.P., et al. *Chem. Eur. J.* **15** (16), 3920-3935, 2009.
- [37] Nishimura, S., et al. *Green Chem.*, **15** (8), 2026-2042, 2013.
- [38] Zhao, J., et al. *RSC Adv.* **4** (12), 6159-6164, 2014.
- [39] Zhao, J., et al. *Appl. Catal. A: Gen.* **467**, 33-37, 2013.

Section 4B: KNO₃ supported MgAl-mixed oxide as solid base catalyst for liquid phase Knoevenagel condensation reaction under microwave irradiation condition

Knoevenagel condensation reaction occupies a fundamental position in the domain of organic chemistry [1-3]. The importance of this reaction lies in the possibility of formation of various intermediates such as α -cyano cinnamates, α,β -unsaturated esters, cinnamic acid and α,β -unsaturated nitriles having significant interests in many areas of sciences including chemical, biological and pharmaceutical sciences [4-9]. In the journey of searching eco-friendly synthesis of these intermediates, a good number of strategies have been investigated by various groups of researchers from different field of sciences. Among these, use of benign reaction media such as ionic liquids and water, solventless synthesis, use of heterogeneous solid catalysts, supported catalysts, microwaves and ultrasound are found successful in the recent years [10-14]. Microwave irradiation technology as alternating heating source has been utilized to enhance chemical reactions from very early days [15-18]. It has become an unavoidable technique for quick synthesis of inorganic and organic compounds in the laboratories [19]. Due to its core heating mechanism, activation and coupling of reactant molecules become more facile to give desired products within short reaction time [20]. Therefore, combining the advantages of microwave energy with heterogeneous solid base catalyst system would be helpful to meet the requirement of cleaner synthesis, high yield, and short reaction time. Among varieties of heterogeneous base catalysts, layered double hydroxides (LDH) are considered as promising solid base catalysts for their excellent basic properties and tunable characteristics [21,22]. Hydrotalcite after activation in the range of 400-500 °C gives mixed metal oxide phase and strong basic sites which make them excellent basic materials for various applications like chemical and pharmaceutical processes, photo catalysis, synthesis of biodiesel and adsorbent purposes [23-27]. Besides, hydrotalcites after impregnation of base precursors like alkali or alkaline earth metal salts over their structures and subsequent calcination further increases the basic properties. Knoevenagel

[Chapter 4]

condensation have been found successful with both supported and unsupported hydrotalcites in the recent years [28-30]. Zhao et al. have shown that KOH loaded MgAl mixed oxide possesses strong base sites ($H_{\text{L}} > 26.5$) and is a highly active catalyst for Knoevenagel condensation reaction at room temperature [31].

In this section, we have described loading of a series of potassium salts i.e. KF, K_2CO_3 , KHCO_3 , KNO_3 and KOH over host MgAl-mixed oxide and their effect on structure and basic properties of the mixed oxide phase after calcination at 450 °C and 550 °C. We have also described the optimization of catalysts and reaction conditions for liquid phase Knoevenagel condensation reaction under microwave irradiation condition. The correlation of catalytic activity and their physico-chemical properties has also been explained here in this section. The detailed methods of modification and characterization techniques are described in Chapter 2.

4B.1 Results and discussion

4B.1.1 Characterization of Potassium Loaded Mg-Al mixed oxides

Powder XRD patterns of MgAl-hydrotalcites (3:1) after loading with KOH, KF, KHCO_3 , K_2CO_3 and KNO_3 salts calcined at 450 °C and 550 °C are shown in figure 4B.1(a-b). All samples undergo phase transition in different speed under the same calcination temperature and display quite different XRD patterns. After calcination at 450 °C, $\text{K}_2\text{CO}_3/\text{MgAl}(\text{O})$ and $\text{KHCO}_3/\text{MgAl}(\text{O})$ samples remain in hydrotalcite phase [32] and slowly convert into MgAl(O) phase while KOH/ MgAl(O) shows both hydrotalcite as well as the mixed oxide phase [33]. On the other hand, KF/MgAl(O) remain slightly in hydrotalcite phase and convert rapidly into MgAl(O) phase. The hydrotalcite phase for $\text{KNO}_3/\text{MgAl}(\text{O})$ has been completely converted into MgAl(O) phase showing additional diffraction lines in the XRD pattern. This clearly confirms the rapid conversion of KNO_3/HT into mixed oxide phase at 450 °C and poor stability in hydrotalcite phase. It is also interesting to observe that KF/MgAl(O) and $\text{KNO}_3/\text{MgAl}(\text{O})$ exhibit similar XRD pattern as the host MgAl(O) at 450 °C and convert easily to mixed metal oxide phase. Therefore, catalysis of calcined hydrotalcites will be more supportive with KF and KNO_3 salts compared to KOH, KHCO_3 and K_2CO_3 . Relative crystallinity (%) study shown in figure 4B.2 reveals that crystallinity (%) due to 003 reflection ($2\theta = 11.5^\circ$) of samples

[Chapter 4]

calcined at 450 °C decreases in the order HT > K₂CO₃/MgAl(O) > KHCO₃/MgAl(O) > KOH/MgAl(O). This signifies that the hydrotalcite phase is retained well by the presence of K₂CO₃ and converts slowly into mixed oxide phase in comparison to the other salts. Conversely, crystallinity of reflection centered at $2\theta = 43^\circ$ due to formation of MgO phase decreases in the order KNO₃/MgAl(O) > MgAl(O) > KF/MgAl(O) > KOH/MgAl(O). This observation confirms the rapid conversion of hydrotalcite phase into mixed oxide phase in presence of KNO₃.

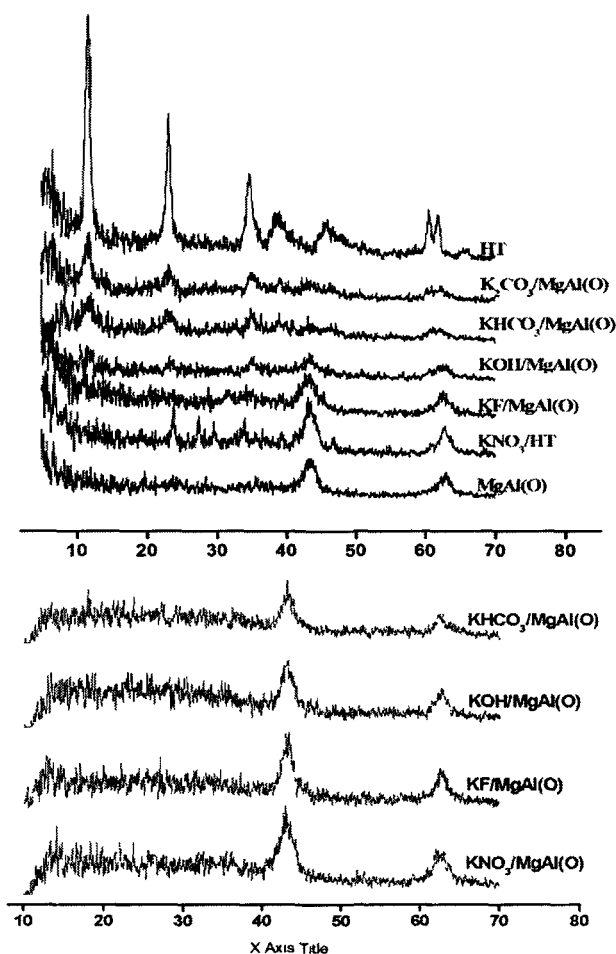


Figure 4B.1: Powder X-ray diffraction pattern of potassium loaded MgAl-mixed oxides, (a) at 450 °C and (b) at 550 °C

However, calcination at 550 °C converts all loaded samples into MgAl mixed oxide phase. At this time also crystallinity (%) trend due to reflection at $2\theta = 43^\circ$ is similar to that observed in case of samples calcined at 450 °C. Thus, quick formation of

the mixed oxide phase in presence of various potassium salts can be understood from the obtained results which follow the trend $\text{KNO}_3/\text{MgAl}(\text{O}) > \text{KF}/\text{MgAl}(\text{O}) > \text{KOH}/\text{MgAl}(\text{O}) > \text{KHCO}_3/\text{MgAl}(\text{O}) > \text{K}_2\text{CO}_3/\text{MgAl}(\text{O})$.

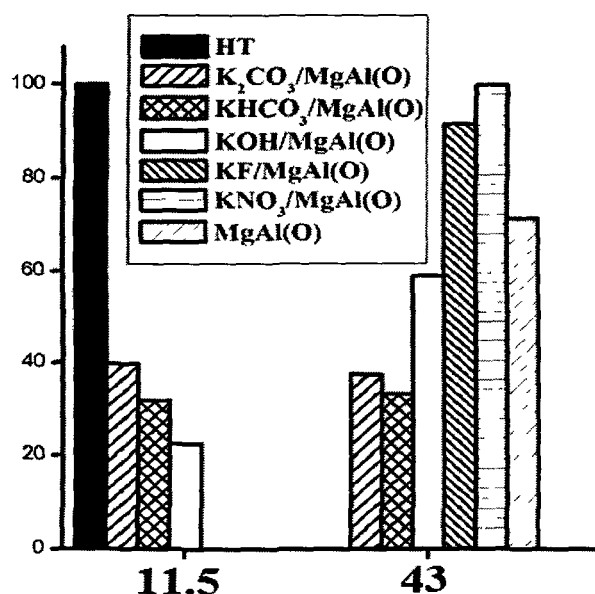


Figure 4B.2: Relative crystallinity (%) of loaded hydrotalcites calcined at 450 °C

FTIR spectra of the loaded mixed oxides and the host $\text{MgAl}(\text{O})$ after activation at 450 °C and 550 °C are presented in Figure 4B.3(a-b). Intensity of bands due to $-\text{OH}$ stretching vibration of surface $-\text{OH}$ groups as well as interlayer water molecules (3450 cm^{-1}), bending mode of water molecules in the interlayer region (1640 cm^{-1}) and CO_3^{2-} vibration (1380 cm^{-1}) are reduced significantly in the calcined samples in comparison to the uncalcined hydrotalcite and suggests the loss of water molecules as well as CO_2 from the structure [34]. The band position at 1640 cm^{-1} is a direct indication of the extent of hydrogen bonding of water molecules inside interlayer region [35]. Since no significant shifting of band position at 1640 cm^{-1} has been observed for all the samples calcined at 450-550 °C, no considerable information about H-bonding can be obtained for interlayer water molecules after calcinations [35]. On the other hand, after calcination at 450 °C, the $-\text{OH}$ stretching vibrational band (3450 cm^{-1}) of all samples other than $\text{KNO}_3/\text{MgAl}(\text{O})$ has been shifted 50-60 cm^{-1} to the lower wave number region from the uncalcined

[Chapter 4]

hydrotalcite sample. This indicates that H-bonding of surface -OH groups with remaining interlayer water molecules and CO_3^{2-} anions are more prominent after calcinations [36]. Conversely, for $\text{KNO}_3/\text{MgAl}(\text{O})$ sample, the -OH stretching band has been shifted around 30 cm^{-1} to higher wavenumber region from uncalcined sample which in turn shows weak H-bonding (free surface -OH groups) in the sample.

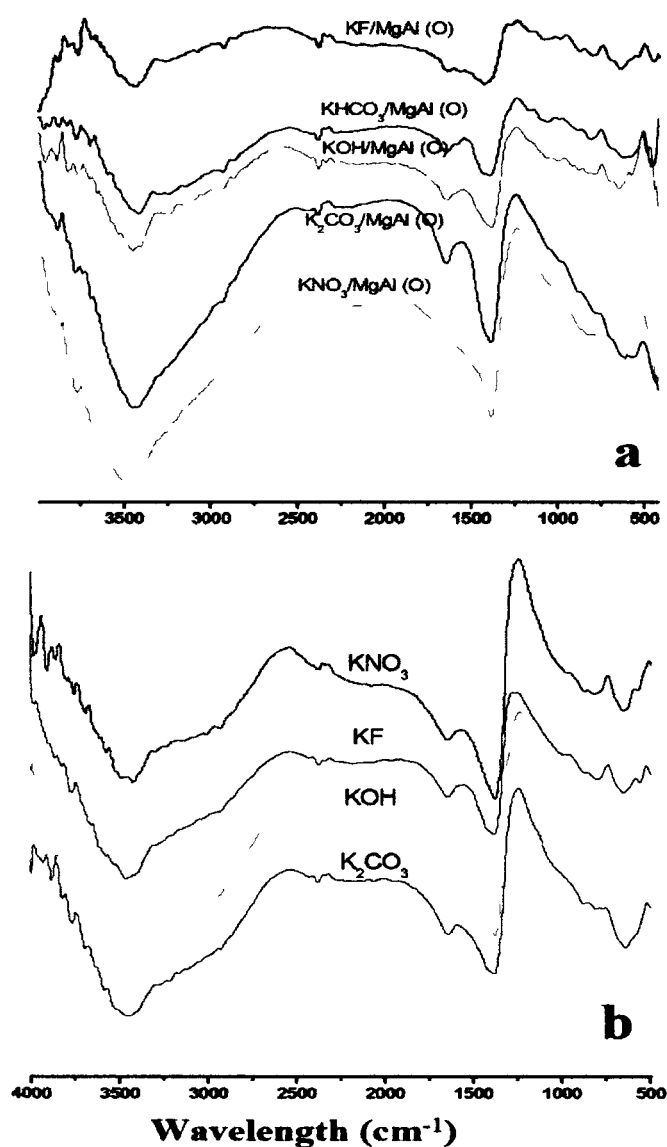


Figure 4B.3: FTIR patterns of MgAl-mixed oxides loaded with potassium salts (a) calcined at 450 °C (b) calcined at 550 °C

This is in accordance with XRD observation confirming the loss of interlayer water more rapidly in presence of KNO_3 . Besides, -OH stretching band is quite sharper for KF/MgAl(O) and $\text{KNO}_3/\text{MgAl(O)}$ in comparison to $\text{K}_2\text{CO}_3/\text{MgAl(O)}$, KOH/MgAl(O) and $\text{KHCO}_3/\text{MgAl(O)}$ samples and thus indicates higher loss of interlayer water molecules from these two samples. Moreover, disappearance of broad band near 3000 cm^{-1} for $\text{KNO}_3/\text{MgAl(O)}$ and KF/MgAl(O) shows decrease of hydrogen bonding [37] between carbonate anions and water molecules in the interlayer galleries. This has been further confirmed by the sharp CO_3^{2-} absorption bands at 1380 cm^{-1} for these samples [38]. Thus, FTIR pattern of the samples calcined at $450\text{ }^\circ\text{C}$ reveals that the interlayer water molecules of hydrotalcite have been lost faster in presence of KF and KNO_3 in comparison to K_2CO_3 , KHCO_3 and KOH . Samples calcined at $550\text{ }^\circ\text{C}$ shows sharp -OH stretching vibrational bands at 3440 cm^{-1} corresponding to hydroxyl groups attached with Al and Mg in the brucite layers [39]. Bands at around 661 and 510 are due to characteristics vibrations for Mg-O and Al-O bonds of metal oxides [40].

The SEM measurements were carried out to determine the morphology and particle size distribution of the modified and calcined Mg-Al hydrotalcites. For this purpose, $\text{KNO}_3/\text{MgAl(O)}$, KF/MgAl(O) , and KOH/MgAl(O) calcined at $450\text{ }^\circ\text{C}$ were selected and observed through SEM at different magnification ranges. Figure 4B.4 (a-c) shows SEM images of the samples having magnification of micrographs at 5,500x and 30,000x. Initial look at the images clearly shows the crystalline nature of all the samples with different particle sizes and agglomeration of particles. It is observed that $\text{KNO}_3/\text{MgAl(O)}$ forms small crystals with homogeneous particle sizes and shape (0.064-1.93 μm), KOH/MgAl(O) forms flat crystals with non-homogeneous particle sizes (0.195-1.24 μm) and KF/MgAl(O) forms agglomerated and homogeneous leaf like crystals (70-90 nm). Due to these variations of morphologies, different catalytic activities can be expected for all the catalysts.

The specific surface area measurements and pore size distribution of calcined hydrotalcites by N_2 adsorption-desorption technique are summarized in table 4A.1. Activation at $450\text{ }^\circ\text{C}$ decreases the surface area of all samples. This is due to gradual collapse of hydrotalcite phase and incomplete formation of the mixed oxide phase. Rehydrated hydrotalcite after calcination at $450\text{ }^\circ\text{C}$ shows type II adsorption isotherms

and H3 hysteresis loops according to IUPAC classification and associate with the of unrestricted monolayer-multilayer adsorption and slit-shaped pores of the structure [41]. Similar isotherm plots and pore types were also found for $\text{KHCO}_3/\text{MgAl}(\text{O})$ and $\text{KNO}_3/\text{MgAl}(\text{O})$ samples showing slit-shaped pores in their structure. It is observed that the $\text{KHCO}_3/\text{MgAl}(\text{O})$ which retained hydrotalcite phase well in the XRD study, has quite low surface area in comparison to the rehydrated $\text{MgAl}(\text{O})$ sample (Table 4B.1, entries 2 & 3). On the other hand, $\text{KNO}_3/\text{MgAl}(\text{O})$ shows similar surface area, pore volume as well as pore diameters as that of the $\text{MgAl}(\text{O})$.

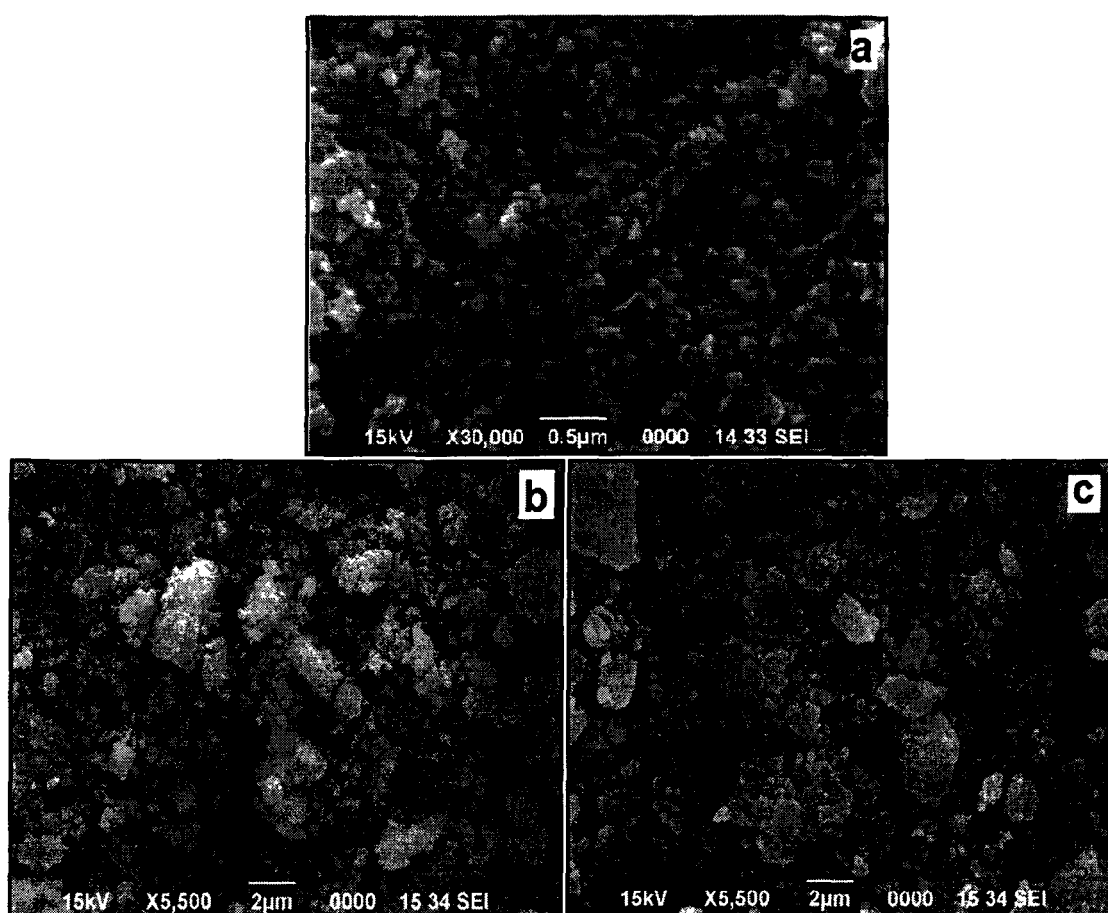


Figure 4B.4: Scanning electron micrographs of (a) HT and (b) KNO_3/HT (c) KF/HT at two different resolutions

Table 4B.1: Textural properties of potassium salt loaded hydrotalcites calcined at 450 °C

Entries	Sample	BET surface area (m ² g ⁻¹)	Pore volume (cm ³ g ⁻¹)	Pore diameter (Å)
1	HT ^a	207	0.23	15
2	MgAl(O) ^b	64	0.07	20
3	KHCO ₃ /MgAl(O)	5	0.01	18
4	KNO ₃ /MgAl(O)	54	0.07	19
5	KNO ₃ /MgAl(O) ^c	4	0.01	16

^aUncalcined hydrotalcite, ^b Rehydrated hydrotalcite calcined at 450 °C, Host mixed oxide, ^cCalcined at 550° C.

Pore volume and average pore diameter of KNO₃/MgAl(O) are 0.07 cm³/g and 19 Å respectively and these are higher in comparison to KHCO₃/MgAl(O) which showed the pore volume and pore radius of 0.01 cm³/g and 18 Å respectively. Surface area of the samples further lowered when the calcination temperature was increased to 550 °C. We have observed that KOH, KF, K₂CO₃ and KHCO₃ have low surface area and pore volumes at both temperatures. Therefore, we have chosen KNO₃/MgAl(O) calcined at 450 °C as the optimum catalyst in this study.

We calculated the base strengths as well as total basic sites of the samples. Table 4B.2 shows the base strengths (HL) and total basic sites of potassium salt loaded MgAl(O) samples after activation at 450 °C. Significant change of base strengths as well as total basic sites were obtained after calcinations at 450 °C which shows the effect of loading over the basic properties. The base strength of unloaded hydrotalcite calcined at 450 °C lies in the range of 15 < pK_{BH+} < 17.2 with total basic sites 0.45 mmolg⁻¹. Loading and calcinations with potassium salts further increases the base strengths and total basic sites. It has been observed that the base strengths of KNO₃/MgAl(O) and KF/MgAl(O) lies in the range 17.2 < pK_{BH+} < 18 and their total basis sites are 0.47 mmol g⁻¹ and 0.42 mmol g⁻¹ respectively. On the other hand, base strengths as well as total basic sites of KOH/MgAl(O), KHCO₃/MgAl(O) and K₂CO₃/MgAl(O) are comparatively

lower than the previous two. This may be due to gradual collapse of hydrotalcite phase at 450 °C and incomplete formation of mixed oxide phase at this temperature (XRD).

Table 4B.2: Basic properties of potassium salt loaded hydrotalcites calcined at 450 °C

Sample	Base Strength (H _L)	Amount of total basic sites (mmol g ⁻¹)
RHT	15 < pK _{BH+} < 17.2	0.45
KNO ₃ / MgAl(O)	17.2 < pK _{BH+} < 18	0.47
KF/ MgAl(O)	17.2 < pK _{BH+} < 18	0.42

4B.1.2 Catalytic reaction

The catalytic activities of the mixed oxides were checked for knoevenagel condensation reaction under microwave irradiation conditions depicted in scheme 4B.1. Since DMF was found as the optimum solvent for this reaction at room temperature (section 4A), we initially studied the reaction with p-nitorbenzaldehyde (1mmol) and malononitrile (1 mmol) in presence of DMF solvent and the mixed oxide catalysts under microwave to check their catalytic activity. The results are summarized in Table 4B.3. It is observed that the reaction proceeds even with host MgAl (O) to give good yield of product within 20 minutes (entry 1, Table 4B.3). However, higher yield and faster reaction was achieved for potassium salt loaded samples. This can be attributed to the increase of base strengths of the materials after incorporation of potassium salts and due to the different numbers of total basic sites of each catalyst. It is observed from table 4B.3 that the reaction with K₂CO₃/ MgAl(O) and KHCO₃/MgAl(O) are comparable to each other in terms of reaction time and yield thus furnishing 92 % and 91 % yield respectively within 15 minutes (entries 2&3, Table 4B.3). This may be due to similarities in their structural pattern which make them comparable to one another. Likewise, KF/MgAl(O) and KNO₃/MgAl(O) furnish 93 % and 99 % yield respectively within 5 minutes. This can be attributed to their low water content in the interlayer space and presence of free surface

hydroxyl groups on the surface. The reaction with KOH/ MgAl(O) is comparatively faster than K₂CO₃/ MgAl(O) and KHCO₃/MgAl(O) and gives 92% yield within 7 minutes. Thus, it can be conferred that KNO₃/ MgAl(O) is the best catalyst in this study. The reactions was further studied with KNO₃/ MgAl(O) catalyst and DMF solvent.

Table 4B.3 Catalyst study for Knoevenagel condensation reaction

Entry	Catalyst ^a	Time (min)	% yield ^b
1	MgAl(O)	20	85
2	K ₂ CO ₃ /MgAl(O)	15	92
3	KHCO ₃ /MgAl(O)	15	91
4	KOH/MgAl(O)	7	92
5	KF/ MgAl(O)	5	93
6	KNO ₃ / MgAl(O)	5	99

Reaction conditions: p-nitrobenzaldehyde (1 mmol), Malononitrile (1 mmol), Catalyst = 30 mg, DMF = 3 ml, MW power = 350 Watt, Temperature = 50 °C

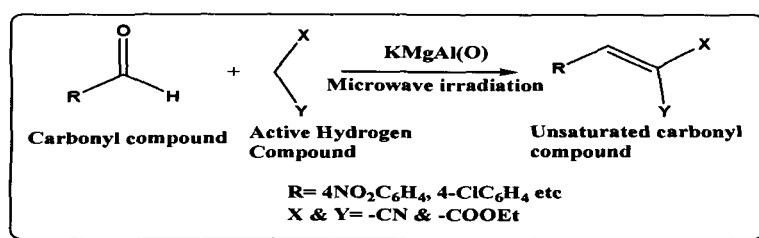
^a Calcined at 450 °C for 6 h.

^b Isolated yield

Having been found the best catalyst, the scope of the reaction was evaluated by performing the reaction with KNO₃/MgAl(O), active methylene compounds (malononitrile and diethyl malonate) and variety of aldehydes such as simple aromatic aldehydes bearing both electron withdrawing and electron donating substituents, heterocyclic aldehyde and polycyclic aromatic aldehyde. The results are summarized in Table 4B.4 (entries 1-14). The reaction becomes faster in comparison to room temperature methodology described in section 3A and gives respectable yields (42-99%) within 2-30 minutes. The catalyst is active for varied reaction centers as mentioned earlier and gives different yields according to the substituents present in the reaction center. Substituent effects on aromatic ring can be elucidated by inspecting entries 1-8 (Table 4B.4). Unsubstituted benzaldehyde reacts smoothly to afford 99 % yield within 7 minutes. In presence of electron withdrawing substituents at ortho, meta or para positions, the reaction becomes faster to afford the desired product with 91-99 % yields within 2 minutes (entries 2-4, Table 4B.4). The electron withdrawing -NO₂ group at

[Chapter 4]

ortho, meta or para positions does not have considerable effect over the speed of the reaction and forms similar yields within 2 minutes. Aldehydes bearing electron donating substituent take comparatively longer reaction time than that with electron withdrawing substituents and afford the product in good to moderate yields (55-87 %) within 30 minutes (entries 6 & 7, Table 4B.4).



Scheme 4B.1: Knoevenagel condensation reaction catalyzed by KNO₃/ MgAl (O)

Table 4B.4: Knoevenagel condensation reaction catalyzed by KNO₃/MgAl(O)

Entry	R	X=Y	Time (min)	Product % Yield ^a
1	Ph	CN	7	99
2	4-NO ₂ C ₆ H ₄	CN	2	99
3	3-NO ₂ C ₆ H ₄	CN	2	91
4	2-NO ₂ C ₆ H ₄	CN	2	93
5	4-ClC ₆ H ₄	CN	5	88
6	4-CH ₃ C ₆ H ₄	CN	25	87
7	4-OHC ₆ H ₄	CN	30	55
8	1-Naphthyl	CN	30	62
9	4-NO ₂ C ₆ H ₄	COOEt	25	77
10	2-NO ₂ C ₆ H ₄	COOEt	25	65
11	4-ClC ₆ H ₄	COOEt	30	52
12	4-CH ₃ C ₆ H ₄	COOEt	30	47
13	4-OHC ₆ H ₄	COOEt	30	42
14	1-Naphthyl	COOEt	30	57

Conditions: aldehyde (1 mmol), malononitrile (1 mmol), DMF (3 mL), 10 % KNO₃/MgAl(O) (30 mg);

^a Isolated yield

[Chapter 4]

The reaction with unsubstituted heterocyclic aldehyde can be compared to the electron donating substituents in benzaldehyde and gives 62 % yield within 30 minutes (entry 8, Table 4B.4) . We have observed further lowering of reaction speed with diethyl malonate as active methylene compound. All the substrates react slowly to give 47-77 % yields within 30 minutes. This is due to decrease of acidity of acidic protons of diethyl malonate in presence of two ester groups. The effect of substituent groups have also been reflected in this case from the obtained yields within 30 minutes (entries 9-14, Table 4B.4).

Table 4B.5: Reusability study of 10 % KNO₃/MgAl(O) under microwave

Entry	Catalyst	Amount	Time (min)	% yield
1	Fresh	50 mg	2	99
2	2 nd run	44 mg	2	99
3	3 rd run	38 mg	2	93
4	4 th run	30 mg	2	91

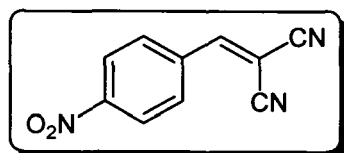
Conditions: p-nitro benzaldehyde (1 mmol), malononitrile (1 mmol), DMF (3 mL)

The scope of the catalyst was further checked by investigating the reusability upto fourth repetitive cycles with recovered catalysts from each run. The catalyst was recovered from the reaction mixture by centrifugation, washed with acetone and calcined again at 450 °C for 2 h before performing the the next run. The results are summarized in Table 4B.5. We have found that the catalyst is active upto fourth cycle and gives similar yields (91-99 %) within 2 minutes.

Thus we have found KNO₃ loaded MgAl(O) as an efficient catalyst for Knoevenagel condensation reaction under microwave irradiations in DMF medium to afford the products within short time.

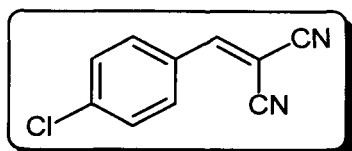
4B.3 Spectral data

1. 2- (4-Nitrobenzylidene)malononitrile [entry 2, Table 4B.4]



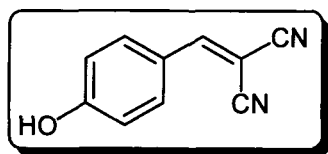
$^1\text{H NMR}$ (400 MHz, CDCl_3): δ 8.39-8.37 (d, $J = 8$ Hz, 2H, ArH), 8.08-8.06 (d, $J = 8$ Hz, 2H, ArH), 7.87 (s, 1H, =CH); $^{13}\text{C NMR}$ (100MHz, CDCl_3): δ 156.80, 150.41, 135.80, 131.30, 124.66, 112.66, 111.59 & 87.62.

2. 2- (4-Chlorobenzylidene)malononitrile



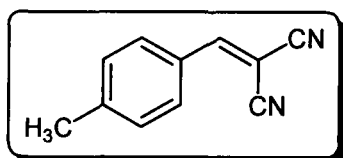
$^1\text{H NMR}$ (400 MHz, CDCl_3): δ 7.88-7.86 (d, $J = 8$ Hz, 2H, ArH), 7.80 (s, 1H, =CH), 7.53-7.51 (d, $J = 8$ Hz, 2H, ArH).

3. 2- (4-Hydroxybenzylidene)malononitrile



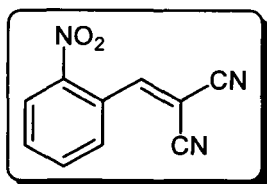
$^1\text{H NMR}$ (400 MHz, CDCl_3): δ 7.88-7.86 (d, $J = 8$ Hz, 2H, ArH), 7.64 (s, 1H, =CH), 6.96-6.94 (d, $J = 8$ Hz, 2H, ArH).

4. 2- (4-Methylbenzylidene)malononitrile



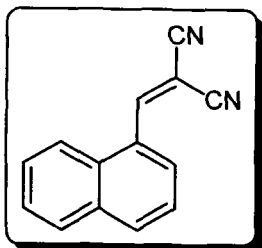
$^1\text{H NMR}$ (400 MHz, CDCl_3): δ 7.82-7.80 (d, $J = 8$ Hz, 2H, ArH), 7.72 (s, 1H, =CH), 7.34-7.32 (d, $J = 8$ Hz, 2H ArH), 2.45 (s, 3H, $-\text{CH}_3$).

5. 2- (2-Nitrobenzylidene)malononitrile



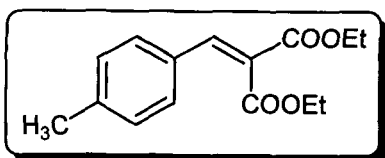
$^1\text{H NMR}$ (400 MHz, CDCl_3): δ 8.46 (s, 1H, =CH), 8.34 (s, 1H, ArH), 7.89-7.84 (m, 2H, ArH), 7.83-7.79 (q, 1H, ArH).

6. 2-Naphthylidene malononitrile



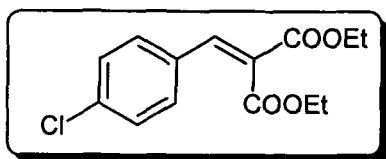
$^1\text{H NMR}$ (400 MHz, CDCl_3): δ 8.46 (s, 1H, =CH), 8.29-8.27 (d, $J = 8$ Hz, 2H, ArH), 8.12-8.10 (d, $J = 8$ Hz, 1H, ArH), 7.97-7.95 (d, $J = 8$ Hz, 1H, ArH), 7.69-7.59 (m, 3H, ArH).

7. 2-(4-methylbenzylidene)-malonic acid diethyl ester



$^1\text{H NMR}$ (400 MHz, CDCl_3): δ 8.34 (s, 1H, =CH), 7.28-7.26 (d, $J = 8$ Hz, 2H, ArH), 7.14-7.12 (d, $J = 8$ Hz, 2H, ArH), 4.14-4.08 (q, 2H, $-\text{OCH}_2$), 4.07-4.01 (q, 2H, $-\text{OCH}_2$), 2.42 (s, 3H, $-\text{CH}_3$), 1.25-1.21 (t, 3H, $-\text{CH}_3$), 1.12-1.08 (t, 3H, $-\text{CH}_3$).

8. 2-(4-chlorobenzylidene)-malonic acid diethyl ester



NMR (400 MHz, CDCl_3): δ 8.35 (s, 1H, =CH), 7.26-7.24 (d, $J = 8$ Hz, 2H, ArH), 7.14-7.12 (d, $J = 8$ Hz, 2H, ArH), 4.15-4.09 (q, 2H, $-\text{OCH}_2$), 4.07-4.01 (q, 2H, $-\text{OCH}_2$), 1.25-1.21 (t, 3H, $-\text{CH}_3$), 1.12-1.08 (t, 3H, $-\text{CH}_3$).

4B.4 References

- [1] Freeman, F. *Chem. Rev.* **80** (4), 329-350, 1980.
- [2] G. Jones, The Knoevenagel condensation. *Org. React.* Wiley, New York, **15**, 204, 1967.
- [3] Zhang, X.R., et al. *Org. Lett.* **8** (12), 2563-2566, 2006.
- [4] Oguchi, M., et al. *J. Med. Chem.* **43** (16), 3052-3066, 2000.
- [5] Jung, J.C., et al. *Molecules* **17** (2), 2091-2012, 2102.
- [6] Raman, N., et al. *Eur. J. Med. Chem.* **80**, 57-70, 2014.
- [7] Malamas, M.S., et al. *J. Med. Chem.* **43** (5), 995-1010, 2000.
- [8] Torre, P.D.L., et al. *Molecules* **17** (2), 12072-12085, 2012.
- [9] Raman, N. & Pravin, N. *Eur. J. Med. Chem.* **80**, 57-70, 2014.
- [10] Zhao, S., et al. *RSC Adv.* **3** (29), 11691-11696, 2013.
- [11] Alizadeh, A., et al. *Micropor. Mesopor. Mat.* **159**, 9-16, 2012.
- [12] Liu, Q., et al. *Ultrason. Sonochem.* **18** (2), 477- 479, 2011.
- [13] Biradar, J.S. & Sasidhar, B.S. *Eur. J. Med. Chem.* **54** (19), 6112-6118, 2011.
- [14] Pahalagedara, M.N., et al. *Langmuir* **30** (27), 8228-8237, 2014.
- [15] Hoz, A.D.L. *Chem. Soc. Rev.* **34** (2), 164-178, 2005.
- [16] Gedye, R.N. & Wei, J.B. *Can. J. Chem.* **76** (5), 525-532, 1998.
- [17] Caddick, S. *Tetrahedron* **51** (38) 10403-10432, 1995.
- [18] Xie, Y.S., et al. *Tetrahedron Lett.* **55** (17) 2796-2800, 2014.
- [19] Baar, M.R., et al. *J. Chem. Educ.*, **87** (1), 84-86, 2010.
- [20] Lidstrom, P., et al. *Tetrahedron* **57** (4)5, 9225-9283, 2001.
- [21] Climent, M.J., et al. *J. Catal.*, **151** (1), 60-66, 1995.
- [22] Cavani, F., et al. *Catal. Today* **11** (2), 173-301, 1991.
- [23] Kantam, M.L., et al. *Chem. Commun.* (9), 1033-1034, 1998.
- [24] Nishimura, S., et al. *Green Chem.* **15** (8), 2026-2042, 2013.
- [25] Mendoza, D.G., et al. *J. Hazard. Mater.* **263** (Part 1) 67-72, 2013.
- [26] Carriazo, D., et al. *J. Mol. Catal. A: Chem.* **342-343**, 83-90, 2011.

- [27] Climent, M.J., et al. *J. Catal.* **269** (1), 140-149, 2010.
- [28] Surpur, M.P., et al. *Tetrahedron Lett.* **50** (6), 719-722, 2009
- [29] Angelescu, E., et al. *Appl. Catal. A: Gen.* **308** (), 13-18, 2006.
- [30] Velosco, C.O., et al. *Micropor. Mesopor. Mat.* **107** (1-2), 23-30, 2008.
- [31] Zhao, J., et al. *Appl. Catal. A: Gen.* **467**, 33-37, 2013.
- [32] Z. Wang, F. Liu, C. Lu, *Chem. Commun.* **47** (19), 5479-5481, 2011.
- [33] Castro, C.S., et al. *Fuel Process. Technol.* **125**, 73-78, 2014.
- [34] Millange, F., et al. *J. Mater. Chem.* **10** (7), 1713-1720, 2000.
- [35] Frost, R.L., et al. *J. Raman Spectros.* **42**, 1163-1167, 2011.
- [36] Frost, R.L., et al. *J. Raman Spectros.* **34** (10), 760-768, 2003.
- [37] Seftel, A.M., et al. *Rev. Roum. Chem.* **52** (11), 1033-1037, 2007.
- [38] Frost, R.L., et al. *J. Raman Spectros.* **34** (10), 760-768, 2003.
- [39] Mustrowski, P., et al. *Mater. Res. Bull.* **39** (2), 263-281, 2004.
- [40] Roelofs, J.C.A.A., et al. *J. Catal.* **203** (1), 184-191, 2001.
- [41] Sing, K.S.W., et al. *Pure Appl. Chem.* **57** (4), 603-619, 1985.

Chapter 5

Synthesis of MgO by hydrothermal and solvothermal methods and their application for Claisen-Schmidt condensation reaction

Chapter 5

Synthesis of MgO particles by hydrothermal and solvothermal methods and their application for Claisen-Schmidt condensation reaction

Synthesis of MgO precursors through different routes has been a fascinating field of catalysis due to the possibility of getting structurally diverse MgO morphologies and excellent basic properties, which can catalyze a good number of base catalyzed organic reactions [1-4]. Besides, MgO has been used in numerous applications such as filler in paints and superconductors [5], modifier [6], catalyst support [7], fertilizers [8], lubricating oils [9] and wastewater treatment [10]. Physico-chemical properties of this class of materials are highly governed by their particle sizes, surface area, crystallinity as well as morphologies which can be well achieved by altering the particle arrangements through various synthesis strategies [11-13]. Among a varieties of synthetic routes [14-18], hydrothermal and solvothermal routes have been widely used in the recent years and found successful in getting varied morphologies [19-22]. However, synthesis of MgO of newer design and improved catalytic activities is still challenge for chemists. It has been found that MgO can effectively catalyze organic reactions such as Aldol condensation, Knoevenagel condensation and Claisen-Schmidt condensation under optimized reaction conditions [23-25]. Among these, the Claisen-Schmidt condensation reaction generally requires elevated reaction temperature and strong base to give the desired product in high yield. Therefore, this reaction is commonly carried out with variety of promoted MgO catalysts and MgO catalysts having various shapes and sizes at high temperatures to obtain the products in high yield and selectivity [26]. However, catalytic activities of these materials are governed by the effect of shape, size, basic properties as well as surface properties which are not yet fully understood. This has inspired us to synthesize MgO precursors via hydrothermal and solvothermal routes and check their morphological features and catalytic activities for Claisen-Schmidt condensation reaction.

In this section, we have described the synthesis of MgO precursors from nitrate salts of magnesium in presence of three bases namely, urea, NaOH and Na₂CO₃ by hydrothermal and solvothermal methods. Complete characterizations of these materials

were done through XRD, FTIR, SEM and N₂ adsorption-desorption measurement methods. Catalytic applications for Claisen-Schmidt condensation reaction was performed under classical heating conditions and described herein. We have also described the effect of ratio of base versus magnesium salt and effect of three bases namely NaOH, Urea and Na₂CO₃ upon growth of particles, phase obtained, crystallinity and their particle sizes. We have observed that the amount of magnesium salt and the base in the mixture has crucial role over the crystal growth. This section also illustrates the basic properties of the as synthesized MgO precursors, calcined MgO and their catalytic activities towards Claisen-Schmidt condensation reaction. The detailed study of effect of solvents, effect of catalysts, reaction time and temperatures on yield was investigated and explained herein. The complete Characterization methods of the materials have been described in Chapter 2.

5.1 Results and discussion

5.1.1 Effect of synthesis parameters on morphologies

Initially, MgO precursors were synthesized through hydrothermal route by mixing base solution and Mg(NO₃)₂.6H₂O salt solution of water in three different molar proportions i.e. 0.1:1, 1:1 and 10:1 respectively at 120 °C for 6 h to understand the effect of ratio of base versus salt over the crystallization pattern of the precursors. The XRD pattern is presented in figure 5.1. Three bases namely urea, sodium hydroxide (NaOH) and sodium carbonate (Na₂CO₃) were used for the synthesis. It was observed that all the precursors were crystalline in nature where presence of the same basic environment leads to similar crystalline phases in the XRD pattern (MgO-U-0.1, MgO-U-1 and MgO-U-10; MgO-OH-1 and MgO-OH-10; MgO-CO-1 and MgO-CO-10). We have noticed that the precursors obtained from urea and Na₂CO₃ form similar crystalline phases in the XRD and may be suggested for the formation of Magnesium Carbonate Hydroxide Hydrate like phase i.e. Mg₅(CO₃)₄(OH)₂.(H₂O)₄ (JCPDS Card Number-701177). On the other hand, precursor obtained from NaOH gives more crystalline and sharp diffraction lines that can be suggested for Mg(OH)₂ phase in the XRD pattern (JCPDS Card Number-860441). Again, ratio of salt versus base and time of crystallization has crucial effect over the growth of crystalline phase. As the amount of base increases in the mixture, crystallinity

of the precursors increases. It can be well explained from the samples synthesized in presence of urea as basic medium (figure 5.1). Increasing the ratio of urea versus salt from 0.1 to 10 in the mixture, crystal growth become more facile showing sharp and well defined diffraction lines in the XRD pattern. It shows that 10:1 ratio of base versus salt gives the highly crystalline phase. It is also observed that increase of hydrothermal treatment time from 6 h to 24 h, the intensity of the XRD peaks diminished (MgO24-U-10, figure 5.1). We have also observed similar dependence of basic environment on crystallization of MgO in case of NaOH and Na₂CO₃ environment. Crystallization becomes more facile on increasing NaOH and Na₂CO₃ in the mixture (Figure 5.1). This shows that the crystallization is highly dependent on the ratio of base versus salt and crystallization time.

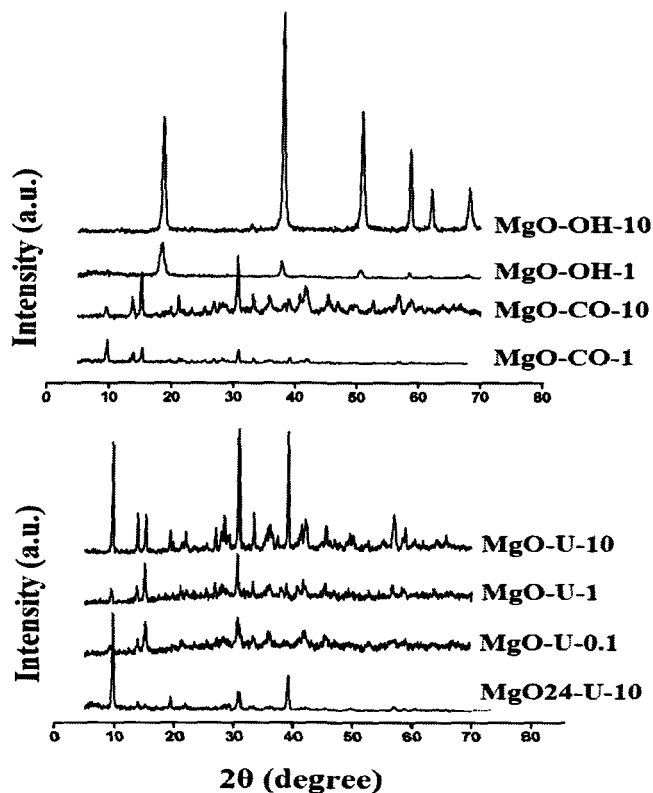


Figure 5.1: XRD pattern of MgO precursors synthesized under hydrothermal treatment for 6 h with different ratio of base versus salt; urea [MgO-U-10 (10:1), MgO-U-1 (1:1), MgO-U-0.1 (0.1:1), MgO24-U-10(10:1 for 24h)]; NaOH [MgO-OH-10 (10:1), MgO-OH-1 (1:1)] and Na₂CO₃ [MgO-CO-10 (10 :1), MgO-CO-1 (1:1)].

The result of relative crystallinity (%) study from integration of XRD peaks at 2θ positions 9.7° , 13.75° and 38.8° are depicted in Figure 5.2. It again reveal that the highest crystallinity is obtained by the sample synthesized from 10: 1 proportion of urea versus $\text{Mg}(\text{NO}_3)_2 \cdot 6\text{H}_2\text{O}$ salt. Therefore, synthesis of MgO through solvothermal route was carried out with 10:1 ratio of urea versus $\text{Mg}(\text{NO}_3)_2 \cdot 6\text{H}_2\text{O}$ salt with three different solvents namely ethanol, ethylene glycol and glycerol. The precursors were named as MgO-U-Et, MgO-U-EG and MgO-U-Gly for ethanol, ethylene glycol and glycerol respectively. It is observed that solvothermal synthesis using urea furnish similar type of XRD pattern as that of the hydrothermal methods (figure 5.3).

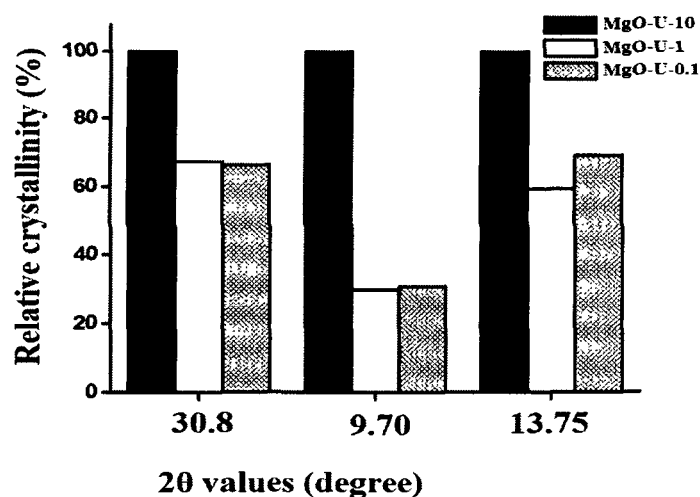


Figure 5.2: Relative crystallinity (%) of MgO precursors obtained from urea

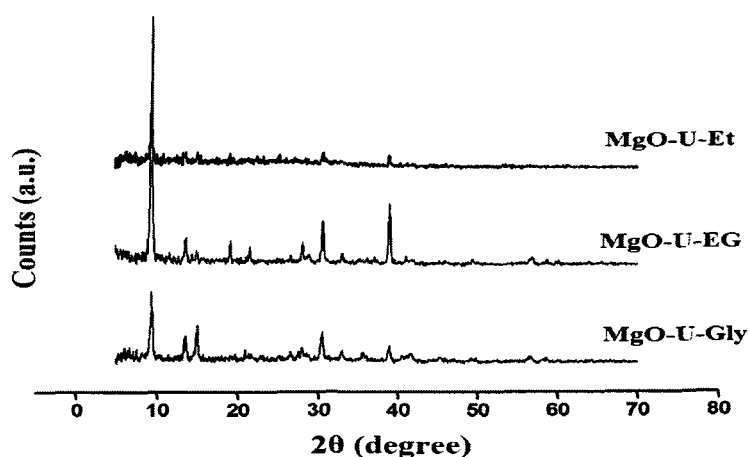


Figure 5.3: XRD pattern of MgO precursors obtained via solvothermal route with ethanol (MgO-U-Et), ethylene glycol (MgO-U-EG) and glycerol (MgO-U-Gly)

However, intensities of the samples are low in comparison to hydrothermal route. Figure 5.4 compares the relative crystallinity of the precursors from solvothermal route to hydrothermal route which reveal that MgO-U-EG has the highest crystallinity among the three obtained through solvothermal route. This indicates slow and improper growth of the crystals obtained through this route.

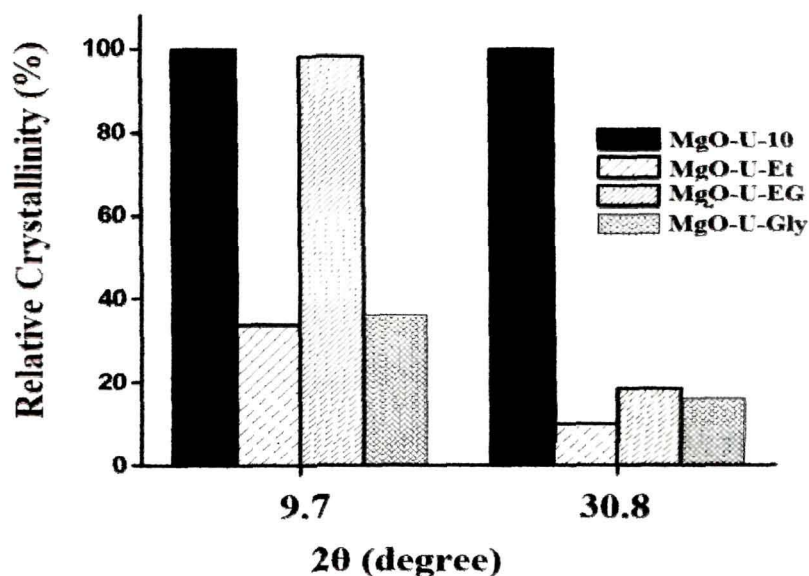


Figure 5.4: Relative crystallinity of MgO precursors obtained via solvothermal route

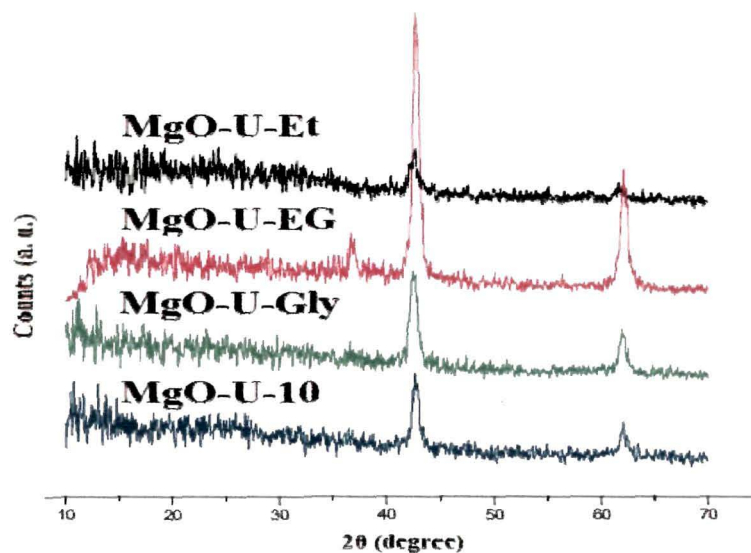


Figure 5.5: XRD pattern of MgO calcined at 500 °C

Following this, all the samples were calcined at 500 °C to obtain MgO phases (Figure 5.5). All the precursors converted into MgO phase showing sharp and distinct peaks at 2θ values 42.75° and 62.15° corresponding to MgO phase.

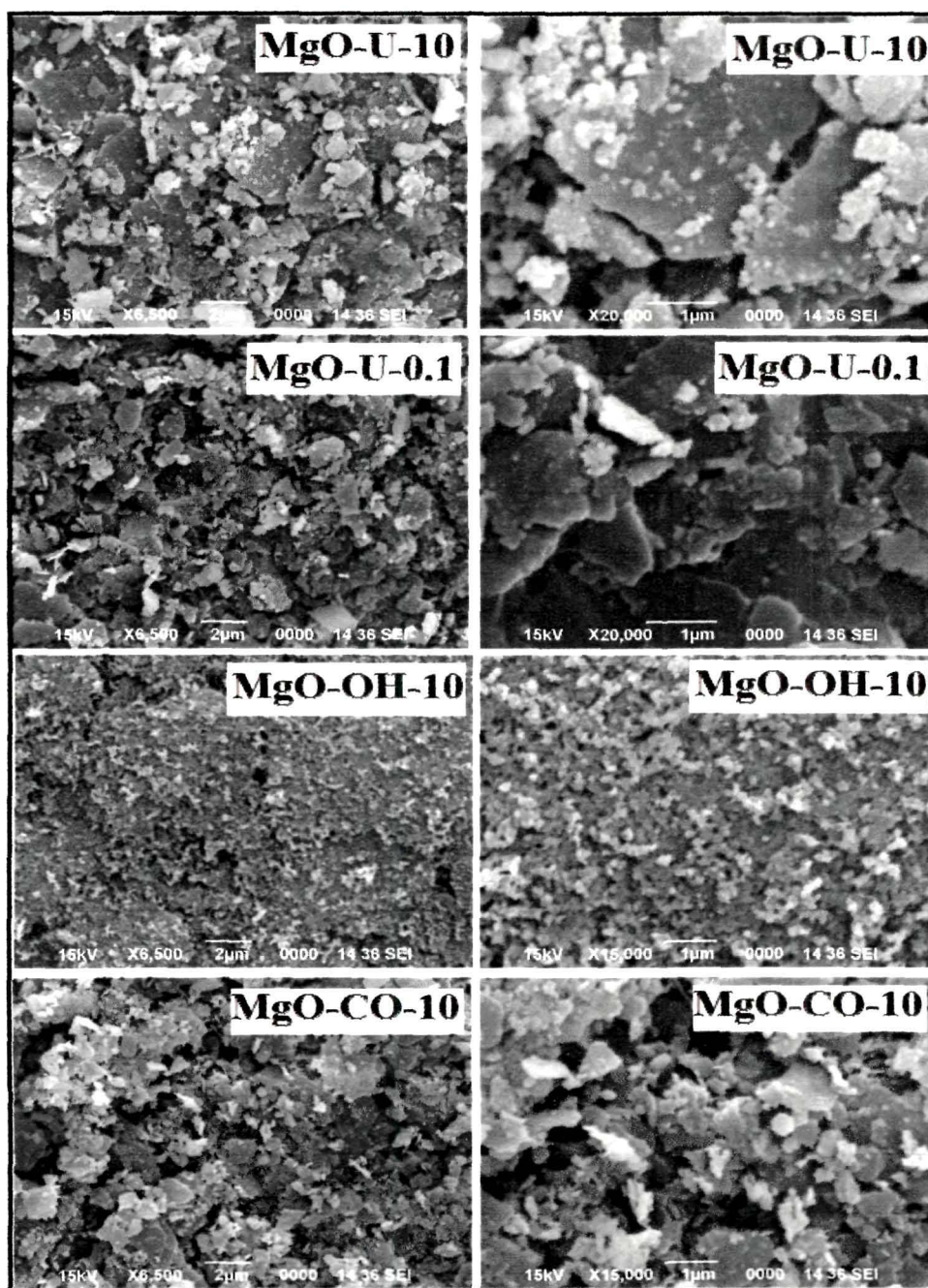


Figure 5.6: SEM images of MgO precursors by hydrothermal route

Figure 5.6 represents the SEM images of MgO precursors obtained by hydrothermal synthesis in presence of urea. Samples MgO-U-10 and MgO-U-0.1 contain non-homogeneous particle shapes and sizes and agglomerated leaf like particles. The morphologies were changed upon changing the basic environment. It is observed from Figure 5.6 that MgO-CO-10 sample (Na_2CO_3) shows similar particle arrangements as that of MgO-U-10 and MgO-U-0.1 which was also evident from XRD analysis (Figure 5.1). However, agglomeration of the particles in MgO-CO-10 is quite less in comparison to MgO-U-0.1 and thus shows leaf like particles with distinct phase. On the other hand, sample obtained from NaOH (MgO-OH-10) has uniform particle shapes and sizes and shows arrangement of homogeneous hexagonal leaf like particles in SEM images. Small and homogeneous particle size of this precursor is reflected from the XRD pattern of the sample showing distinct peaks (Figure 5.1).

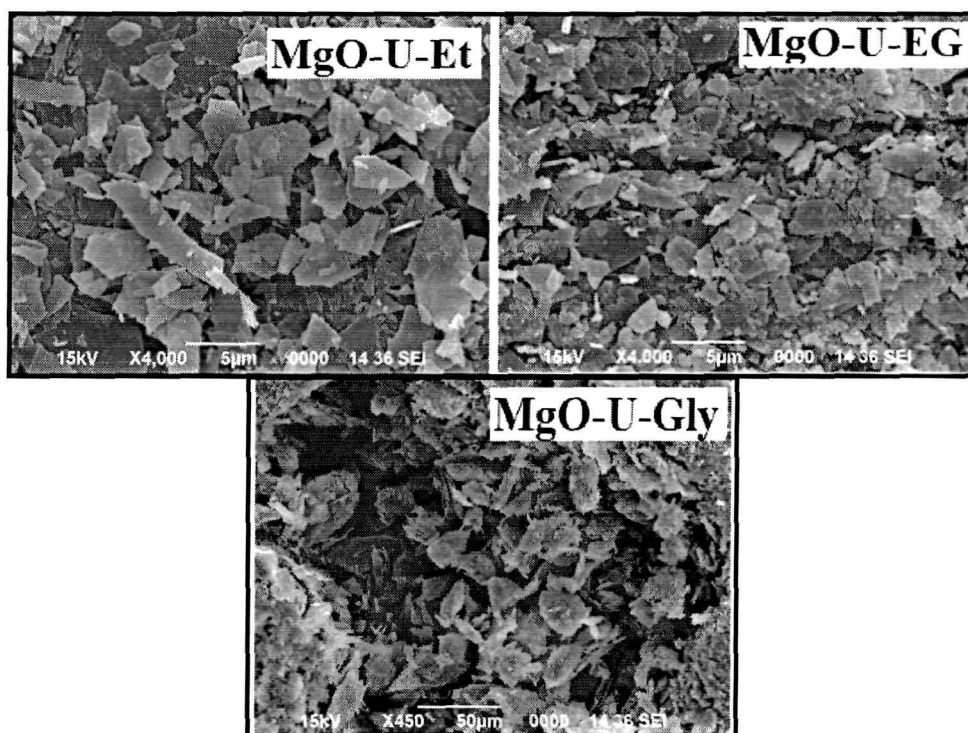


Figure 5.7: SEM images of MgO precursors obtained by solvothermal route

The SEM images of the samples obtained through solvothermal synthesis shows amorphous sheets of structures with nonhomogeneous shapes (Figure 5.7). This has been

further confirmed by looking at the XRD pattern which showed less intense peaks in comparison to hydrothermal route. Therefore, it can be conferred that the presence of urea in the mixture does not favour particle growth to form definite shapes. On the other hand, NaOH as base favours the nucleation process to form uniform particles under hydrothermal method.

The surface area measurement of the calcined MgO samples showed varied specific area and pore volumes. It is observed from Table 5.1 that in MgO sample obtained from solvothermal route has larger surface area than that with hydrothermal route using the same basic environment i.e. urea. It may be due to smaller particle sizes of MgO obtained through solvothermal method. Among the studied oxides, BET area and pore volume of MgO obtained by using NaOH is the highest. This can be attributed to the small and uniform particles of this sample. We have also found comparable crystallite sizes of the precursors through hydrothermal and solvothermal route.

Table 5.1: Surface area and pore volumes of MgO calcined at 500 °C.

Entry	Sample	BET area m^2g^{-1}	Pore volume $(\text{cm}^3\text{g}^{-1})$	Pore diameter (Å)	Crystallite size (Å)
1	MgO-U-10	63	0.26	25	222
2	MgO-OH-10	283	0.46	37	-
3	MgO-CO-10	105	0.18	65	-
4	MgO-U-EG	208	0.46	41	269
5	MgO-U-Gly	217	0.50	36	275

The N_2 -adsorption desorption isotherm of the calcined samples show type II isotherms according to the IUPAC classification. This type of isotherm is the characteristics of monolayer and multilayer adsorption in the samples. Again, we have observed that the samples MgO-U-EG, MgO-U-Gly and MgO-U-10, shows type A hysteresis loop according to “de Boer” [27] classification and characterize the presence of cylindrical pores. On the other hand, the samples MgO-OH-10 and MgO-CO-10 showed type C hysteresis loop characteristics of wedge shaped pores having open ends.

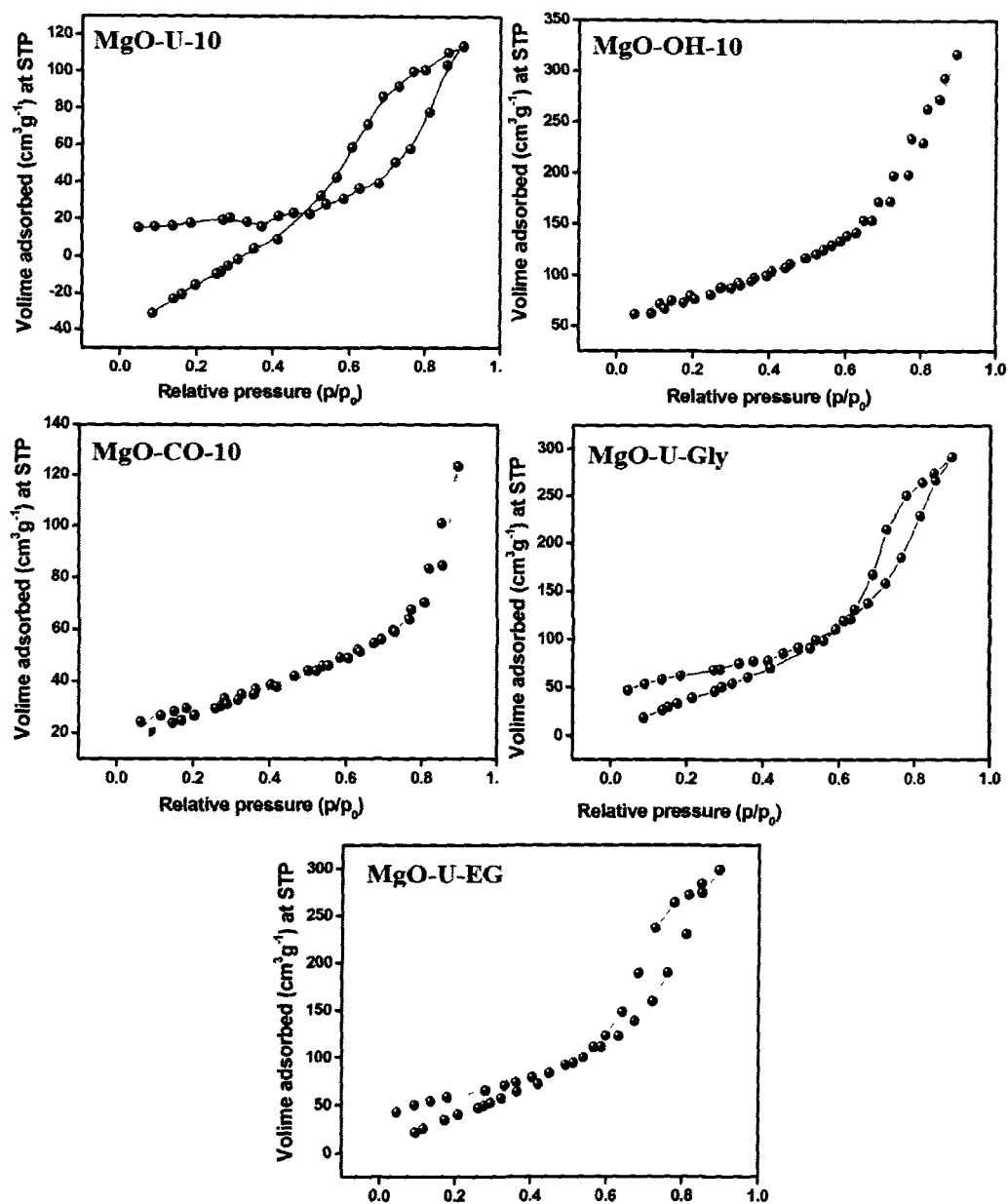
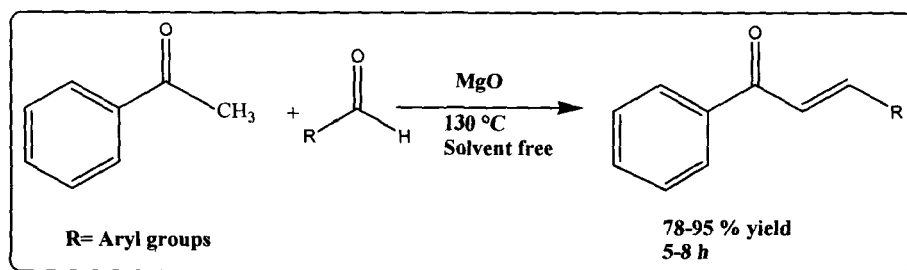


Figure 5.8: BET isotherms of Calcined MgO at 500 °C.

5.1.2 Catalytic reaction

To understand the relationship between the effect of morphologies and catalytic activity, Claisen-Schmidt condensation reaction was carried out with the prepared MgO samples calcined at 500 °C under solvent free condition (Scheme 5.1). For this purpose, 1 mmol p-nitrobenzaldehyde, 1 mmol acetophenone and 35 mg MgO was taken in a round

bottomed flask and heated in an oil bath at 130° C with constant stirring. The results of catalytic reactions are presented in Table 5.2. We have seen that all the prepared MgO are active for this reaction and give respectable yields within 5-8 hours.



Scheme 5.1: Claisen-Schmidt condensation reaction catalyzed by MgO calcined at 500 °C

Table 5.2: Effect of various MgO catalysts calcined at 500 °C

Sl No	Catalyst	Time (h)	Yield
1	MgO-U-10	8	78
2	MgO-OH-10	5	87
3	MgO-CO-10	8	67
5	Mg-U-EG	5	86
6	MgO-U-Gly	5	95

Conditions: Acetophenone = 1 mmol, p-nitrobenzaldehyde = 1 mmol, MgO = 35 mg, Temperature = 130 °C.

The reaction between acetophenone and p-nitrobenzaldehyde was faster with MgO obtained from NaOH base through hydrothermal method (MgO-OH-10) in comparison to the other two samples obtained via this route. This can be attributed to the well crystalline uniform MgO particles and high surface area. On the other hand, acetophenone conversion of 95 % was achieved from MgO obtained from glycerol base (MgO-U-Gly) in comparison to the other catalysts.

Therefore, the reaction was further carried out with MgO-U-Gly sample with a variety of aldehydes bearing electron withdrawing groups and electron donating groups (Table 5.3). We have observed that electron withdrawing substituents in aromatic ring

[Chapter 5]

(entries 1, 2 & 3, Table 5.3) react faster than that having electron donating substituents (entry 5, Table 5.3) to give 91-95 % yield within 5-6 hours. The reaction with naphthaldehyde was slow and showed 23 % yield within 8 hours. The reusability of the catalyst was also tested for three repetitive cycles where the catalyst was found active to give good yield of product within 8 hours (entry 7, table 5.3). However, the activity was reduced gradually after each run. This may be due to loss of some MgO in each cycle or deactivation of some active sites during the reaction.

Table 5.3 Claisen-Schmidt reaction with MgO at 130 °C.

SL No	R	Time (h)	Yield (%) ^a	Yield (%) ^d (Time in minutes)
1	4-NO ₂ C ₆ H ₄	5	95	97 (35)
2	3-NO ₂ C ₆ H ₄	6	90	92 (35)
3	2-NO ₂ C ₆ H ₄	5	91	89 (35)
4	4-ClC ₆ H ₄	6	87	88 (40)
5	4-CH ₃ C ₆ H ₄	8	68	79 (40)
6	1-Naphthyl	8	23	47 (40)
7	4-NO ₂ C ₆ H ₄	8	82 ^b 73 ^c	

Conditions: Acetophenone= 1 mmol, p-nitrobenzaldehyde = 1 mmol, MgO = 35 mg, solvent free

^aIsolated yields, ^bSecnd run, ^cThird run

^d Reactions under microwave irradiation (Conditions: Acetophenone=1 mmol, aldehyde = 1 mmol, MgO = 35 mg, solvent free, 490 Watt)

The scope of the catalysts was further checked by performing the reaction under microwave irradiation condition (490 Watt). It is observed that the reaction time reduces from hours to minutes under microwave condition to afford moderate to excellent yield (47-97 %) within 40 minutes.

Thus, we have prepared an effective MgO catalyst of high surface area for Claisen-Schmidt condensation reaction under classical heating as well as microwave irradiation conditions.

5A.3: References

- [1] Chintareddy, V.R. & Kantam, M.L. *Catal. Surv. Asia* **15**, 89-110, 2011.
- [2] Hattori H., *Chem. Rev.* **95**, 537-550, 1995.
- [3] Ding, Y., et al. *Chem. Mater.* **13**, 435-440, 2001.
- [4] Cosimo, J.I.D., et al. *Catalysis* **26**, 1-28, 2014.
- [5] Kovac, P., et al. *Supercond. Sc. Technol.* **17** (10), L1-L6, 2004.
- [6] Mladenov, M., et al. *Electrochem. Commun.* **3** (8), 410-416, 2001.
- [7] Leofanti, G., et al. *Appl. Catal.* **3**, 131-139, 1982.
- [8] Thiel, H.E.V. & Tucker, W.J. *J. Agric. Food Chem.* **5** (6), 442-444, 1957.
- [9] Huang, W., et al. *Wear* **260** (1-2), 140-148, 2006.
- [10] Huang, H., et al. *Chem. Eng. J.* **254**, 418-425, 2014.
- [11] Sutradhar, N., et al. *J. Phys. Chem. C* **115** (25), 12308-12316, 2011.
- [12] Pashchanka, M. et al. *J. Mater. Chem.*, **20**, 957-963, 2010.
- [13] Nagashima, K., et al. *Appl. Phys. Lett.* **90**, 233103, 2007.
- [14] Kern, W. & Roster, R. S. *J. Vac. Sci. Technol.* **14**, 1082, 1977.
- [15] Haubold, V. *Mater. Sci. Eng.* **679**, 1992.
- [16] Ouraipryvan, P., et al. *Mater. Lett.* **63** (21), 1862-1865, 2009.
- [17] Wahab, R., *Mater. Sci. forum* **558-559**, 983-986, 2007.
- [18] Matthew. R., et al. *Carbon* **44**, 10-18, 2006.
- [19] Yi Ding, Y., et al. *Chem. Mater.* **13**, 435-440, 2001.
- [20] Cui, H., et al. *Mater. Res. Bull.* **50**, 307-311, 2014.
- [21] Selvamani, T., et al. *Catal. Commun.* **11** (6), 537-541, 2010.
- [22] Zhang, Y., et al. *J. Alloy Comp.* **590**, 373-379, 2014.
- [23] Chen, S., et al., Theoretical study on the reaction mechanisms of the aldol-condensation of 5-hydroxymethylfurfural with acetone catalyzed by MgO and MgO⁺, *Catal. Today*, in press.
- [24] Diez, V.K., et al. *Catal. Today* **173** (1), 21-27, 2011.
- [25] Ganguly, A., et al. *J. Colloid Interf. Sci.* **353** (1), 137-142.
- [26] Sutradhar, N., et al. *Mater. Res. Bull.* **46** (11), 2163-2167, 2011.
- [27] S. Brunauer, S., et al., *J. Am. Chem. Soc.* **62**, 1723, 1940.

Chapter 6

Conclusions and Future scope

6.1 Conclusions

The overall intention of the present study was to develop benign catalyst systems and suitable reaction media for three important base catalyzed organic reactions i.e Henry reaction, Knoevenagel condensation reaction and Claisen-Schmidt condensation reaction. Inspired by some excellent literatures, we selected three important solid base materials namely, *zeolite*, *MgAl-hydrotalcite* and *MgO* particles to synthesize and modify for this purpose.

In Chapter 3, we have successfully loaded KF amount of 5 w % over NaY and KL zeolites by a wet impregnation method and activated at 450 °C. The base strength of the loaded zeolites was found higher ($8.0 < H_L < 10.0$) than the parent zeolites ($6.8 < H_L < 8.0$) after activation. The importance of this observation is the perseverance of zeolite framework structure along with simultaneous increase of base strengths after calcination at 450 °C. We have found that KF/NaY is an efficient catalyst for nitroaldol reaction in presence of MeOH–H₂O solvent at room temperature and furnishes good to moderate yields (47-92 %) within 4-48 hours. Reaction parameters such as temperature, molar ratio of nitromethane with aldehydes and effect of solvents were optimized to understand the reaction fully. We have observed that increasing temperature speed up the reaction and reduces the selectivity while increasing amount of nitromethane increases both selectivity and conversions. Among a series of screened solvents, methanol gives the highest conversion of 92 % within 48 h. Addition of H₂O with the solvents further enhances the reaction rate and selectivity. The catalyst is found active up to fourth run showing similar conversions in each run.

To enhance the scope of the reaction, NaY zeolite was modified with 0.5 - 20 % KF (w/w) by a wet impregnation method and characterized by X-ray diffraction and FT-IR techniques. Framework structure was found preserved even after 20 % loading of KF while crystallinity reduced from lower to higher loading. Optimization of reaction conditions with different solvents, microwave power and microwave irradiation time, was carried out for the reaction in presence of 10 % KF/NaY catalyst to get good to excellent yields within 2-15 minutes. Again, higher basicity of modified samples than their parent one was observed from basicity measurement by Hammett indicator method. Thus, we have described an efficient method of synthesis of β -nitro alcohols catalyzed by KF

modified NaY zeolite under microwave irradiation condition which can be a good alternative for conventional synthesis with liquid bases. The method is fast and selective and superior to many literature methods. Optimization of reaction conditions such as solvents, microwave power and amount of solvents serve to suppress the possible competitive reactions during the reaction and aid in the formation of selective product. The reaction rate greatly enhances due to the combined effect of microwave and water-alcohol mixture as reaction medium.

In Chapter 4, we have described a simple and efficient protocol for liquid phase Knoevenagel condensation reaction catalyzed by KOH loaded MgAl hydrotalcite prepared through wet impregnation of KOH over calcined MgAl hydrotalcite. Among five different potassium salt loaded MgAl hydrotalcites i.e. KF, KOH, KNO₃, KHCO₃ and K₂CO₃, the host structure is more stable in presence of KOH and least stable with KNO₃. Introduction of potassium species increases the basicities and shows higher activities for Knoevenagel condensation reaction at room temperature. It is found that 10% (w/w) KOH/HT is the best catalyst and DMF is the best solvent in the study and catalyzes the reaction efficiently giving 99 % conversion and 100 % selectivity within 10 minutes. It is also observed that polar aprotic solvent like DMF and acetonitrile speed up the reaction while non-polar solvents slower the reaction. The combination of the use of recyclable solid base catalyst, DMF as reaction medium, room temperature reaction, high yield and selectivity make this protocol eco-friendly and superior to various reported methods. Renewability of the solid base and its easy and simple preparation method makes the protocol attractive to chemists practicing green synthetic processes.

The scope of the reaction and catalytic materials were further enhanced by performing the reaction with calcined hydrotalcites under microwave irradiation. Calcined Mg-Al hydrotalcite was used as support to load KNO₃, KOH, K₂CO₃, KHCO₃ and KF by a wet impregnation method and calcined again at 450-550 °C temperatures to obtain potassium salt loaded MgAl-mixed oxides. The obtained materials were characterized by XRD, FTIR, BET, DSC, TGA and SEM techniques and the catalytic activities were checked for liquid phase Knoevenagel condensation reaction under microwave irradiation. The materials showed different structural and basic properties and gives good to excellent yield of within 1 hour at room temperature. It is found that KNO₃

loaded mixed oxide is the best catalyst in the study to afford 99 % conversion within 5 minutes. The catalyst was active for varieties of aldehydes and gave 47-99 % yield within 2-30 minutes. The results can be well correlated to the basicity, BET surface area and pore sizes.

In Chapter 5, we have successfully synthesized different MgO precursors through hydrothermal and hydrothermal routes by mixing base solution and $\text{Mg}(\text{NO}_3)_2 \cdot 6\text{H}_2\text{O}$ salt solution of water in three different molar proportions i.e. 1: 0.1, 1:1 and 0.1:1 at 120 °C for 6 h. It is found that increasing the amount of base in the reaction mixture facilitates the crystallization procedure. Among the three molar ratio of base versus salt, the highest crystallinity was observed from 1: 0.1 ratio of base: $\text{Mg}(\text{NO}_3)_2 \cdot 6\text{H}_2\text{O}$. Solvothermal synthesis of MgO precursors were synthesized from 1:0.1 ratio of the base versus $\text{Mg}(\text{NO}_3)_2 \cdot 6\text{H}_2\text{O}$ using three different solvents namely ethanol, ethylene glycol and glycerol. Calcination of all the precursors gave MgO phase, which showed high catalytic activities for Claisen-Schmidt reaction at 130 °C. It was observed that MgO obtained through solvothermal method possesses higher surface area than that from hydrothermal route. The optimized catalyst in the study is the MgO obtained from ethylene glycol solvent through solvothermal route and gives moderate to good yield (47-92 %) within 8 hours.

6.1 Future scope of work

Synthesis and modification of solid strong bases has become a necessary tool for achieving cleaner catalytic alternatives for liquid bases which can be used for a good number of base catalyzed reactions. From the understanding of experimental results found in the research work presented in this thesis and going through various literatures, the following points can be highlighted for future scope of the present study.

- i) Zeolite NaY can be loaded with other fluoride salts of alkali and alkaline earth metals to understand the role of basic guest precursors over the stability of the framework.
- ii) Effect of calcination temperatures over structure and basicity of zeolite structure would be interesting. Thermal treatment of loaded zeolites at

temperature ranges 300-800 °C would be curious to know about the change in basic properties.

- iii) Metal loaded zeolites can be tested for other base catalyzed organic reactions such as Knoevenagel condensation reaction and aldol condensation reaction which can be run with mild base catalysts.
- iv) Hydrotalcite with various amount of KOH over its structure and simultaneous calcination into mixed oxide phase would be helpful to understand the effect of loading and calcination temperature on change of basic properties.
- v) Solvothermal synthesis of MgO with different bases can be done to check on the effect of basic environment on formation of morphologies and physic chemical properties.
- vi) Optimization of reaction conditions such as solvents and temperatures is a necessary step to check on the reactions carried out with these solid bases.
- vii) These techniques can be extended to mesoporous materials such as MCM-41, SBA-15 etc.

Appendices

A. List of Publications

1. **Devi, R., Borah, R. & Deka, R.C.** Design of zeolite catalysts for nitroaldol reaction under mild condition, *Appl. Catal. A: Gen.* **433-434**, 122-127, 2012.
2. **Devi, R., Borah, R. & Deka, R.C.** Investigation of Structural Change and Basicity of NaY Zeolite upon Loading KF and Their Application in Henry Nitroaldol Reaction Under Microwave Irradiation Condition, *Catal. Lett.*, **144** (10), 1751-1758, 2014.
3. **Bharali, D., Devi, R., Bharali, P., Deka, R.C.** *New. J. Chem.* Synthesis of high surface area mixed metal oxide from NiMgAl LDH precursor for Nitro-aldol condensation reaction. (*Under review*)
4. **Devi R., Baruah, P.J., Begum, P., Bharali, P., Deka R. C.,** Comparative study of structure and basicity of potassium salt modified MgAl- hydrotalcites and their application for Knoevenagel condensation reaction. (*Communicated*)
5. **Devi, R. & Deka, R. C.** Investigation of microwave assisted Knoevenagel condensation reaction catalyzed by KNO₃ promoted MgAl-hydrotalcite. (*Communicated*)
6. **Devi, R., Bharali, P., Deka, R. C.** Synthesis of MgO from hydrothermal and solvothermal routes for Claisen-Schmidt condensation reaction. (*Communicated*)

B. List of Seminar/Conference/Workshop/Symposium attended

1. **Summer School on green Chemistry**, from 2-22nd June 2009, Tezpur University.
2. **Frontier Lecture Series**, from 20-22 November 2009, Tezpur University
3. **Orientation Programme in Catalysis Research**, from 28th November to 16th December, 2009, IIT Madras.
4. **14th National Workshop on Catalysis**, from 21st-23rd December 2009, Tezpur University.

[Publications and conference attended]

5. **Workshop on Intellectual Property Right Sensitization-2010**, Tezpur University.
6. **Workshop on Integrated arsenic and iron removal from groundwater: Arsiron Nilogon**, 25th June, 2011, Tezpur University.
7. **National workshop on Nuclear and Atomic Techniques Based Pure and Applied Sciences**, 1st -3rd February, 2011.
8. **National Conference on Chemistry, Chemical Technology and Society**, from 11th -12th November, 2011, Tezpur University.
9. **Indo-Finnish Symposium on Role of catalyst on production of green fuel**, 1st February, 2013, Tezpur University.
10. **Workshop on spectroscopic tools and their applications**, 6th April 2013, Tezpur University.